

Control of Vein Patterning by Auxin Transport and Signaling

by

Sree Janani Ravichandran

A thesis submitted in partial fulfillment of the requirements for the degree of

Master of Science

in

Plant biology

Department of Biological Sciences
University of Alberta

© Sree Janani Ravichandran, 2019

ABSTRACT

Tissue networks such as the vascular networks of mammalian embryos and the vein network of plant leaves transport water, signals and nutrients; what controls the formation of these networks is thus a key question in biology. In animals, the formation of tissue networks requires direct cell-cell communication and often cell movements, both of which are precluded in plants by a wall that holds cells in place; therefore, plants form tissue networks such as the vein networks in their leaves by a different mechanism.

The details of the mechanism by which plants form leaf vein networks are poorly understood, but available evidence places the plant signal auxin and its polar transport through plant tissues at the core of such mechanism. (1) Expression of the PIN-FORMED1 (PIN1) auxin transporter of *Arabidopsis* is initiated in broad domains of leaf inner cells that become gradually restricted to files of vein precursor cells in contact with pre-existing, narrow PIN1 expression domains. Within broad expression domains, PIN1 is localized isotropically — or nearly so — to the plasma membrane of leaf inner cells. As expression of PIN1 becomes gradually restricted to files of vein precursor cells, PIN1 localization becomes polarized to the side of the plasma membrane facing the pre-existing, narrow PIN1 expression domains with which the narrowing domains are in contact. (2) Auxin application to developing leaves induces the formation of broad expression domains of isotropically localized PIN1. Such domains become restricted to the sites of auxin-induced vein formation, and PIN1 localization becomes polarized toward pre-existing PIN1 expression domains. (3) Both restriction of PIN1 expression and polarization of PIN1 localization are delayed by chemical

inhibition of auxin transport. (4) Auxin transport inhibitors induce characteristic vein-pattern defects, similar to — though stronger than — those of *pin1* mutants. Therefore, available evidence suggests that auxin induces the polar formation of veins and that such inductive and orienting property of auxin strictly depends on the function of *PIN1* and possibly other *PIN* genes.

How auxin coordinates PIN polarity between auxin-transporting cells to induce the polar formation of veins is unclear, but for the past 20 years the prevailing hypothesis has been that the GNOM (GN) guanine-nucleotide exchange factor for ADP-ribosylation-factor GTPases, which regulates vesicle formation in membrane trafficking, controls the cellular localization of PIN1 and other PIN proteins; the resulting cell-to-cell, polar transport of auxin would coordinate PIN polarity between auxin-transporting cells and control polar developmental processes such as vein formation. Here I tested this hypothesis by a combination of cellular imaging, molecular genetic analysis, and chemical induction and inhibition. Contrary to predictions of the hypothesis, my results suggest that: (1) auxin-induced polar-vein-formation occurs in the absence of PIN proteins or any known intercellular auxin transporter; (2) the residual auxin-transport-independent vein-patterning activity relies on auxin signaling; (3) GN controls both auxin transport and signaling to induce vein formation.

Whereas mechanisms by which GN may control PIN polarity and derived polar auxin transport have been suggested, it is unclear how GN could control auxin signaling, which takes place in the nucleus and is inherently non-polar. The most parsimonious account is that auxin signaling leads to the production of proteins which control vein patterning and whose localization is controlled by GN. Here I tested this hypothesis by a combination of gene

expression screen and molecular genetic analysis, and identified four putative candidates for such proteins.

Finally, to further characterize in the future the function of such putative candidate proteins which are targets of auxin signaling, which control vein patterning, and whose localization is controlled by GN, I have identified and characterized GAL4/GFP enhancer-trap lines for the targeted misexpression of genes of interest in specific cells and tissues of developing leaves.

My results suggest synergism between auxin transport and signaling and their unsuspected control by GN in the formation of plant tissue networks, a control whose logic is unprecedented in multicellular organisms.

ACKNOWLEDGEMENTS

My master's work would not have been possible without the generous contributions of many other people.

First and foremost, I would like to express my deepest gratitude and appreciation to Dr. Enrico Scarpella for his unparalleled knowledge, constructive criticism and relentless support throughout my master's program.

For kindly providing plasmids and seeds, I thank the Arabidopsis Biological Resource Center (ABRC), Thomas Berleth, Ikram Blilou, Mark Estelle, Jiří Friml, Hidehiro Fukaki, Hiroo Fukuda, Markus Geisler, Gerd Jürgens, Cris Kuhlemeier, Elliot Meyerowitz, Ikram Blilou, Miyo Morita, Satoshi Naramoto, Sandra Richter, Ben Scheres, Masao Tasaka, Jian Xu and Michael Prigge.

I would like to extend my thanks to Dr. Neil Harris for agreeing to be in my supervisory committee and Dr. Jocelyn Hall for agreeing to be my arm's length examiner.

I would also like to thank Dr. Mike Deyholos for collaborating and sharing his insightful expertise for Chapter 3 of my thesis.

I very much appreciate my fellow lab mates Anmol Krishna, Brindhi Amalraj, Linh Manh Nguyen, Priyanka Govindaraju and Dr. Dhruv Lavania for helping me with parts of this thesis and creating a fun-filled environment in the lab. I thank Carla Verna for training me with techniques in the lab.

And my biggest thanks to my family for all the support you have shown me throughout, the culmination of three years of distance learning: my parents Ravichandran and Meenambikai, and my brother Vigneshh. This dissertation would not have been possible without their warm love, continued patience, and endless support.

Table of contents

Chapter 1: General Introduction	1
1.1 The plant vascular system	1
1.2 Leaf vein development	1
1.3 Auxin transport and vascular strand formation	3
1.4 Auxin signaling and vascular strand formation	4
1.5 Scope and outline of the thesis	5
Chapter 2: Coordination of tissue cell polarity by auxin transport and signaling	7
2.1 Introduction	7
2.2 Results	9
2.2.1 Contribution of the <i>GNOM</i> gene to coordination of tissue cell polarity during Arabidopsis vein formation	9
2.2.2 Contribution of <i>GN</i> to vein patterning	15
2.2.3 Contribution of plasma-membrane-localized PIN proteins to vein patterning	20
2.2.4 Contribution of <i>PIN</i> genes to vein patterning	30
2.2.5 Genetic versus chemical inhibition of auxin transport during vein patterning	30
2.2.6 Contribution of <i>ABCB</i> genes to vein patterning	35
2.2.7 Contribution of <i>AUX1/LAX</i> genes to vein patterning	43
2.2.9 Response of <i>pin</i> leaves to auxin application	60

2.2.10 Contribution of auxin signaling to vein patterning _____	62
2.2.11 Contribution of <i>GN</i> to auxin signaling _____	69
2.2.12 Contribution of auxin transport and signaling to coordination of tissue cell polarity during vein formation _____	76
2.3 Discussion _____	81
2.3.1 Control of vein patterning by carrier-mediated polar auxin-transport _____	82
2.3.2 Control of vein patterning by auxin signaling _____	85
2.3.3 A tissue-cell-polarizing signal upstream of auxin transport and signaling ____	86
2.4 Materials & Methods _____	89
2.4.1 Notation _____	89
2.4.2. Plants _____	89
2.4.3 Chemicals _____	89
2.4.4 RT-PCR _____	89
2.4.5 Imaging _____	90
Chapter 3: Identification of new auxin-signaling-dependent regulators of vein patterning _____	97
3.1 Introduction _____	97
3.2 Results and Discussion _____	98
3.2.1 A gene expression screen for auxin signaling targets that control vein patterning synergistically with auxin transport _____	98
3.2.2 Contribution of auxin signaling targets to vein patterning _____	101
3.2.3 Interaction between auxin signaling targets and auxin transport in vein patterning _____	104

3.2.4 <i>PXY</i> redundancy in vein patterning _____	107
3.2.5 Conclusions and prospects _____	107
3.3 Materials & Methods _____	111
3.3.1 Plants _____	111
3.3.2 Imaging _____	111
3.3.3 RNA isolation and sequencing _____	111
3.3.4 Gene expression analysis _____	112
Chapter 4: GAL4/GFP enhancer-trap lines for identification and manipulation of cells and tissues in developing Arabidopsis leaves _____	118
4.1 Introduction _____	118
4.2 Results and Discussion _____	119
4.3 Materials & Methods _____	144
4.3.1 Plants _____	144
4.3.2 Chemicals _____	144
4.3.3 Imaging _____	145
Chapter 5: General discussion _____	146
5.1 Conclusion summary _____	146
5.2 The Canalization hypothesis: challenges and alternatives _____	147
5.2.1 The Canalization hypothesis _____	148
5.2.2 Challenges to the canalization hypothesis _____	151
5.2.3 Alternatives to the canalization hypothesis _____	155

5.2.4 Conclusions	154
Literature cited	156

List of tables

Chapter 2

Table 2.1. Origin and nature of lines.	10
Table 2.2. Embryo viability of WT, <i>pin3;4;7</i> and <i>pin2;3;4;7</i> .	27
Table 2.3. Embryo viability of <i>toz</i> , <i>mp</i> , <i>pin1</i> , <i>pin1;3;4;7</i> , <i>pin1;2;3;4;7</i> and <i>pin1;3;4;6;7;8</i> .	28
Table 2.4. Embryo viability of <i>pin1</i> , <i>pin1;3;4;7</i> , <i>pin1;2;3;4;7</i> and <i>pin1;3;4;6;7;8</i> .	29
Table 2.5. Embryo viability of WT, <i>abcb1</i> , <i>abcb19</i> , <i>abcb1;19</i> and <i>twd1</i> .	38
Table 2.6. Embryo viability of <i>toz</i> , <i>mp</i> , <i>pin1;3;6</i> and <i>pin1;3;6;abcb1;19</i> .	41
Table 2.7. Embryo viability of <i>pin1;3;6</i> and <i>pin1;3;6;abcb1;19</i> .	42
Table 2.8. Embryo viability of WT, <i>aux1</i> , <i>lax1</i> , <i>aux1;lax1</i> and <i>aux1;lax1;2;3</i> .	46
Table 2.9. Embryo viability of <i>toz</i> , <i>mp</i> , <i>pin1;3;6</i> and <i>pin1;3;6;aux1;lax1</i> .	48
Table 2.10. Embryo viability of <i>pin1;3;6</i> and <i>pin1;3;6;aux1;lax1</i> .	49
Table 2.11. Embryo viability of <i>axr1;axl</i> , <i>tir1;afb2</i> , <i>gn;pin1,3;4;7</i> and <i>gn;pin1,3,6;4;7;8</i> .	56
Table 2.12. Embryo viability of <i>gn;pin1,3;4;7</i> and <i>gn;pin1,3,6;4;7;8</i> .	57
Table 2.13. Embryo viability of WT, <i>axr1</i> and <i>tir1;afb2</i> .	65
Table 2.14. Embryo viability of <i>toz</i> , <i>mp</i> , <i>pin1,3,6;4;7;8</i> , <i>pin1,3,6;4;7;8;axr1</i> , <i>pin1,3,6;4;7;8;tir1;afb2</i> .	70
Table 2.15. Embryo viability of <i>pin1,3,6;4;7;8;axr1</i> and <i>pin1,3,6;4;7;8;tir1;afb2</i> .	71
Table 2.16. Embryo viability of <i>toz</i> , <i>mp</i> , <i>gn</i> and <i>gn;axr1</i> .	77
Table 2.17. Embryo viability of <i>gn</i> and <i>gn;axr1</i> .	78
Table 2.18. Genotyping strategies.	91

Table 2.19. Oligonucleotide sequences.	93
-----------------------------------------------	----

Table 2.20. Light paths.	95
---------------------------------	----

Chapter 3

Table 3.1. Genes that are co-expressed with <i>GN</i> , <i>PINI</i> or <i>MP</i> , whose expression was both ≥ 1.5 -fold lower in NPA-grown <i>tir1;afb2</i> than in NPA-grown WT and ≥ 1.5 -fold lower in PBA- and NPA-grown WT than in NPA-grown WT, and which encoded proteins that are predicted to be localized to the plasma membrane or to be secreted to the extracellular space.	101
------------------------------------------------------------------------------------------------------------------------------------------------------------------------------------------------------------------------------------------------------------------------------------------------------------------------------------------------------------------------------------------------------------	-----

Table 3.2. Origin and nature of lines.	112
-----------------------------------------------	-----

Table 3.3. Genotyping strategies.	114
------------------------------------------	-----

Table 3.4. Oligonucleotide sequences.	
----------------------------------------------	--

Chapter 4

Table 4.1. Origin and nature of lines.	121
-----------------------------------------------	-----

Table 4.2. Reproducibility indices of expression features.	139
-------------------------------------------------------------------	-----

List of Figures

Chapter 2

Figure 2.1. Contribution of the <i>GNOM</i> gene to coordination of tissue cell polarity during Arabidopsis vein formation.	12
Figure 2.2. Contribution of <i>GN</i> to vein patterning.	16
Figure 2.3. Effect of the <i>gn-18</i> mutation on <i>GN</i> expression.	19
Figure 2.4. Contribution of plasma-membrane-localized PIN proteins to vein patterning.	22
Figure 2.5. <i>pin</i> mutant seedlings.	24
Figure 2.6. Cotyledon patterns of <i>pin</i> mutants.	25
Figure 2.7. Contribution of <i>PIN</i> genes to vein patterning.	31
Figure 2.8. Genetic versus pharmacological inhibition of auxin transport.	33
Figure 2.9. Contribution of <i>ABCB</i> genes to vein patterning.	35
Figure 2.10. Cotyledon patterns of <i>pin</i> , <i>abcb</i> and <i>aux1/lax</i> mutants.	40
Figure 2.11. Contribution of <i>AUX1/LAX</i> genes to vein patterning.	44
Figure 2.12. <i>pin</i> and <i>gn</i> mutant seedlings.	51
Figure 2.13. Seedling axes of <i>pin</i> and <i>gn</i> mutants.	52
Figure 2.14. Cotyledon patterns of <i>pin</i> and <i>gn</i> mutants.	53
Figure 2.15. Cotyledon vein patterns of <i>pin</i> and <i>gn</i> mutants.	54
Figure 2.16. Genetic interaction between <i>GN</i> and <i>PIN</i> genes.	59
Figure 2.17. Response of <i>pin</i> leaves to auxin application.	61

Figure 2.18. Contribution of auxin signaling to vein patterning.	63
Figure 2.19. <i>pin</i> and <i>axr1</i> mutant seedlings.	67
Figure 2.20. Cotyledon patterns of <i>pin</i> , <i>axr1</i> and <i>tir1;afb2</i> mutants.	68
Figure 2.21. <i>pin</i> and <i>tir1;afb2</i> mutant seedlings.	69
Figure 2.22. Auxin response in developing leaves.	73
Figure 2.23. <i>gn</i> and <i>axr1</i> mutant seedlings.	74
Figure 2.24. Cotyledon patterns of <i>gn</i> and <i>axr1</i> mutants.	75
Figure 2.25. Genetic interaction between <i>GN</i> and <i>AXR1</i> .	76
Figure 2.26. Contribution of auxin transport and signaling to coordination of tissue cell polarity during vein formation.	80
Figure 2.27. Interpretation Summary.	83

Chapter 3

Figure 3.1. Flowchart of screen for auxin signaling targets that control vein patterning synergistically with auxin transport.	99
Figure 3.2. Contribution of auxin signaling targets to vein patterning.	104
Figure 3.3. Contribution of auxin signaling targets and auxin transport to vein patterning.	107
Figure 3.4. <i>PXY</i> redundancy to vein patterning.	109

Chapter 4

Figure 4.1. Expression of E100>>, E861>> and E4295>>erGFP in Arabidopsis leaf development.	119
---------------------------------------------------------------------------------------------------	-----

Figure 4.2. Expression of E4259>>, E4722>>, E2408>> and E4716>>erGFP in leaf development.	132
Figure 4.3. Expression of E2331>> and E3912>>erGFP in leaf development.	135
Figure 4.4. E2331-mediated visualization and manipulation of developing veins.	137

Chapter 5

Figure 5.1. Induction of vascular strand formation by wounding and auxin application.	146
Figure 5.2. Leaf vein networks and carrier-mediated polar auxin transport.	150

LIST OF ABBREVIATIONS

ABCB	ATP-BINDING CASSETTE B
AFB	AUXIN SIGNALLING F-BOX
ARF	AUXIN RESPONSE FACTOR
ARF GEF	ADP-ribosylation factor guanine-nucleotide exchange factor
AXR1	AUXIN RESISTANT1
AUX1	AUXIN RESISTANT1
Col-0	Columbia
DAG	Days after germination
DR5	DIRECT REPEAT5
EMB30	EMBRYO DEFECTIVE30
ER	endoplasmic reticulum
Fig	Figure
GFP	green fluorescent protein
GN	GNOM
hv	higher vein
IAA	indole-3-acetic acid
l1	first loop
l2	second loop
LAX	LIKE AUX1
LUT	look-up-table
MP	MONOPTEROS
mv	midvein
NPA	1-N-naphthylphthalamic acid
PBA	phenylboronic acid
PILS	PIN-LIKES
PIN	PIN-FORMED
PM	plasma membrane

pm	plasma-membrane-localization signal
PXY	PHLOEM XYLEM INTERCALATED
RNA	Ribonucleic acid
RPS5A	RIBOSOMAL PROTEIN S5A
SCM	SCRAMBLED/STRUBBELIG
TIR1	TRANSPORT INHIBITOR RESPONSE1
TOZ	TORMOZ
TWD1	TWISTED DWARF1
UBQ10	UBIQUITIN10
WT	wild type
YFP	yellow fluorescent protein

Gene and Protein Notation

Uppercase Italics	WT Gene (e.g., <i>PIN1</i>)
Uppercase Roman	WT Protein (e.g., PIN1)
Lowercase Italics	Mutant Allele (e.g., <i>pin1</i>)
Multiple Mutant of Gene A and B	<i>a;b</i> (e.g.; <i>pin1;pin6</i>)

Gene Fusion Notation

Transcriptional Fusion of Gene A to Gene B (Fusion of promoter A to gene B)	A::B
Translational Fusion of Gene A to Gene B (Fusion of gene A to gene B)	A:B

Gene Coordinates

All gene coordinates are relative to the adenine (position +1) of the start codon.

Chapter 1: General Introduction

1.1 The plant vascular system

Most multicellular organisms transport signals, nutrients and water by means of vascular systems. In vascular plants, such vascular system is composed of a network of continuous vascular strands that connect to one another different parts of an organ and different organs of the plant (Esau, 1965). Vascular strands are named differently in different organs: veins in flat organs such as cotyledons, leaves, sepals and petals; vascular bundles in the stem; and vascular cylinder in the root.

Mature vascular strands are cylinders composed of two vascular tissues: xylem — toward the inside in cylindrical organs and the upper side in flat organs — and phloem — toward the outside in cylindrical organs and the lower side in flat organs (Esau, 1965). Xylem mainly transports water and minerals, and is composed of tracheary elements, parenchyma cells and fibers; phloem mainly transports the products of photosynthesis and is composed of sieve elements, parenchyma cells, fibers and sclereids.

During plant growth by lengthening, vascular tissues differentiate from within bundles of files of vascular-precursor procambial cells (Esau, 1965). In plants and organs that undergo growth by radial thickening, a layer of procambial cells remains in each vascular strand between the xylem and phloem formed during growth by lengthening; this layer of procambial cells resumes proliferation to give rise to the vascular cambium, from which new xylem and phloem will differentiate to thicken vascular strands.

1.2 Leaf vein development

In the rounded leaves of many non-monocots, lateral veins branch from a central midvein and connect to distal veins to form vein loops; minor veins branch from midvein and loops, and either end freely or contact other veins; and minor veins and loops curve near the leaf margin to lend a scalloped outline to the vein network (Gifford and Foster, 1988; Nelson and Dengler, 1997). In the elongated leaves of many monocots — for example, grasses like

maize — vein loops are compressed laterally and are stretched along the length of the leaf, such that midvein and lateral veins seem to be parallel to one another.

In flowering plants, polar localization of the auxin transporter PIN-FORMED1 (PIN1) and related proteins at the plasma membrane of epidermal cells at the shoot apex suggests that auxin transport converges toward sites of leaf primordium formation (Bayer 2009; Benkova 2003; Carraro 2006; Johnston 2015). Epidermal “convergence points” of PIN1 polarity correlated with sites of primordium formation become associated with broad inner PIN1-expression-domains that will narrow to sites of midvein formation. Likewise, sites of leaf lateral growth and positions of broad inner PIN1-expression-domains correlated with lateral vein formation seem to be connected to one another through epidermal convergence points of PIN1 polarity at the leaf margin (Hay et al. 2006; Scarpella et al. 2006; Wenzel et al. 2007).

By contrast, minor veins form from PIN1 expression domains with no association with epidermal convergence points and that branch from pre-existing veins (Scarpella et al. 2006; Wenzel et al. 2007). Initially, all minor veins end freely in the leaf inner tissue, and PIN1 is localized to the side of the plasma membrane toward the pre-existing veins. However, over time, some minor veins can become connected to pre-existing veins at both sides; at the ends of these “connected” veins, PIN1 is localized to the side of the plasma membrane toward the pre-existing veins, and the two, opposite PIN1 polarities are joined by a “bipolar” cell: a cell with PIN1 localized to two opposite sides of the plasma membrane.

PIN1 expression behavior during loop formation shows that each loop is formed by a minor vein branching from a lateral vein (Scarpella et al., 2006; Wenzel et al., 2007). Initially the minor vein ends freely in the leaf inner tissue, but over time it connects to the midvein or to more apically located lateral veins. As in all other connected veins, at the ends of each loop, PIN1 is localized to the side of the plasma membrane toward the pre-existing veins it connects to, and the two, opposite PIN1 polarities are joined by a bipolar cell.

Domains of PIN1 expression in the leaf inner tissue are initially broad and overlap with broad domains of expression of the auxin-response transcription factor MONOPTEROS (MP) (Donner et al., 2009; Wenzel et al., 2007). Like broad domains of PIN1 expression,

broad domains of MP expression narrow over time until they become restricted to sites of vein formation.

1.3 Auxin transport and vascular strand formation

The plant signal auxin is the only known molecule that can induce the formation of vascular strands: application of auxin to various plant tissues indeed induces the differentiation of continuous files of vascular cells that connect the applied auxin to the pre-existing vascular strands basally to the site of auxin application (Sachs, 1981; Berleth et al., 2000). The auxin-induced vascular-differentiation response is characterized by distinctive and reproducible properties: (1) the response is local, as it is initiated at the site of auxin application; (2) it is polar, as it is oriented toward the pre-existing vascular strands basal to the site of auxin application; (3) it is continuous, as it generates uninterrupted files of vascular cells; (4) it is constrained in the planes perpendicular to the main axis of the vascular differentiation response, as it originates slender bundles of vascular cell files; (5) it depends on polar transport through plant tissues and is obstructed in the presence of auxin transport inhibitors (Dalessandro and Roberts, 1971; Gersani, 1987). These observations suggest that the auxin-induced vascular-differentiation response recruits polar signals that already exist in plant tissues and that probably correspond to the polar transport of auxin.

Indeed, auxin is primarily synthesized in immature apical organs, such as leaf and flower primordia, and is transported basally to the roots through the vascular strands (Michniewicz et al., 2007; Normanly, 2010; Zhao, 2010). The resulting apical-basal transport of auxin seems to depend on the polar localization of auxin efflux carriers of the PIN-FORMED (PIN) family to the basal plasma-membrane of auxin-transporting cells (Wiśniewska *et al.*, 2006). Indeed, indole-3-acetic acid (IAA), the most common auxin in plants, is non-charged in the acidic cell wall and can thus freely diffuse into cells through the plasma membrane (Raven, 1975; Rubery and Sheldrake, 1974). However, in the more alkaline cytoplasm, IAA becomes negatively charged and can no longer passively diffuse through the plasma membrane but requires efflux carrier proteins to leave the cell.

These observations and considerations form the basis of the “canalization hypothesis”, which postulates that a positive feedback between auxin transport through a cell and the cell’s auxin conductivity progressively restricts an initially dispersed auxin flow to narrow, preferred canals, which will eventually differentiate into vascular strands (Sachs, 1981).

In *Arabidopsis* (*Arabidopsis thaliana* (L.) Heynh), the plasma-membrane localization of PIN1 marks the presumed site of cellular auxin efflux (Petrásek and Friml, 2009). Consistent with prediction of the canalization hypothesis, inhibition of polar auxin transport or higher auxin levels, either occurring naturally at leaf margin outgrowths or induced experimentally by direct auxin application, lead to the formation of broader inner PIN1-expression-domains in which PIN1 is homogeneously distributed throughout the plasma membrane (Aloni et al. 2003; Mattsson et al. 2003; Hay et al. 2006; Scarpella et al. 2006; Wenzel et al. 2007). Over time, these broader domains of PIN1 expression become restricted to cell files that will differentiate into vascular strands in which PIN1 becomes polarly localized to the side of the cell closest to the pre-existing vascular strands (Sauer et al., 2006; Scarpella et al., 2006). Consistent with a role for polar auxin transport in vascular strand formation, mutation in multiple *PIN* genes or development in the presence of polar auxin transport inhibitors leads to defects in vein network formation (Mattsson et al., 1999; Sawchuk et al., 2013; Sieburth, 1999; Verna et al., 2015).

1.4 Auxin signaling and vascular strand formation

The auxin signal is transduced by multiple pathways (Leyser, 2010); best understood is that which ends with the transcriptional activation or repression of auxin-responsive genes by transcription factors of the AUXIN RESPONSE FACTOR (ARF) family (Chapman and Estelle, 2009).

At low concentrations of auxin, transcriptional repressors of the AUXIN/INDOLE-3-ACETIC ACID (Aux/IAA) family interact with ARFs and prevent them from inducing transcription of their target genes (Mockaitis and Estelle, 2008). At higher concentrations of auxin, nuclear-localized TRANSPORT INHIBITOR RESPONSE1/AUXIN SIGNALING F-

BOX PROTEIN (TIR1/AFB) receptor complexes bind auxin and thereby associate with Aux/IAAs, directing them to degradation by the 26S proteasome. Degradation of AUX/IAAs releases ARFs from inhibition, thus allowing them to induce transcription of their target genes, including *AUX/IAAs*. While this model of auxin-dependent, ARF-mediated activation of gene expression has been well characterized, it is certainly an over-simplification because it only explains the function of those ARFs that contain a transcriptional activation domain and not the function of those ARFs that act as repressors of transcription (Guilfoyle and Hagen, 2007).

Two pieces of evidence suggests that auxin signaling is required for vein formation: (1) veins form along expression domains of targets of activating ARFs and domains of activity of synthetic auxin-responsive promoters that contain binding sites for activating ARFs (Donner et al., 2009; Mattsson et al., 2003); (2) mutations in genes that encode auxin signaling components leads to the formation of fewer and incompletely differentiated veins (Alonso-Peral et al., 2006; Candela et al., 1999; Esteve-Bruna et al., 2013; Hardtke and Berleth, 1998; Przemeck et al., 1996; Strader et al., 2008).

1.5 Scope and outline of the thesis

The scope of my M.Sc. thesis was to understand the contribution of auxin transport and signaling to vein patterning in *Arabidopsis* leaves.

The evidence discussed above suggests that auxin induces the polar formation of veins and that such inductive and orienting property of auxin strictly depends on the function of *PIN1* and possibly other *PIN* genes. How auxin precisely controls *PIN* function and derived polar formation of veins is unclear, but the current hypothesis is that the GNOM (GN) guanine-nucleotide exchange factor for ADP-ribosylation-factor GTPases, which regulates vesicle formation in membrane trafficking, coordinates the cellular localization of PIN proteins between cells (Steinmann et al., 1999); the resulting cell-to-cell, polar transport of auxin would coordinate PIN polarity between auxin-transporting cells and control polar developmental processes such as vein formation (reviewed in, e.g., (Berleth et al., 2000; Richter et al., 2010; Nakamura et al., 2012; Linh et al., 2018)). In Chapter 2, we tested this

hypothesis. Contrary to predictions of the hypothesis, we found that auxin-induced polar vein-formation occurs in the absence of PIN proteins or any known intercellular auxin transporter, that the residual auxin-transport-independent vein-patterning activity relies on auxin signaling, and that GN controls both auxin transport and signaling to induce vein formation.

Whereas mechanisms by which GN may control PIN polarity and derived polar auxin transport have been suggested (reviewed in (Richter et al., 2010; Luschnig and Vert, 2014); see also (Naramoto et al., 2014) and references therein), it is unclear how GN could control auxin signaling, which takes place in the nucleus and is inherently non-polar (reviewed in (Leyser, 2018)). The most parsimonious account is that auxin signaling leads to the production of proteins which control vein patterning and whose localization is controlled by GN. In Chapter 3, we tested this hypothesis and identified four putative candidates for such proteins.

The identification of putative candidate proteins which are targets of auxin signaling, which control vein patterning and whose localization is controlled by GN required gene misexpression by different promoters. This imposed the burden of generating different constructs for different gene and promoter combinations. This approach could be simplified if GAL4/GFP enhancer-trap lines existed in Columbia-0, the genotype of reference in Arabidopsis (Koorneef and Meinke, 2010), with which to drive expression of genes of interest in desired cells and tissues of developing leaves. Unfortunately, such lines are not available. In Chapter 4, we addressed this limitation and provided GAL4/GFP enhancer-trap lines in the Col-0 background of Arabidopsis for the identification and manipulation of cells and tissues in developing leaves. The canalization hypothesis was originally formulated to account for the formation of vascular strands in plant tissues that had been wounded and/or to which auxin had been applied (Sachs, 1968; Sachs, 1981). All modern interpretations of the hypothesis assume that PIN proteins are essential to auxin-induced vein formation (e.g., (Hartmann et al; Alim and Frey, 2010; Runions et al., 2014; Cieslak et al., 2015)). As such, our findings in Chapter 2 seem to challenge the canalization hypothesis. In Chapter 5, we discuss whether accounts can be proposed to reconcile our findings with the hypothesis.

Chapter 2: Coordination of tissue cell polarity by auxin transport and signaling

2.1 Introduction

How the polarity of the cells in a tissue is coordinated is a central question in biology. In animals, the coordination of this tissue cell polarity requires direct cell-cell communication and often cell movements (Goodrich and Strutt, 2011), both of which are precluded in plants by a wall that holds cells in place; therefore, tissue cell polarity is coordinated by a different mechanism in plants.

Plant veins are an expression of coordinated tissue cell polarity (Sachs, 1991b; Sachs, 2000; Boutte et al., 2007; Nakamura et al., 2012). This is reflected in the relation between the parts of the vein, and between the veins and the parts of the plant: vascular elements are elongated along the length of the vein and are connected to one another at their ends (Esau, 1942), and veins primarily connect shoot organs with roots (Dengler, 2006); therefore, veins and their elements are unequal at their ends — one end connects to shoot tissues, the other to root tissues — and are thus polar (Sachs, 1975). Not all the veins in closed networks such as those of *Arabidopsis* (*Arabidopsis thaliana* (L.) Heynh) leaves have unambiguous shoot-to-root polarity, but the vein networks themselves are polar (Sachs, 1975).

Just as veins are an expression of coordinated tissue cell polarity, their formation is an expression of coordination of tissue cell polarity; this is most evident in developing leaves. Consider, for example, the formation of the midvein at the centre of the cylindrical leaf primordium. Initially, the plasma-membrane (PM)-localized PIN-FORMED1 (PIN1) protein of *Arabidopsis* (Galweiler et al., 1998), which catalyzes cellular efflux of the plant signal auxin (Petrasek et al., 2006), is expressed in all the inner cells of the leaf primordium (Benkova et al., 2003; Reinhardt et al., 2003; Heisler et al., 2005; Scarpella et al., 2006; Wenzel et al., 2007; Bayer et al., 2009; Verna et al., 2015); over time, however, PIN1 expression becomes gradually restricted to the file of cells that will form the midvein. PIN1 localization at the PM of the inner cells is initially isotropic, or nearly so, but as PIN1

expression becomes restricted to the site of midvein formation, PIN1 localization becomes polarized: in the cells surrounding the developing midvein, PIN1 localization gradually changes from isotropic to medial, i.e. toward the developing midvein, to mediobasal; and in the cells of the developing midvein, PIN1 becomes uniformly localized toward the base of the leaf primordium, where the midvein will connect to the pre-existing vasculature. Both the restriction of PIN1 expression and the polarization of PIN1 localization initiate and proceed away from pre-existing vasculature and are thus polar.

The correlation between (1) coordination of tissue cell polarity, as expressed by the coordination of PIN1 polar localization between cells, (2) polar auxin transport, as expressed by the auxin-transport-polarity-defining localization of PIN1 (Wisniewska et al., 2006), and (3) the polar formation of veins, themselves polar, does not seem to be coincidental. Auxin application to developing leaves induces the formation of broad expression domains of isotropically localized PIN1; such domains become restricted to the sites of auxin-induced vein formation, and PIN1 localization becomes polarized toward the pre-existing vasculature (Scarpella et al., 2006). Both the restriction of PIN1 expression domains and the polarization of PIN1 localization are delayed by chemical inhibition of auxin transport (Scarpella et al., 2006; Wenzel et al., 2007), which induces vein pattern defects similar to, though stronger than, those of *pin1* mutants (Mattsson et al., 1999; Sieburth, 1999; Sawchuk et al., 2013).

Therefore, available evidence suggests that auxin coordinates tissue cell polarization to induce polar-vein-formation, and it seems that such coordinative and inductive property of auxin strictly depends on the function of *PIN1* and possibly other *PIN* genes. How auxin precisely coordinates tissue cell polarity to induce polar-vein-formation is unclear, but the current hypothesis is that the GNOM (GN) guanine-nucleotide exchange factor for ADP-ribosylation-factor GTPases, which regulates vesicle formation in membrane trafficking, controls the cellular localization of PIN1 and other PIN proteins; the resulting cell-to-cell, polar transport of auxin would coordinate tissue cell polarity and control polar developmental processes such as vein formation (reviewed in, e.g., (Berleth et al., 2000; Richter et al., 2010; Nakamura et al., 2012; Linh et al., 2018)). Here we tested this hypothesis by a combination of cellular imaging, molecular genetic analysis and chemical induction and inhibition.

Contrary to predictions of the hypothesis, we found that auxin-induced polar-vein-formation occurs in the absence of PIN proteins or any known intercellular auxin transporter; that auxin-transport-independent vein-patterning activity relies on auxin signaling; and that a GN-dependent tissue-cell-polarizing signal acts upstream of both auxin transport and signaling.

2.2 RESULTS

2.2.1 Contribution of the *GNOM* gene to coordination of tissue cell polarity during *Arabidopsis* vein formation

The current hypothesis of how auxin coordinates tissue cell polarity to induce polar-vein-formation proposes that the GNOM (GN) guanine-nucleotide exchange factor for ADP-ribosylation-factor GTPases, which regulates vesicle formation in membrane trafficking, controls the cellular localization of PIN1; the resulting cell-to-cell, polar transport of auxin would coordinate cell polarity between cells, and control polar developmental processes such as vein formation (reviewed in, e.g., (Berleth et al., 2000; Richter et al., 2010; Nakamura et al., 2012; Linh et al., 2018)). As such, the hypothesis predicts that the restriction of PIN1 expression domains and coordination of PIN1 polar localization that normally occur during vein formation (Benkova et al., 2003; Reinhardt et al., 2003; Heisler et al., 2005; Scarpella et al., 2006; Wenzel et al., 2007; Bayer et al., 2009; Sawchuk et al., 2013; Marcos and Berleth, 2014; Verna et al., 2015) would occur abnormally, or fail to occur altogether, during *gn*-mutant leaf development.

We first tested this prediction by imaging expression domains of PIN1::PIN1:YFP (PIN1:YFP fusion protein expressed by the PIN1 promoter (Xu et al., 2006)) in WT and in the new strong allele *gn-13* (Table 2.1) during first-leaf development.

Consistent with previous reports (Benkova et al., 2003; Reinhardt et al., 2003; Heisler et al., 2005; Scarpella et al., 2006; Wenzel et al., 2007; Bayer et al., 2009; Sawchuk et al., 2013; Marcos and Berleth, 2014; Verna et al., 2015), in WT leaves PIN1::PIN1:YFP was expressed in all the cells at early stages of tissue development; over time, epidermal expression became restricted to the basal-most cells and inner tissue expression became restricted to files of vascular cells (Fig 2.1A–J).

Table 2.1. Origin and nature of lines

Line	Origin/Nature
PIN1::PIN1:YFP	(Xu et al., 2006)
<i>gn-13</i>	ABRC; SALK_045424 (Alonso et al., 2003); contains a T-DNA insertion after +2835 of <i>GN</i> (AT1G13980)
PIN1::PIN1:GFP	(Benkova et al., 2003)
<i>gn-18</i>	ABRC; SALK_026031; contains a T-DNA insertion after -1047 of <i>GN</i> (AT1G13980)
<i>fwr (gn^{fwr})</i>	(Okumura et al., 2013)
<i>gn^{B/E}</i>	(Geldner et al., 2004)
<i>gn^{R5}</i>	(Geldner et al., 2004)
<i>van7/emb30-7 (gn^{van7})</i>	(Koizumi et al., 2000)
<i>gn^{van7+fwr}</i>	<i>gn^{van7}</i> (-2127 to +5388; primers: ‘GN Fwd NotI’ and ‘GN Rev NotI’) containing the <i>fwr</i> mutation (primers: ‘fwr-mutagenesis F’ and ‘fwr-mutagenesis R’)
<i>gn^{SALK_103014}</i>	ABRC; (Okumura et al., 2013)
<i>emb30-8 (gn^{emb30-8})</i>	ABRC; (Franzmann et al., 1989; Moriwaki et al., 2013)
PIN2::PIN2:GFP	(Xu and Scheres, 2005)
PIN3::PIN3:GFP	(Zadnikova et al., 2010)
PIN4::PIN4:GFP	(Bennett et al., 2016; Belteton et al., 2018)
PIN7::PIN7:GFP	(Belteton et al., 2018)
<i>pin1-1</i>	ABRC; WT at the TTG1 (AT5G24520) locus (Goto N, 1987; Galweiler et al., 1998; Sawchuk et al., 2013)
<i>pin1-134</i>	Derived from <i>Atpin1::En134</i> (Galweiler et al., 1998); contains a 4-bp (AATT) insertion between +134 and +135 of <i>PIN1</i> (AT1G73590), resulting in a stop codon after amino acid 62.
<i>pin3-3</i>	(Friml et al., 2002b)

<i>pin4-2</i>	(Friml et al., 2002a)
<i>pin7^{En}</i>	(Blilou et al., 2005)
<i>eir1-1 (pin2)</i>	ABRC; (Roman et al., 1995; Luschnig et al., 1998)
<i>toz-1</i>	(Griffith et al., 2007)
<i>mp^{G12}</i>	(Hardtke and Berleth, 1998)
<i>pin6</i>	ABRC; (Sawchuk et al., 2013)
<i>pin8-1</i>	ABRC; (Bosco et al., 2012)
ABCB1::ABCB1:GFP	(Dhonukshe et al., 2008; Mravec et al., 2008)
ABCB19::ABCB19:GFP	(Dhonukshe et al., 2008; Mravec et al., 2008)
<i>pgp1-100 (abcb1)</i>	ABRC; (Lin and Wang, 2005)
<i>mdr1-101 (abcb19)</i>	ABRC; (Lin and Wang, 2005)
<i>ucu2-4 (twd1)</i>	ABRC; (Perez-Perez et al., 2004)
<i>aux1-21;lax1;2-1;3</i>	(Bainbridge et al., 2008)
<i>aux1-355</i>	ABRC; SALK_020355 (Alonso et al., 2003); contains a T-DNA insertion after +631 of <i>AUX1</i> (AT2G38120)
<i>lax1-064</i>	ABRC; SALK_071064 (Alonso et al., 2003); contains a T-DNA insertion after +814 of <i>LAX1</i> (AT5G01240)
<i>axr1-3</i>	ABRC; (Lincoln et al., 1990)
<i>axr1-12</i>	ABRC; (Lincoln et al., 1990)
<i>axl</i>	ABRC; SAIL_673_C11 (Sessions et al., 2002); contains a T-DNA insertion after +1390 of <i>AXL</i> (AT2G32410)
<i>tir1-1;afb2-3</i>	(Savaldi-Goldstein et al., 2008)
DR5rev::nYFP	(Heisler et al., 2005; Sawchuk et al., 2013)

All gene coordinates are relative to the adenine (position +1) of the start codon.

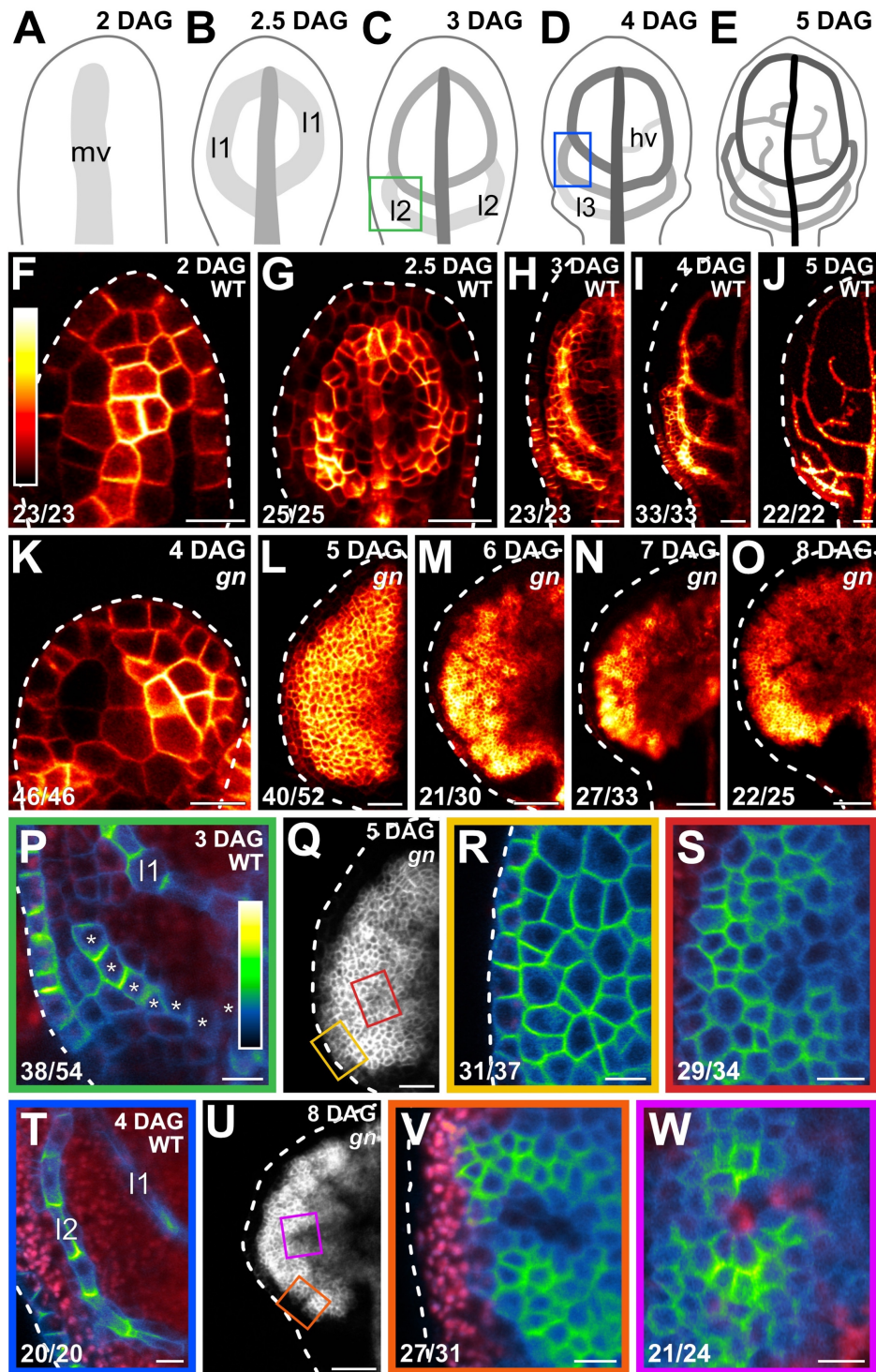


Figure 2.1. Contribution of the *GNOM* gene to coordination of tissue cell polarity during Arabidopsis vein formation. (A–Q,T,U) Top right: leaf age in days after germination (DAG). (A–E) Veins form sequentially during Arabidopsis leaf development:

the formation of the midvein (mv) is followed by the formation of the first loops of veins (“first loops”; l1), which in turn is followed by the formation of second loops (l2) and minor veins (hv) (Mattsson et al., 1999; Sieburth, 1999; Kang and Dengler, 2004; Scarpella et al., 2004). Loops and minor veins differentiate in a tip-to-base sequence during leaf development. Increasingly darker grays depict progressively later stages of vein development. Boxes in C and D illustrate positions of closeups in P and T. l3: third loop. (F–W) Confocal laser scanning microscopy. First leaves. For simplicity, only half-leaves are shown in H–J and L–O. Dashed white line in F–R, T, U and V delineates leaf outline. (F–Q,T,U) Top right: genotype. (F–P,R–T,V,W) Bottom left: reproducibility index. (F–O) PIN1::PIN1:YFP expression; look-up table (ramp in F) visualizes expression levels. (P,R–T,V,W) PIN1::PIN1:GFP expression; look-up table (ramp in P) visualizes expression levels. Red: autofluorescence. Stars in P label cells of the developing second loop. (Q,U) PIN1::PIN1:YFP expression. Boxes in Q and in U illustrate positions of closeups in R and S and in V and W, respectively. Bars: (F,P,R–T,V,W) 10 μm ; (G,I,L,Q) 30 μm ; (H,K) 20 μm ; (J,M–O,U) 60 μm .

In *gn* leaves too, PIN1::PIN1:YFP was expressed in all the cells at early stages of tissue development and over time epidermal expression became restricted to the basal-most cells; however, inner tissue expression failed to become restricted to files of vascular cells and instead remained nearly ubiquitous even at very late stages of leaf development (Fig 2.1K–O).

We next tested the prediction by imaging cellular localization of expression of PIN1::PIN1:GFP (Benkova et al., 2003) in WT and *gn-13* during first-leaf development. Hereafter, we use “basal” to describe localization of PIN1::PIN1:GFP expression oriented toward pre-existing veins, irrespective of how those veins are positioned within a leaf.

Consistent with previous reports (Benkova et al., 2003; Reinhardt et al., 2003; Heisler et al., 2005; Scarpella et al., 2006; Wenzel et al., 2007; Bayer et al., 2009; Sawchuk et al., 2013; Marcos and Berleth, 2014; Verna et al., 2015), in the cells of the second pair of vein loops (“second loop” hereafter) at early stages of its development in WT leaves, PIN1::PIN1:GFP expression was mainly localized to the basal side of the plasma membrane (PM), toward the midvein; in the inner cells flanking the developing loop, PIN1::PIN1:GFP expression was mainly localized to the side of the PM facing the developing loop; and in the inner cells further away from the developing loop, PIN1::PIN1:GFP expression was localized isotropically, or nearly so, at the PM (Fig 2.1C,P). At later stages of second-loop development, by which time PIN1::PIN1:GFP expression had become restricted to the sole, elongated cells of the developing loop, PIN1::PIN1:GFP expression was localized to the basal side of the PM, toward the midvein (Fig 2.1D,T).

At early stages of development of the tissue that in *gn* leaves corresponds to that from which the second loop forms in WT leaves, PIN1::PIN1:GFP was expressed uniformly in the outermost inner tissue and expression was localized isotropically, or nearly so, at the PM (Fig 2.1Q,R). PIN1::PIN1:GFP was expressed more heterogeneously in the innermost inner tissue, but expression remained localized isotropically, or nearly so, at the PM, except in cells near the edge of higher-expression domains (Fig 2.1Q,S); in those cells, localization of PIN1::PIN1:GFP expression at the PM was weakly polar, but such weak cell polarities pointed in seemingly random directions (Fig 2.1Q,S).

At late stages of *gn* leaf development, heterogeneity of PIN1::PIN1:GFP expression had spread to the outermost inner tissue, but expression remained localized isotropically, or nearly so, at the PM, except in cells near the edge of higher-expression domains (Fig 2.1U,V); in those cells, localization of PIN1::PIN1:GFP expression at the PM was weakly polar, but such weak cell polarities pointed in seemingly random directions (Fig 2.1U,V). Heterogeneity of PIN1::PIN1:GFP expression in the innermost inner tissue had become more pronounced at late stages of *gn* leaf development, and the weakly polar localization of PIN1::PIN1:GFP expression at the PM had spread to the center of the higher-expression domains (Fig 2.1U,W); nevertheless, such weak cell polarities still pointed in seemingly random directions (Fig 2.1U,W). Finally, none of the cells had acquired the elongated shape characteristic of vascular cells in WT (Fig 2.1U–W).

In conclusion, consistent with previous observations (Steinmann et al., 1999; Kleine-Vehn et al., 2008), both restriction of PIN1 expression domains and coordination of PIN1 polar localization occur only to a very limited extent or fail to occur altogether during *gn* leaf development, which is consistent with the current hypothesis of how auxin coordinates tissue cell polarity to induce polar-vein-formation.

2.2.2 Contribution of *GN* to vein patterning

We tested whether the very limited or altogether absent restriction of PIN1 expression domains and coordination of PIN1 polar localization occurring during *gn* leaf development (Figure 2.1) were associated with vein pattern defects in mature *gn* leaves.

WT *Arabidopsis* grown under normal conditions forms separate leaves whose vein networks are defined by at least four reproducible features (Telfer and Poethig, 1994; Nelson and Dengler, 1997; Kinsman and Pyke, 1998; Candela et al., 1999; Mattsson et al., 1999; Sieburth, 1999; Steynen and Schultz, 2003; Sawchuk et al., 2013; Verna et al., 2015) (Fig 2.2A,B): (1) a narrow I-shaped midvein that runs the length of the leaf; (2) lateral veins that branch from the midvein and join distal veins to form closed loops; (3) minor veins that branch from midvein and loops and either end freely or join other veins; (4) minor veins and loops that curve near the leaf margin, lending a scalloped outline to the vein network.

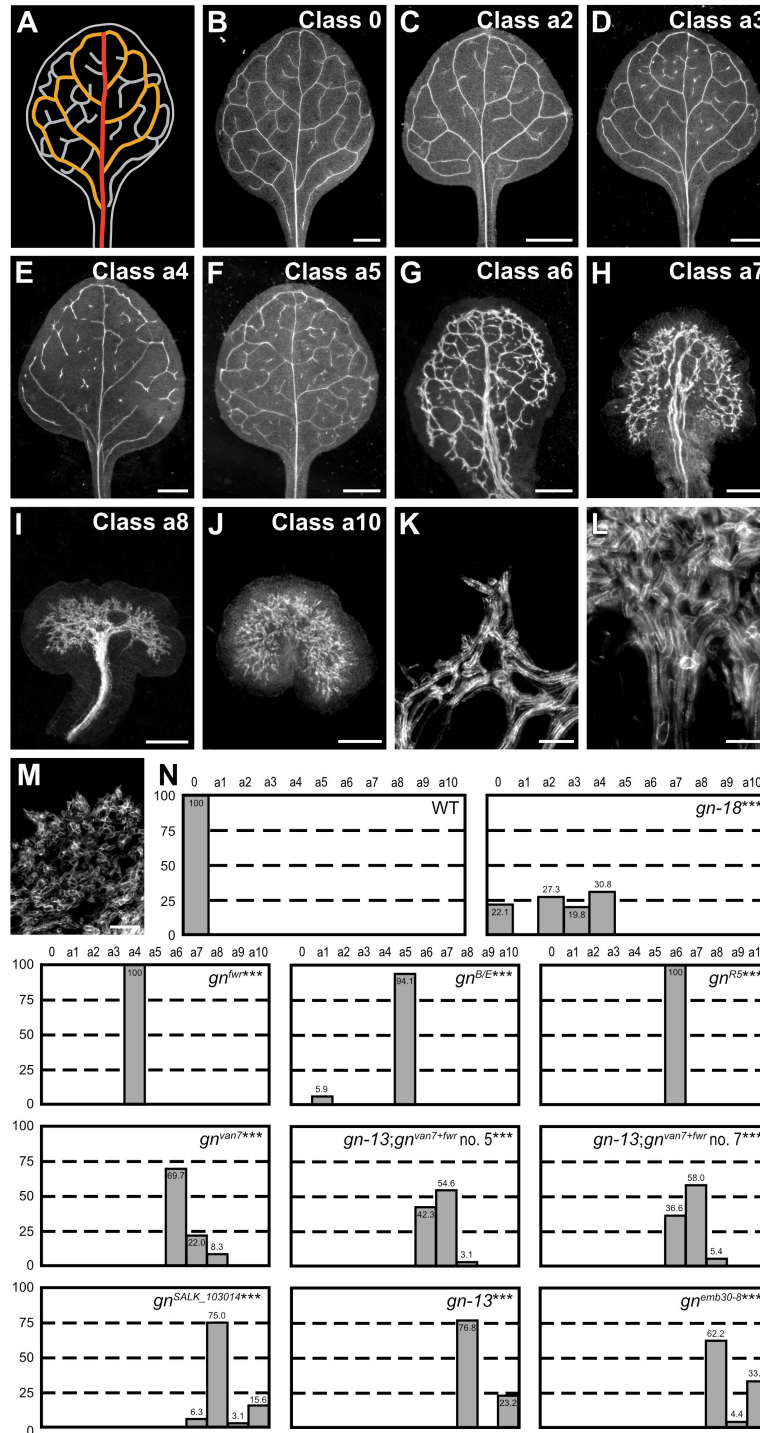


Figure 2.2. Contribution of GN to vein patterning.(A,B) Vein pattern of WT mature first leaf. In A: red, midvein; orange, loops; gray, minor veins. (B–J) Dark-field illumination of mature first leaves illustrating phenotype classes (top right): class 0, narrow I-shaped

midvein and scalloped vein-network outline (B); class a1, dense vein network and apically thickened vein-network outline (not shown); class a2, open vein-network outline (C); class a3, fragmented vein network (D); class a4, open vein-network outline and fragmented vein network (E); class a5, open vein-network outline, fragmented vein network and apically thickened vein-network outline (F); class a6, wide midvein, dense network of thick veins and jagged vein-network outline (G); class a7, dense network of thick veins that fail to join the midvein in the bottom half of the leaf and pronouncedly jagged vein-network outline (H); class a8, wide midvein and shapeless vascular cluster (I); class a9, fused leaves with wide midvein and shapeless vascular cluster (not shown); class a10, shapeless vascular cluster (J). (K–M) Details of vascular clusters illustrating vascular elements uniformly oriented perpendicular to the leaf margin (K) (class a6), vascular elements oriented seemingly randomly at the distal side of the cluster and parallel to the leaf axis at the proximal side of the cluster (L) (classes a8 and a9) and seemingly random orientation of vascular elements (M) (classes a8–a10). (N) Percentages of leaves in phenotype classes. Difference between *gn-18* and WT, between *gn^{fwr}* and WT, between *gn^{B/E}* and WT, between *gn^{R5}* and WT, between *gn^{van7}* and WT, between *gn^{van7+fwr}*; *gn-13* and WT, between *gn^{SALK_103014}* and WT, between *gn-13* and WT and between *emb30-8* and WT was significant at $P < 0.001$ (***) by Kruskal-Wallis and Mann-Whitney test with Bonferroni correction. Sample population sizes: WT, 58; *gn-18*, 172; *gn^{fwr}*, 43; *gn^{B/E}*, 80; *gn^{R5}*, 93; *gn^{van7}*, 109; *gn^{van7+fwr}*; *gn-13* no. 5, 97; *gn^{van7+fwr}*; *gn-13* no. 7, 93; *gn^{SALK_103014}*, 32; *gn-13*, 56; *gn^{emb30-8}*, 45. Bars: (B–F) 1 mm; (G) 0.75 mm; (H,I) 0.5 mm; (J) 0.25 mm; (K–M) 50 μ m.

In ~25% of the leaves of the new weak allele *gn-18* (Table 2.1) (Figure 2.3) closed loops were often replaced by open loops, i.e. loops that contact the midvein or other loops at only one of their two ends (Fig 2.2C,N). Moreover, in ~50% of *gn-18* leaves veins were often replaced by “vein fragments”, i.e. stretches of vascular elements that fail to contact other stretches of vascular elements at either one of their two ends (Fig 2.2D,E,N). Loops were open and veins were fragmented also in the leaves of both *gn^{fwr}* (Okumura et al., 2013) and *gn^{B/E}* (Geldner et al., 2004) (Fig 2.2N). In addition, the vein network of *gn^{B/E}* leaves was denser and its outline was thicker near the leaf tip (Fig 2.2F,N).

The vein network was denser also in all the leaves of *gn^{R5}* (Geldner et al., 2004), in nearly 70% of those of *gn^{van7}* (Koizumi et al., 2000) and in ~40% of those of *gn^{van7+fwr};gn-13* — in which we had combined the *van7* and *fwr* mutations (Table 2.1) (Fig 2.2G,N). However, in the leaves of these backgrounds — unlike in those of *gn^{B/E}* — all the veins were thicker; lateral veins failed to join the midvein but ran parallel to it to form a “wide midvein”; and the vein network outline was jagged because of narrow clusters of vascular elements that were oriented perpendicular to the leaf margin and that were laterally connected by veins (Fig 2.2G,K,N). These features were enhanced in ~20% of the leaves of *gn^{van7}*, in ~55% of those of *gn^{van7+fwr};gn-13* and in ~5% of those of *gn^{SALK_103014}* (Okumura et al., 2013): the vein network was denser, veins failed to join the midvein in the bottom half of the leaf, and the vein network outline was pronouncedly jagged (Fig 2.2H,N). Consistent with previous observations (Shevell et al., 2000), in the few remaining leaves of *gn^{van7}* and *gn^{van7+fwr};gn-13*, and in most of those of *gn^{SALK_103014}*, *gn-13* and *gn^{emb30-8}* (Franzmann et al., 1989; Moriwaki et al., 2014), a central, shapeless vascular cluster was connected with the basal part of the leaf by a wide midvein; and vascular elements were oriented seemingly randomly at the distal side of the cluster and progressively more parallel to the leaf axis toward the proximal side of the cluster (Fig 2.2I,L–N). Finally, in the remaining leaves of *gn^{SALK_103014}*, *gn-13* and *gn^{emb30-8}*, vascular differentiation was limited to a central, shapeless cluster of seemingly randomly oriented vascular elements (Fig 2.2J,M,N).

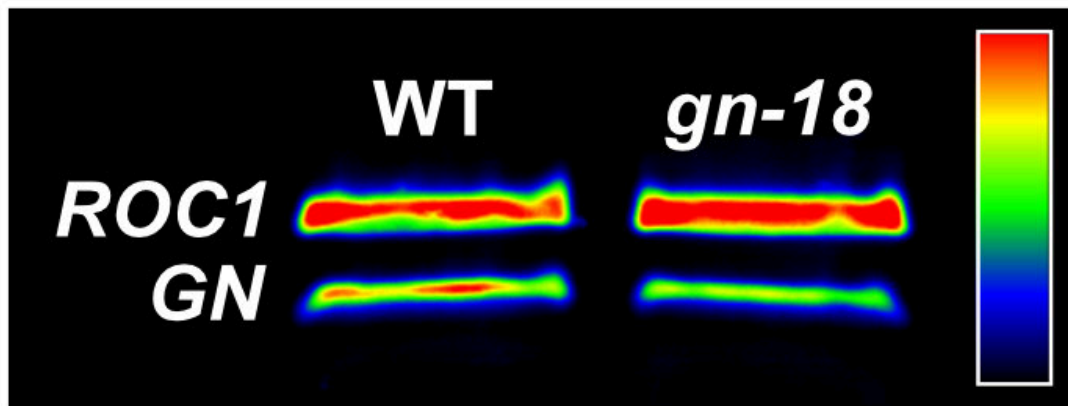


Figure 2.3. Effect of the *gn-18* mutation on *GN* expression. RT-PCR analysis of *GN* expression in 4-day-old seedlings of wild type and *gn-18*. The nearly evenly expressed *ROC1* (Lippuner et al., 1994) was used as control. Look-up table visualizes expression levels.

We conclude that defects in coordination of PIN1 polar localization and possible derived defects in polar auxin transport during *gn* leaf development are associated with vein pattern defects in mature *gn* leaves.

2.2.3 Contribution of plasma-membrane-localized PIN proteins to vein patterning

Were the vein pattern defects of *gn* the sole result of loss of PIN1-mediated polar auxin-transport induced by defects in coordination of PIN1 polar localization, the vein pattern defects of *gn* would be phenocopied by simultaneous mutation in all the *PIN* genes with function in *PIN1*-dependent vein patterning; we tested whether that were so.

In Arabidopsis, the PIN family of auxin transporters is composed of eight members (Paponov et al., 2005; Krecek et al., 2009; Viaene et al., 2012): PIN5, PIN6 and PIN8, which are primarily localized to the endoplasmic reticulum (ER) (Mravec et al., 2009; Bosco et al., 2012; Ding et al., 2012; Sawchuk et al., 2013); and PIN1, PIN2, PIN3, PIN4 and PIN7 are primarily localized to the plasma membrane (PM) and catalyze cellular auxin efflux (Chen et al., 1998; Galweiler et al., 1998; Luschnig et al., 1998; Muller et al., 1998; Friml et al., 2002a; Friml et al., 2002b; Friml et al., 2003; Petrasek et al., 2006; Yang and Murphy, 2009; Zourelidou et al., 2014). Sequence analysis divides the PM-localized subfamily of PIN (PM-PIN) proteins into three groups: the PIN1 group, the PIN2 group and the PIN3 group, which also contains PIN4 and PIN7 (Krecek et al., 2009; Viaene et al., 2012).

Mutants of *PIN1* are the only *pin* single mutants with vein pattern defects, and the vein pattern defects of double mutants between *pin1* and mutants of *PIN2*, *PIN3*, *PIN4* or *PIN7* are no different from those of *pin1* single mutants (Sawchuk et al., 2013), suggesting that either *PIN2*, *PIN3*, *PIN4* and *PIN7* have no function in *PIN1*-dependent vein patterning or their function in this process is redundant. To discriminate between these possibilities, we first assessed the collective contribution to *PIN1*-dependent vein patterning of the *PM-PIN* genes of the *PIN3* group (*PIN3*, *PIN4* and *PIN7*), whose translational fusions to GFP (Zadnikova et al., 2010; Bennett et al., 2016; Belteton et al., 2018) (Table 2.1) are all expressed — as are translational fusions of PIN1 to GFP (Benkova et al., 2003; Heisler et al.,

2005; Scarpella et al., 2006; Wenzel et al., 2007; Bayer et al., 2009; Marcos and Berleth, 2014) — in both epidermal and inner cells of the developing leaf (Fig 2.4A,C–E).

Consistent with previous reports (Sawchuk et al., 2013; Verna et al., 2015), the vein patterns of most of the *pin1* leaves were abnormal (Fig 2.4F,G,L). *pin3;pin4;pin7* (*pin3;4;7* hereafter) embryos were viable and developed into seedlings (Table 2.2) whose vein patterns were no different from those of WT (Fig 2.4L). *pin1,3;4;7* embryos were viable (Table 2.3) and developed into seedlings (Table 2.4) that were smaller than *pin1* seedlings (Fig 2.5A,B). The cotyledon pattern defects of *pin1,3;4;7* were more severe than those of *pin1* (Fig 2.6A–H), and the vein pattern defects of *pin1,3;4;7* were more severe than those of *pin1*: no *pin1,3;4;7* leaf had a WT vein pattern; *pin1,3;4;7* veins were thicker; and ~15% of *pin1,3;4;7* leaves were fused (Fig 2.4H–L). However, as in WT, in *pin1,3;4;7* vascular elements were elongated and aligned along the length of the vein (Fig 2.4J,K).

Next, we tested whether mutation of *PIN2* — whose translational fusion to GFP (Xu and Scheres, 2005) is only expressed in epidermal cells in the developing leaf (Fig 2.4B) — changed the spectrum of vein pattern defects of *pin1,3;4;7*.

pin2;3;4;7 embryos were viable and developed into seedlings (Table 2.2) whose vein patterns were no different from those of WT (Fig 2.4L). *pin1,3;2;4;7* embryos were viable (Table 2.3) and developed into seedlings (Table 2.4) whose vein pattern defects were no different from those of *pin1,3;4;7* (Fig 2.4L). The cotyledon pattern defects of *pin1,3;2;4;7* were more severe than those of *pin1,3;4;7* (Fig 2.6A–H), but the size of *pin1,3;2;4;7* seedlings was similar to that of *pin1,3;4;7* seedlings (Fig 2.5A–C).

In conclusion, the *PIN3* group of *PM-PIN* genes (*PIN3*, *PIN4* and *PIN7*) provides no nonredundant function in vein patterning, but it contributes to *PIN1*-dependent vein patterning; *PIN1* and the *PIN3* group of *PM-PIN* genes redundantly restrict vascular differentiation to narrow zones; and *PIN2* seems to have no function in any of these processes. Most important, loss of *PM-PIN* function fails to phenocopy the vein pattern defects of *gn*.

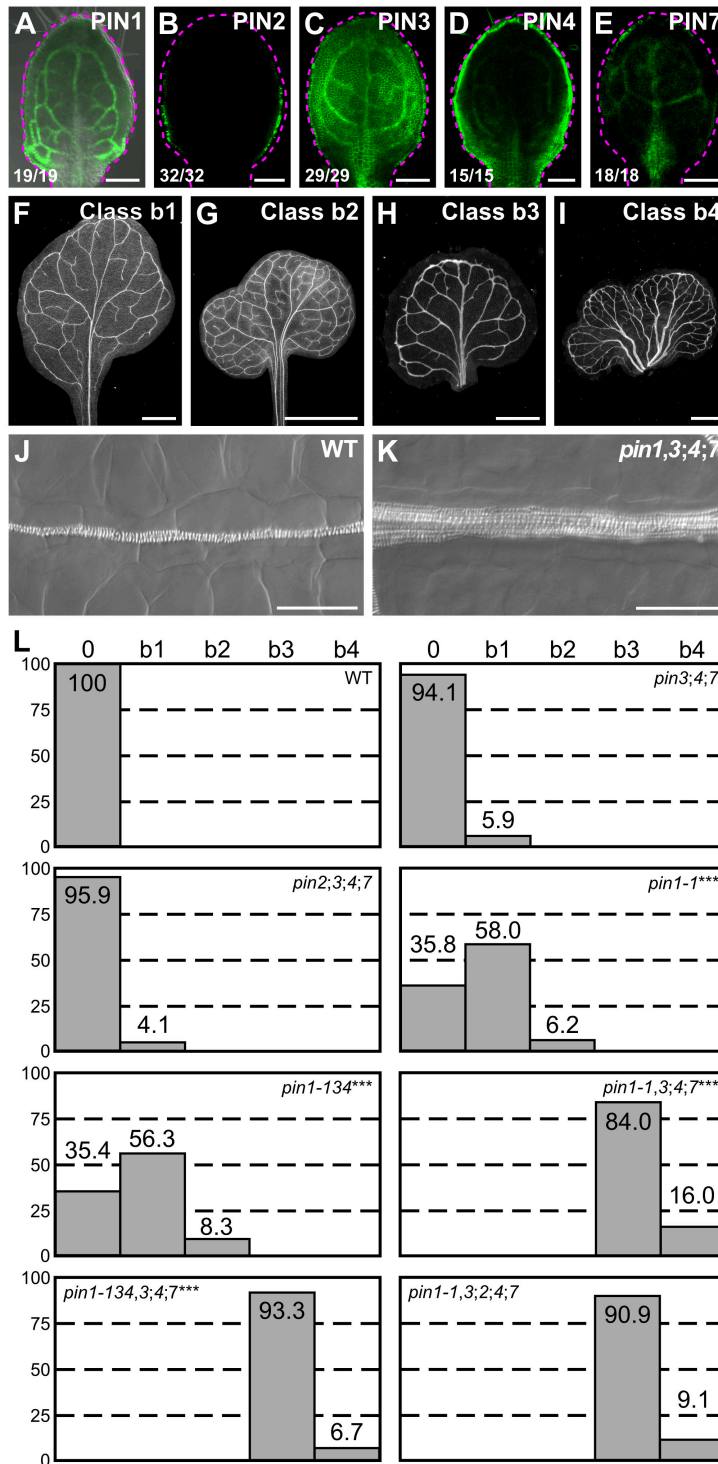


Figure 2.4. Contribution of plasma-membrane-localized PIN proteins to vein patterning. (A–K) Top right: expression-reported gene, phenotype class or genotype. (B–E) Bottom left: reproducibility index. (A–E) Confocal laser scanning microscopy with (A) or

without (B–E) transmitted light; 4-day-old first leaves. Dashed magenta line delineates leaf outline. (A) PIN1::PIN1:GFP expression. (B) PIN2::PIN2:GFP expression. (C) PIN3::PIN3:GFP expression. (D) PIN4::PIN4:GFP expression. (E) PIN7::PIN7:GFP expression. (F–I) Dark-field illumination images of mature first leaves illustrating phenotype classes: class b1, Y-shaped midvein and scalloped vein-network outline (F); class b2, fused leaves with scalloped vein-network outline (G); class b3, thick veins and scalloped vein-network outline (H); class b4, fused leaves with thick veins and scalloped vein-network outline (I). (J,K) Differential interference images of details of WT (J) or *pin1-1,3;4;7* (K) illustrating normal (classes 0, b1 and b2) or thick (classes b3 and b4) veins, respectively. (L) Percentages of leaves in phenotype classes. Difference between *pin1-1* and WT, between *pin1-134* and WT, between *pin1-1,3;4;7* and *pin1-1*, and between *pin1-134,3;4;7* and *pin1-134* was significant at $P < 0.001$ (***) by Kruskal-Wallis and Mann-Whitney test with Bonferroni correction. Sample population sizes: WT, 58; *pin2;3;4;7*, 49; *pin3;4;7*, 102; *pin1-1*, 81; *pin1-134*, 48; *pin1-1,3;4;7*, 75; *pin1-134,3;4;7*, 45; *pin1-1,3;2;4;7*, 99. Bars: (A–E) 0.1 mm; (F–H) 1 mm; (I) 5 mm; (J,K) 50 μm .

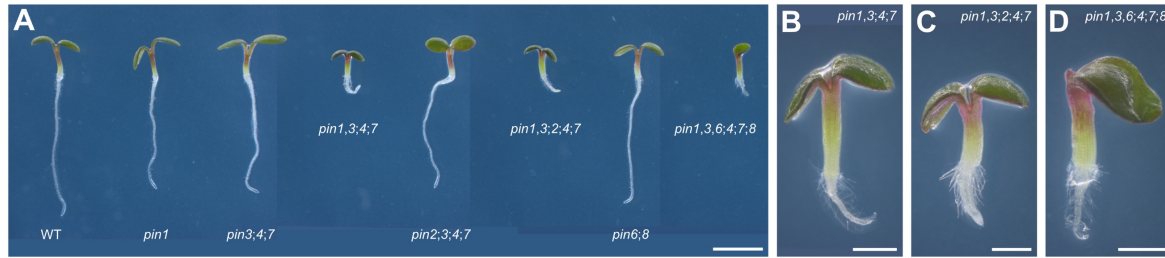


Figure 2.5. *pin* mutant seedlings. (A–D) Dark-field illumination composite of 3-day-old seedlings; genotypes below respective seedlings (A) or top right (B–D). (A) Overview. Because the seedling lineup was wider than the stereomicroscope’s field of view, overlapping images of parts of the lineup were acquired and combined to reconstruct the original lineup. (B–D) Details. Bars: (A) 2 mm; (B–D) 0.5 mm.

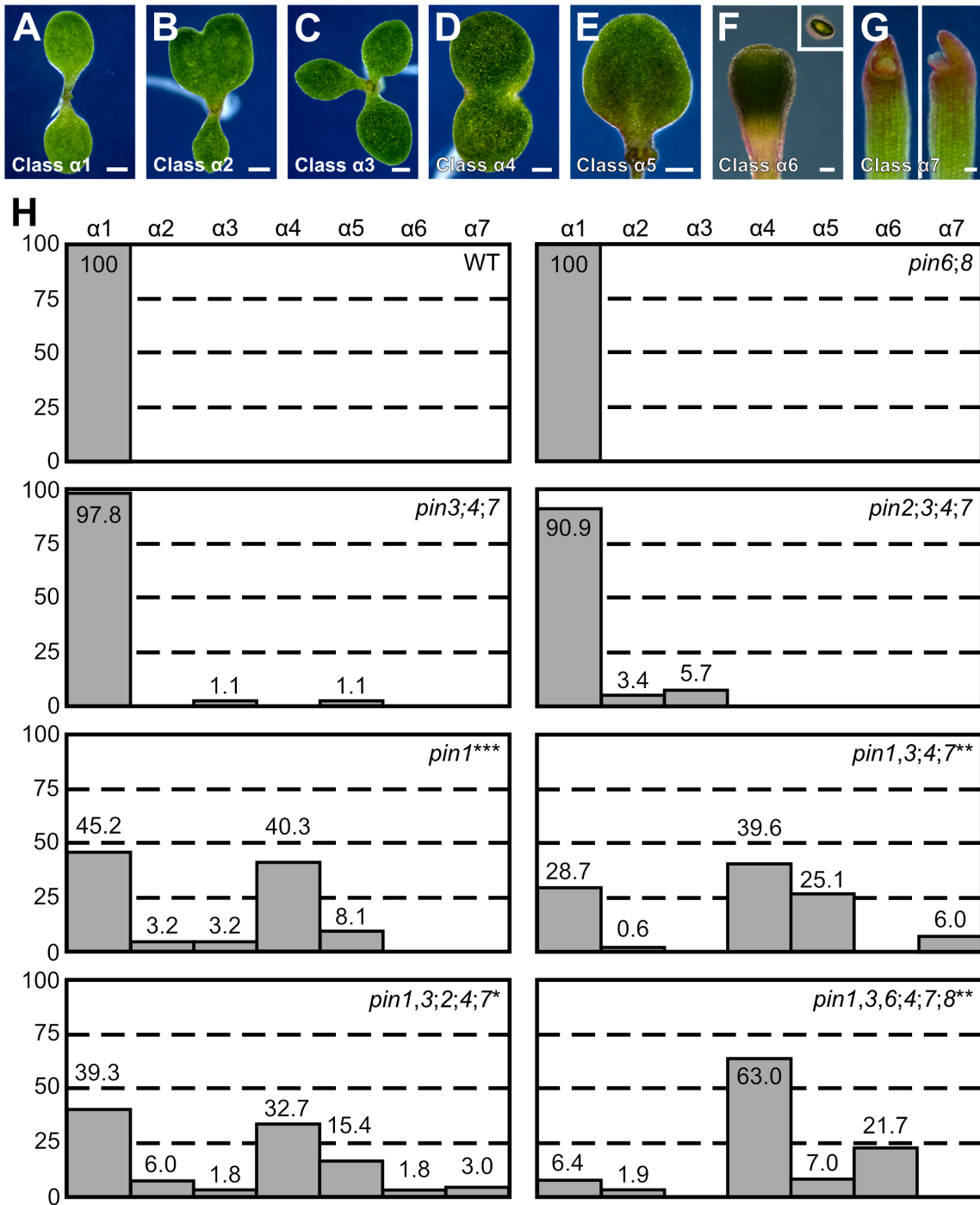


Figure 2.6. Cotyledon patterns of *pin* mutants. (A–G) Dark-field illumination of 3-day-old seedlings illustrating phenotype classes (bottom left): class α_1 , two separate cotyledons (A); class α_2 , fused cotyledons and separate single cotyledon (B); class α_3 , three separate cotyledons (C); class α_4 , fused cotyledons (D); class α_5 , single cotyledon (E); class α_6 , cup-

shaped cotyledon, side view (inset: top view) (F); class $\alpha 7$, small, hood-like outgrowth (G: left, front view; right, side view). (H) Percentages of seedlings in phenotype classes. Difference between *pin1-1* and WT was significant at $P < 0.001$ (***) , between *pin1-1,3;4;7* and *pin1-1* and between *pin1-1,3,6;4;7;8* and *pin1-1* was significant at $P < 0.01$ (**) and between *pin1-1,3;2;4;7* and *pin1-1,3;4;7* was significant at $P < 0.05$ (*) by Kruskal-Wallis and Mann-Whitney test with Bonferroni correction. Sample population sizes: WT, 58; *pin3;4;7*, 55; *pin2;3;4;7*, 55; *pin6;8*, 50; *pin1-1,3;4;7*, 76; *pin1-1,3;2;4;7*, 80; *pin1-1,3,6;4;7;8*, 65. Bars: (A–E) 0.5 mm; (F) 0.25 mm; (G) 0.2 mm.

Table 2.2. Embryo viability of WT, *pin3;4;7* and *pin2;3;4;7*

Genotype of self-fertilized parent	Proportion of viable embryos in siliques of self-fertilized parent (no. of non-aborted seeds / total no. of seeds)	Percentage of viable seeds in siliques of self-fertilized parent
WT	293/293	100
<i>pin3/pin3;pin4/pin4;pin7/pin7</i>	275/276	99.6
<i>pin2/pin2;pin3/pin3;pin4/pin4;pin7/pin7</i>	271/271	100

Difference between *pin3;4;7* and WT and between *pin2;3;4;7* and WT was not significant by Kruskal-Wallis and Mann-Whitney test with Bonferroni correction.

Table 2.3. Embryo viability of *toz*, *mp*, *pin1*, *pin1,3;4;7*, *pin1,3;2;4;7* and *pin1,3,6;4;7;8*

Genotype of self-fertilized parent	Proportion of viable embryos in siliques of self-fertilized parent (no. of non-aborted seeds / total no. of seeds)	Percentage of viable seeds in siliques of self-fertilized parent
<i>TOZ/toz-1</i>	202/278	72.7
<i>MP/mp</i> ^{G12}	264/265***	99.6
<i>PIN1/pin1-1</i>	254/260***	97.7
<i>PIN1/pin1-134</i>	257/258***	99.6
<i>PIN1/pin1-1,pin3/pin3;pin4/pin4;pin7/pin7</i>	269/272***	98.9
<i>PIN1/pin1-134,pin3/pin3;pin4/pin4;pin7/pin7</i>	280/281***	99.6
<i>PIN1/pin1-1,pin3/pin3;pin2/pin2;pin4/pin4;pin7/pin7</i>	276/278***	99.3
<i>PIN1/pin1-1,pin3/pin3,pin6/pin6;pin4/pin4;pin7/pin7;pin8/pin8</i>	266/268***	99.2

Difference between negative control for completely penetrant embryo lethality (*mp*^{G12}) and positive control for completely penetrant embryo lethality (*toz-1*), between *pin1-1* and *toz-1*, between *pin1-134* and *toz-1*, between *pin1-1,3;4;7* and *toz-1*, between *pin1-134,3;4;7* and *toz-1*, between *pin1-1,3;2;4;7* and *toz-1* and between *pin1-1,3,6;4;7;8* and *toz-1* was significant at $P < 0.001$ (***) by Kruskal-Wallis and Mann-Whitney test with Bonferroni correction. Difference between *pin1-1* and *mp*^{G12}, between *pin1-134* and *mp*^{G12}, between *pin1-1,3;4;7* and *mp*^{G12}, between *pin1-134,3;4;7* and *mp*^{G12}, between *pin1-1,3;2;4;7* and *mp*^{G12} and between *pin1-1,3,6;4;7;8* and *mp*^{G12} was not significant by Kruskal-Wallis and Mann-Whitney test with Bonferroni correction.

Table 2.4. Embryo viability of *pin1*, *pin1,3;4;7*, *pin1,3;2;4;7* and *pin1,3,6;4;7;8*

Genotype of self-fertilized parent	Proportion of embryo-viable mutants in progeny of self-fertilized parent (no. of mutant seedlings / total no. of seedlings)	Percentage of embryo-viable mutants in progeny of self-fertilized parent
<i>PIN1/pin1-1</i>	66/239	27.6
<i>PIN1/pin1-134</i>	53/227	23.3
<i>PIN1/pin1-1,pin3/pin3;pin4/pin4;pin7/pin7</i>	52/196	26.5
<i>PIN1/pin1-1-134,pin3/pin3;pin4/pin4;pin7/pin7</i>	56/228	24.6
<i>PIN1/pin1-1,pin3/pin3;pin2/pin2;pin4/pin4;pin7/pin7</i>	61/263	23.2
<i>PIN1/pin1-1,pin3/pin3,pin6/pin6;pin4/pin4;pin7/pin7;pin8/pin8</i>	65/260	25.0

Difference between observed and theoretical frequency distributions of embryo-viable mutants in the progeny of self-fertilized heterozygous parents was not significant by Pearson's chi-squared (χ^2) goodness-of-fit test ($\alpha=0.05$, dF=1).

2.2.4 Contribution of *PIN* genes to vein patterning

Expression and genetic analyses suggest that PIN1, PIN3, PIN4 and PIN7 redundantly define a single auxin-transport pathway with vein patterning functions whose loss fails to phenocopy the vein pattern defects of *gn* (Figure 2.2; Figure 2.4). The ER-localized PIN (ER-PIN) proteins PIN6 and PIN8, but not the ER-PIN protein PIN5, define a distinct auxin-transport pathway with vein patterning functions that overlap with those of *PIN1* (Sawchuk et al., 2013; Verna et al., 2015). We tested what the collective contribution of these two auxin-transport pathways were to vein patterning and whether simultaneous mutation in all the *PIN* genes with vein patterning function phenocopied the vein pattern defects of *gn*.

As previously reported (Sawchuk et al., 2013), the vein pattern of *pin6;8* was no different from that of WT (Fig. 2.7C). *pin1,3,6;4;7;8* embryos were viable (Table 2.3) and developed into seedlings (Table 2.4) whose vein patterns differed from those of *pin1,3;4;7* in four respects: (1) the vein network comprised more lateral veins; (2) lateral veins failed to join the midvein but ran parallel to it to form a wide midvein; (3) lateral veins ended in a marginal vein that closely paralleled the leaf margin, lending a smooth outline to the vein network; (4) veins were thicker (Figure 2.4; Fig 2.7A–C). Simultaneous mutation of *PIN6* and *PIN8* in the *pin1,3;4;7* background shifted the distribution of *pin1,3;4;7* cotyledon pattern phenotypes toward stronger classes (Fig 2.6A–H), but the size of *pin1,3,6;4;7;8* seedlings was similar to that of *pin1,3;4;7* seedlings (Fig 2.5A,B,D). Because *pin6;8* synthetically enhanced vein pattern defects of *pin1,3;4;7*, we conclude that the auxin-transport pathway mediated by PIN1, PIN3, PIN4 and PIN7 and that mediated by PIN6 and PIN8 provide overlapping functions in vein patterning. Nevertheless, loss of *PIN*-dependent vein patterning function fails to phenocopy the vein pattern defects of *gn*.

2.2.5 Genetic versus chemical inhibition of auxin transport during vein patterning

Loss of *PIN*-dependent vein patterning function fails to phenocopy the vein pattern defects of *gn* (Figure 2.2; Figure 2.7), suggesting that these latter are not the sole result of loss of *PIN*-dependent polar auxin-transport induced by defects in coordination of PIN polar localization.

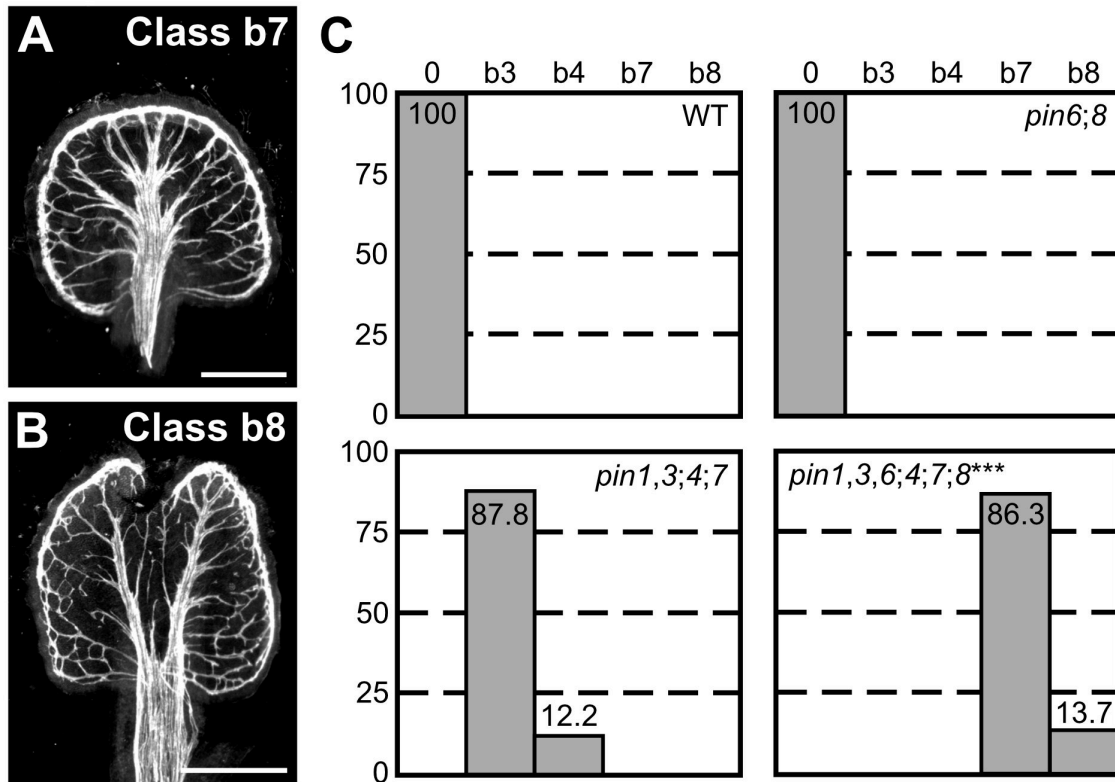


Figure 2.7. Contribution of *PIN* genes to vein patterning. (A,B) Dark-field illumination of mature first leaves illustrating phenotype classes (top right): class b7, wide midvein, more lateral-veins and conspicuous marginal vein (A); class b8, fused leaves with wide midvein, more lateral-veins and conspicuous marginal vein (B). (C) Percentages of leaves in phenotype classes (Classes 0, b3 and b4 defined in Figures 2.2 and 2.4). Difference between *pin1-1,3,6;4;7;8* and *pin1-1,3;4;7* was significant at $P < 0.001$ (***) by Kruskal-Wallis and Mann-Whitney test with Bonferroni correction. Sample population sizes: WT, 51; *pin6;8*, 47; *pin1-1,3;4;7*, 49; *pin1-1,3,6;4;7;8*, 73. Bars: (A,B) 0.5 mm.

However, it is possible that the vein pattern defects of *gn* result from additional or exclusive defects in *PIN*-independent polar auxin-transport pathways; we tested whether that were so.

Cellular auxin efflux is inhibited by a class of structurally related compounds referred to as phytotropins, exemplified by N-1-naphthylphthalamic acid (NPA) (Cande and Ray, 1976; Katekar and Geissler, 1980; Sussman and Goldsmith, 1981). Because PM-PIN proteins catalyze cellular auxin efflux (Chen et al., 1998; Petrasek et al., 2006; Yang and Murphy, 2009; Zourelidou et al., 2014), we first tested whether defects resulting from simultaneous mutation of all the *PM-PIN* genes with vein patterning function were phenocopied by growth of WT in the presence of NPA. To address this question, we compared defects of *pin1,3;4;7* to those induced in WT by growth in the presence of 100 μ M NPA, which is the highest concentration of NPA without toxic, auxin-efflux-unrelated effects (Petrasek et al., 2003; Dhonukshe et al., 2008). Because leaves develop more slowly at this concentration of NPA (Mattsson et al., 1999; Sieburth, 1999), to ensure maximal vascular differentiation we allowed them to grow for four weeks before analysis.

Consistent with previous reports (Mattsson et al., 1999; Sieburth, 1999), NPA only rarely induced leaf fusion in WT (see Fig. 2.9I for one such rare occurrence) but reproducibly induced characteristic vein-pattern defects: (1) the vein network comprised more lateral veins; (2) lateral veins failed to join the midvein but ran parallel to it to form a wide midvein; (3) lateral veins ended in a marginal vein that closely paralleled the leaf margin, lending a smooth outline to the vein network; (4) veins were thicker, though vascular elements were elongated and aligned along the length of the vein (Fig. 2.8A,D,E,H).

By contrast, 20% of *pin1,3;4;7* leaves were fused, and though *pin1,3;4;7* veins were thick, *pin1,3;4;7* vein patterns lacked all the other characteristic defects induced in WT by NPA (Fig. 2.8B,H). However, such defects were induced in *pin1,3;4;7* by NPA (Fig. 2.8F,H), suggesting that this background has residual NPA-sensitive vein-patterning activity. The vein pattern defects induced in WT or *pin1,3;4;7* by NPA were no different from those of *pin1,3,6;4;7;8* (Fig. 2.8C,D–F,H). Because no additional defects were induced in *pin1,3,6;4;7;8* by NPA (Fig. 2.8G,H), the residual NPA-sensitive vein-patterning activity of *pin1,3;4;7* is likely provided by *PIN6* and *PIN8*.

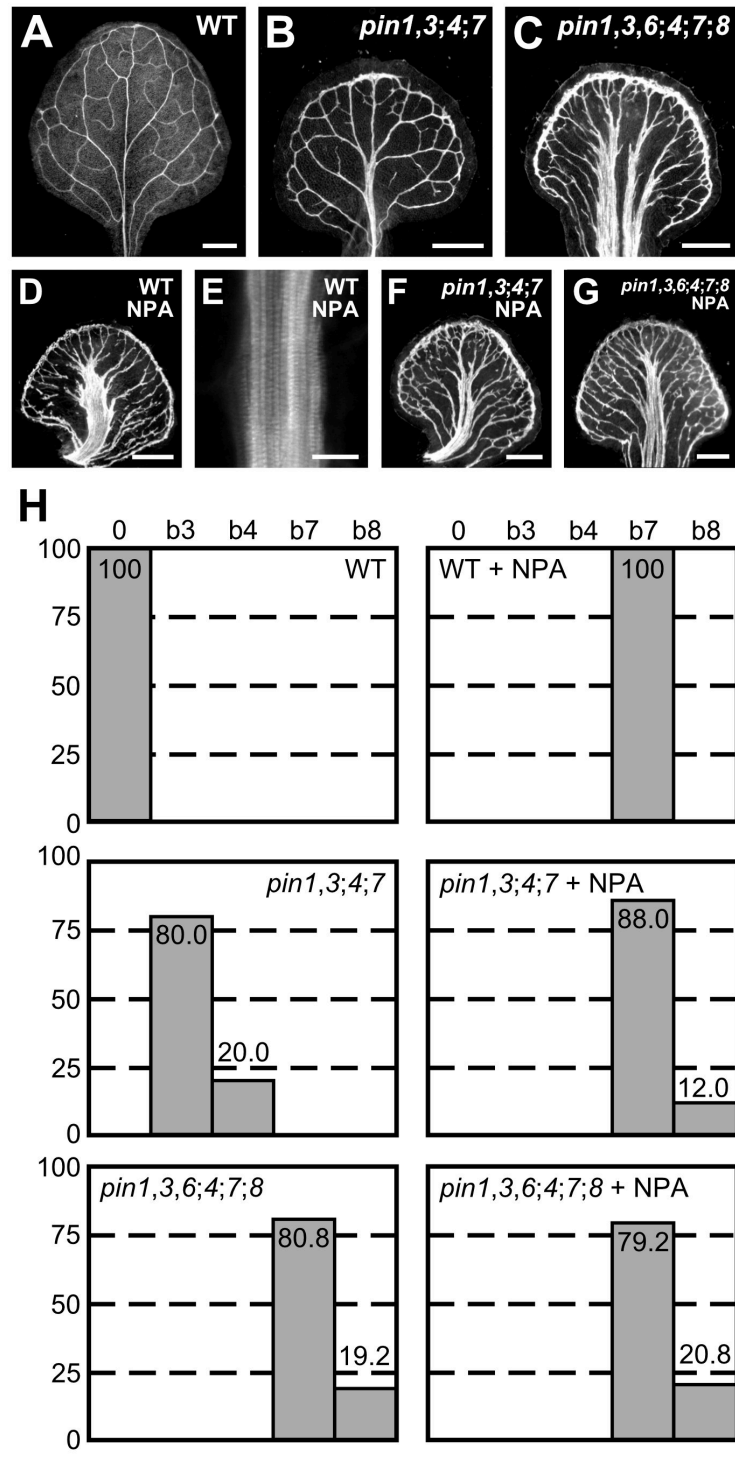


Figure 2.8. Genetic versus pharmacological inhibition of auxin transport. (A–G) Top right: genotype and treatment. (A–G) Dark-field illumination (A–D,F,G) or confocal laser scanning microscopy (E) of mature first leaves. (A) WT. (B) *pin1-1,3,4;7*. (C) *pin1-*

1,3,6;4;7;8. (D) NPA-grown WT. (E) Detail illustrating thick veins in NPA-grown WT (compare with Fig 2.4J). (F) NPA-grown *pin1-1,3;4;7*. (G) NPA-grown *pin1-1,3,6;4;7;8*. (H) Percentages of leaves in phenotype classes (defined in Figures 2.2,2.4,2.7). Sample population sizes: WT, 38; *pin1-1,3;4;7*, 30; *pin1-1,3,6;4;7;8*, 73; NPA-grown WT, 41; NPA-grown *pin1-1,3;4;7*, 58; NPA-grown *pin1-1,3,6;4;7;8*, 48. Bars: (A–D,F,G) 0.5 mm, (E) 25 μ m.

In conclusion, our results suggest that growth in the presence of NPA phenocopies defects of loss of *PIN*-dependent vein patterning function; that in the absence of this function any residual NPA-sensitive vein-patterning activity — if existing — becomes inconsequential; and that loss of neither *PIN*-dependent vein-patterning function nor NPA-sensitive vein-patterning activity phenocopies the vein pattern defects of *gn*.

2.2.6 Contribution of *ABCB* genes to vein patterning

Loss of *PIN*-dependent vein-patterning function or of NPA-sensitive vein-patterning activity fails to phenocopy the vein pattern defects of *gn* (Figure 2.2; Figure 2.8), suggesting that these latter are not the sole result of loss of *PIN*-dependent or NPA-sensitive polar auxin-transport induced by defects in coordination of PIN polar localization. However, it is possible that the vein pattern defects of *gn* result from additional or exclusive defects in another polar auxin-transport pathway; we tested whether that were so.

Cellular auxin efflux is catalyzed not only by PM-PIN proteins but by the PM-localized ATP-BINDING CASSETTE B1 (*ABCB1*) and *ABCB19* proteins (Geisler et al., 2005; Bouchard et al., 2006; Petrasek et al., 2006; Blakeslee et al., 2007; Yang and Murphy, 2009), whose fusions to GFP (Dhonukshe et al., 2008; Mravec et al., 2008) are expressed at early stages of leaf development (Fig. 2.9A,B). We tested whether *ABCB1/19*-mediated auxin efflux were required for vein patterning.

The embryos of *abcb1* and *abcb19* were viable, but ~15% of *abcb1;19* embryos died during embryogenesis (Table 2.5); nevertheless, the vein patterns of *abcb1*, *abcb19* and *abcb1;19* were no different from the vein pattern of WT (Fig. 2.9E,F,I), suggesting that *ABCB1/19*-mediated auxin efflux is dispensable for vein patterning.

Developmental functions of *ABCB1/19*-mediated auxin transport overlap with those of PIN-mediated auxin transport (Blakeslee et al., 2007; Mravec et al., 2008). We therefore tested whether vein pattern defects resulting from simultaneous mutation of *PIN1*, *PIN3* and *PIN6*, or induced in WT by 100 μ M NPA — which phenocopies loss of *PIN*-dependent vein-patterning function (Figure 2.8) — were enhanced by simultaneous mutation of *ABCB1* and *ABCB19*.

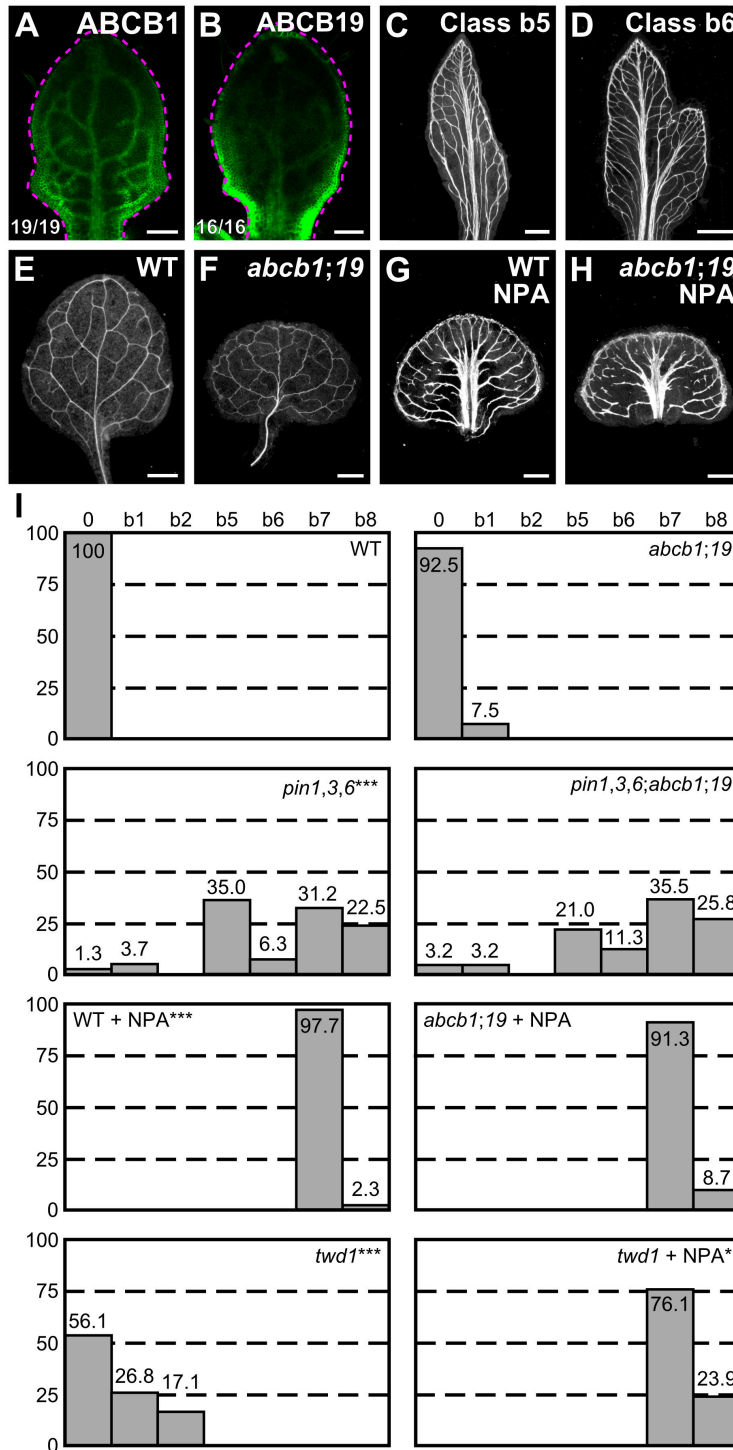


Figure 2.9. Contribution of *ABCB* genes to vein patterning. (A,B,E–H) Top right: expression-reported gene, genotype and treatment. (A–B) Bottom left: reproducibility index. (A–B) Confocal laser scanning microscopy; 5-day-old first leaves. Dashed magenta line

delineates leaf outline. (A) ABCB1::ABCB1:GFP expression. (B) ABCB19::ABCB19:GFP expression. (C–H) Dark-field illumination of mature first leaves. (C,D) Phenotype classes: class b5, thick veins and conspicuous marginal vein (C); class b6, fused leaves with thick veins and conspicuous marginal vein (D). (I) Percentages of leaves in phenotype classes (Classes 0, b1, b2, b7 and b8 defined in Figures 2.2, 2.4 and 2.7). Difference between *pin1-1,3,6* and WT, between *twd1* and WT and between NPA-grown WT and WT was significant at $P < 0.001$ (***) and between NPA-grown *twd1* and NPA-grown WT was significant at $P < 0.05$ (*) by Kruskal-Wallis and Mann-Whitney test with Bonferroni correction. Sample population sizes: WT, 41; *abcb1;19*, 40; *pin1-1,3,6*, 80; *pin1-1,3,6;abcb1;19*, 62; NPA-grown WT, 43; NPA-grown *abcb1;19*, 46; *twd1*, 41; NPA-grown *twd1*, 46. Bars: (A–B) 0.1 mm; (C–H) 0.5 mm.

Table 2.5. Embryo viability of WT, *abcb1*, *abcb19*, *abcb1;19* and *twd1*

Genotype of self-fertilized parent	Proportion of viable embryos in siliques of self-fertilized parent (no. of non-aborted seeds / total no. of seeds)	Percentage of viable seeds in siliques of self-fertilized parent
WT	294/294	100
<i>abcb1/abcb1</i>	269/272	98.9
<i>abcb19/abcb19</i>	271/276	98.2
<i>abcb1/abcb1;abcb19/a bcb19</i>	276/332***	83.1
<i>twd1/twd1</i>	245/265***	92.4

Difference between *abcb1;19* and WT and between *twd1* and WT was significant at $P < 0.001$ (***) and between *abcb1* and WT and between *abcb19* and WT was not significant by Kruskal-Wallis and Mann-Whitney test with Bonferroni correction.

pin1,3,6 embryos were viable (Table 2.6) and developed into seedlings (Table 2.7). The proportion of embryos derived from the self-fertilization of *PIN1,PIN3,PIN6/pin1,pin3,pin6;abcb1/abcb1;abcb19/abcb19* that died during embryogenesis was no different from the proportion of embryos derived from the self-fertilization of *abcb1/abcb1;abcb19/abcb19* that died during embryogenesis (Table 2.6), suggesting no nonredundant functions of *PIN1*, *PIN3* and *PIN6* in *ABCB1/ABCB19*-dependent embryo viability.

Consistent with previous reports (Blakeslee et al., 2007; Mravec et al., 2008), simultaneous mutation of *ABCB1* and *ABCB19* in the *pin1,3,6* background shifted the distribution of *pin1,3,6* cotyledon pattern phenotypes toward stronger classes (Figure 2.10). However, the spectrum of vein pattern phenotypes of *pin1,3,6;abcb1;19* was no different from that of *pin1,3,6*, and the vein pattern defects induced in *abcb1;19* by NPA were no different from those induced in WT by NPA (Fig. 2.9C,D,G–I), suggesting no vein-patterning function of *ABCB1* and *ABCB19* in the absence of function of *PIN1*, *PIN3* and *PIN6* or of NPA-sensitive, *PIN*-dependent vein-patterning function.

ABCB1 and *ABCB19* are members of a large family (Geisler and Murphy, 2006); therefore, vein patterning functions of *ABCB1/19*-mediated auxin efflux might be masked by redundant functions provided by other *ABCB* transporters.

The TWISTED DWARF1/ULTRACURVATA2 (*TWD1/UCU2*; *TWD1* hereafter) protein (Kamphausen et al., 2002; Perez-Perez et al., 2004) is a positive regulator of *ABCB*-mediated auxin transport (Geisler et al., 2003; Bouchard et al., 2006; Bailly et al., 2008; Wu et al., 2010; Wang et al., 2013). Consistent with this observation, defects of *twd1* are more severe than, though similar to, those of *abcb1;19* (Geisler et al., 2003; Bouchard et al., 2006; Bailly et al., 2008; Wu et al., 2010; Wang et al., 2013). We therefore reasoned that analysis of *twd1* vein patterns might uncover vein patterning functions of *ABCB*-mediated auxin transport that could not be inferred from the analysis of *abcb1;19*.

Approximately 25% of *twd1* leaves had Y-shaped midveins and ~15% of *twd1* leaves were fused (Fig. 2.9I), suggesting possible vein-patterning functions of *TWD1*-dependent *ABCB*-

Table 2.6. Embryo viability of *toz*, *mp*, *pin1,3,6* and *pin1,3,6;abcb1;19*

Genotype of self-fertilized parent	Proportion of viable embryos in siliques of self-fertilized parent (no. of non-aborted seeds / total no. of seeds)	Percentage of viable seeds in siliques of self-fertilized parent
<i>TOZ/toz-1</i>	202/277	72.9
<i>MP/mp^{G12}</i>	255/256***	99.6
<i>PIN1/pin1-1,pin3/pin3,PIN6/pin6</i>	263/266***	98.9
<i>PIN1/pin1-1,PIN3/pin3,PIN6/pin6;abcb1/abcb1;abcb19/abcb19</i>	240/284*/***	84.5

Difference between negative control for completely penetrant embryo lethality (*mp^{G12}*) and positive control for completely penetrant embryo lethality (*toz-1*) and between *pin1-1,3,6* and *toz-1* was significant at $P < 0.001$ (***) and between *pin1-1,3,6;abcb1;19* and *toz-1* was significant at $P < 0.05$ (*) by Kruskal-Wallis and Mann-Whitney test with Bonferroni correction. Difference between *pin1-1,3,6;abcb1;19* and *mp^{G12}* was significant at $P < 0.001$ (***) and between *pin1-1,3,6* and *mp^{G12}* was not significant by Kruskal-Wallis and Mann-Whitney test with Bonferroni correction. Linkage in *cis* between *pin1-1* and *pin6* in *PIN1/pin1-1,pin3/pin3,PIN6/pin6* was confirmed by phenotyping the progeny of the self-fertilized *PIN1/pin1-1,pin3/pin3,PIN6/pin6* plants used for the embryo viability analysis for the presence of seedlings with cup-shaped cotyledons, which are characteristic of *pin1,6* double homozygous mutant (Sawchuk et al., 2013). Linkage in *cis* between *pin1-1*, *pin3* and *pin6* in *PIN1/pin1-1,PIN3/pin3,PIN6/pin6;abcb1/abcb1;abcb19/abcb19* was confirmed by phenotyping the progeny of the self-fertilized *PIN1/pin1-1,PIN3/pin3,PIN6/pin6;abcb1/abcb1;abcb19/abcb19* plants used for the embryo viability analysis for the presence of seedlings with cup-shaped cotyledons and by genotyping those cup-shaped-cotyledon seedling for the *pin3* mutation.

Table 2.7. Embryo viability of *pin1,3,6* and *pin1,3,6;abcb1;19*

Genotype of self-fertilized parent	Proportion of embryo-viable mutants in progeny of self-fertilized parent (no. of mutant seedlings / total no. of seedlings)	Percentage of embryo-viable mutants in progeny of self-fertilized parent
<i>PIN1/pin1-1,pin3/pin3,PIN6/pin6</i>	80/361	22.2
<i>PIN1/pin1-1,PIN3/pin3,PIN6/pin6;abcb1/abcb1;abcb19/abcb19</i>	74/335	22.1

Difference between observed and theoretical frequency distributions of embryo-viable mutants in the progeny of self-fertilized heterozygous parents was not significant by Pearson's chi-squared (χ^2) goodness-of-fit test ($\alpha=0.05$, dF=1). Genotype of the mutants seedlings of *PIN1/pin1-1,pin3/pin3,PIN6/pin6* was confirmed by genotyping all mutant seedlings for *pin1-1* and *pin6* mutation. Genotype of the mutants seedlings of *PIN1/pin1-1,PIN3/pin3,PIN6/pin6;abcb1/abcb1;abcb19/abcb19* was confirmed by genotyping all mutant seedlings for *pin1-1*, *pin3* and *pin6* mutation.

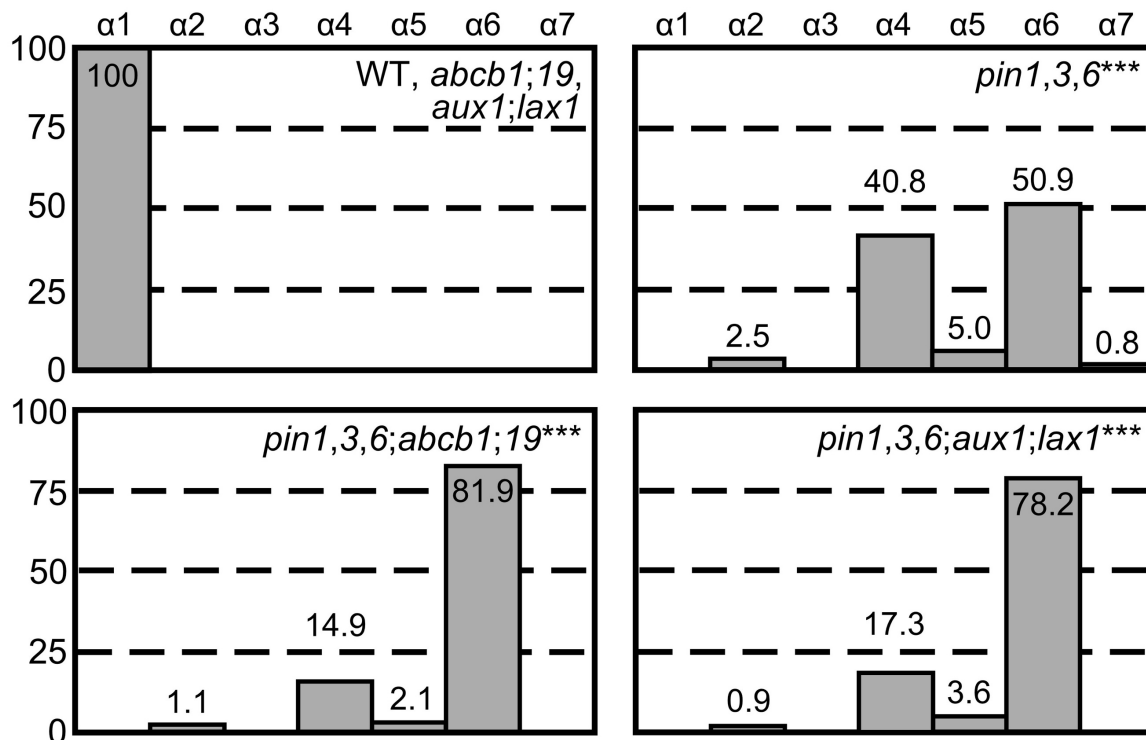


Figure 2.10. Cotyledon patterns of *pin*, *abcb* and *aux1/lax* mutants. Percentages of seedlings in phenotype classes (defined in Figure 2.6). Difference between *pin1-1,3,6* and WT, between *pin1-1,3,6;abcb1;19* and *pin1-1,3,6* and between *pin1-1,3,6;aux1-355;lax1-064* and *pin1-1,3,6* was significant at $P < 0.001$ (***) by Kruskal-Wallis and Mann-Whitney test with Bonferroni correction. Sample population sizes: WT, 56; *abcb1;19*, 75; *aux1-355;lax1-064*, 87; *pin1-1,3,6*, 120; *pin1-1,3,6;abcb1;19*, 94; *pin1-1,3,6;aux1-355;lax1-064*, 110.

mediated auxin transport. However, vein pattern defects induced in *twd1* by 100 μ M NPA were no different from those induced in WT or *abcb1;19* by NPA (Fig. 2.9I), suggesting that vein patterning functions of *TWD1*-dependent ABCB-mediated auxin transport — if existing — become inconsequential in the absence of NPA-sensitive, *PIN*-dependent vein-patterning function. By contrast, NPA enhanced leaf separation defects of *twd1* (Fig. 2.9I), suggesting overlapping functions of *TWD1*-dependent ABCB-mediated auxin transport and NPA-sensitive, *PIN*-dependent auxin transport in leaf separation.

In conclusion, the residual vein patterning activity in *pin* mutants or in their NPA-induced phenocopy is not provided by *ABCB1*, *ABCB19* or *TWD1*-dependent ABCB-mediated auxin transport, and loss of *PIN*- and ABCB-mediated auxin transport fails to phenocopy vein pattern defects of *gn*.

2.2.7 Contribution of *AUX1/LAX* genes to vein patterning

Loss of *PIN*- and ABCB-mediated auxin transport fails to phenocopy vein pattern defects of *gn* (Figure 2.2; Figure 2.9), suggesting that these latter are not the sole result of loss of *PIN*-dependent, NPA-sensitive or ABCB-dependent polar auxin-transport. However, it is possible that the vein pattern defects of *gn* result from additional or exclusive defects in yet another auxin-transport pathway; we tested whether that were so.

Auxin is predicted to enter the cell by diffusion and through an auxin influx carrier (Rubery and Sheldrake, 1974; Raven, 1975). In Arabidopsis, auxin influx activity is encoded by the *AUX1*, *LAX1*, *LAX2* and *LAX3* (*AUX1/LAX*) genes (Parry et al., 2001; Yang et al., 2006; Swarup et al., 2008; Peret et al., 2012). We tested whether *AUX1/LAX*-mediated auxin influx were required for vein patterning.

aux1;lax1;2;3 embryos were viable (Table 2.8). Because the vein patterns of *aux1;lax1;2;3* were no different from those of WT (Fig. 2.11A,C,D), we conclude that *AUX1/LAX* function is dispensable for vein patterning.

We next tested whether contribution of *AUX1/LAX* genes to vein patterning only became apparent in conditions of extremely reduced *PIN*-mediated auxin transport. To address this

Table 2.8. Embryo viability of WT, *aux1*, *lax1*, *aux1;lax1* and *aux1;lax1;2;3*

Genotype of self-fertilized parent	Proportion of viable embryos in siliques of self-fertilized parent (no. of non-aborted seeds / total no. of seeds)	Percentage of viable seeds in siliques of self-fertilized parent
WT	272/274	99.3
<i>aux1/aux1-355</i>	266/267	99.6
<i>lax1/lax1-064</i>	265/267	99.2
<i>aux1/aux1-355;lax1/lax1-064</i>	278/281	98.9
<i>aux1/aux1-21;lax1/lax1;lax2/lax2-1;lax3/lax3</i>	261/262	99.6

Difference between *aux1-355* and WT, between *lax1-064* and WT, between *aux1-355;lax1-064* and WT and between *aux1-21;lax1;2-1;3* and WT was not significant by Kruskal-Wallis and Mann-Whitney test with Bonferroni correction.

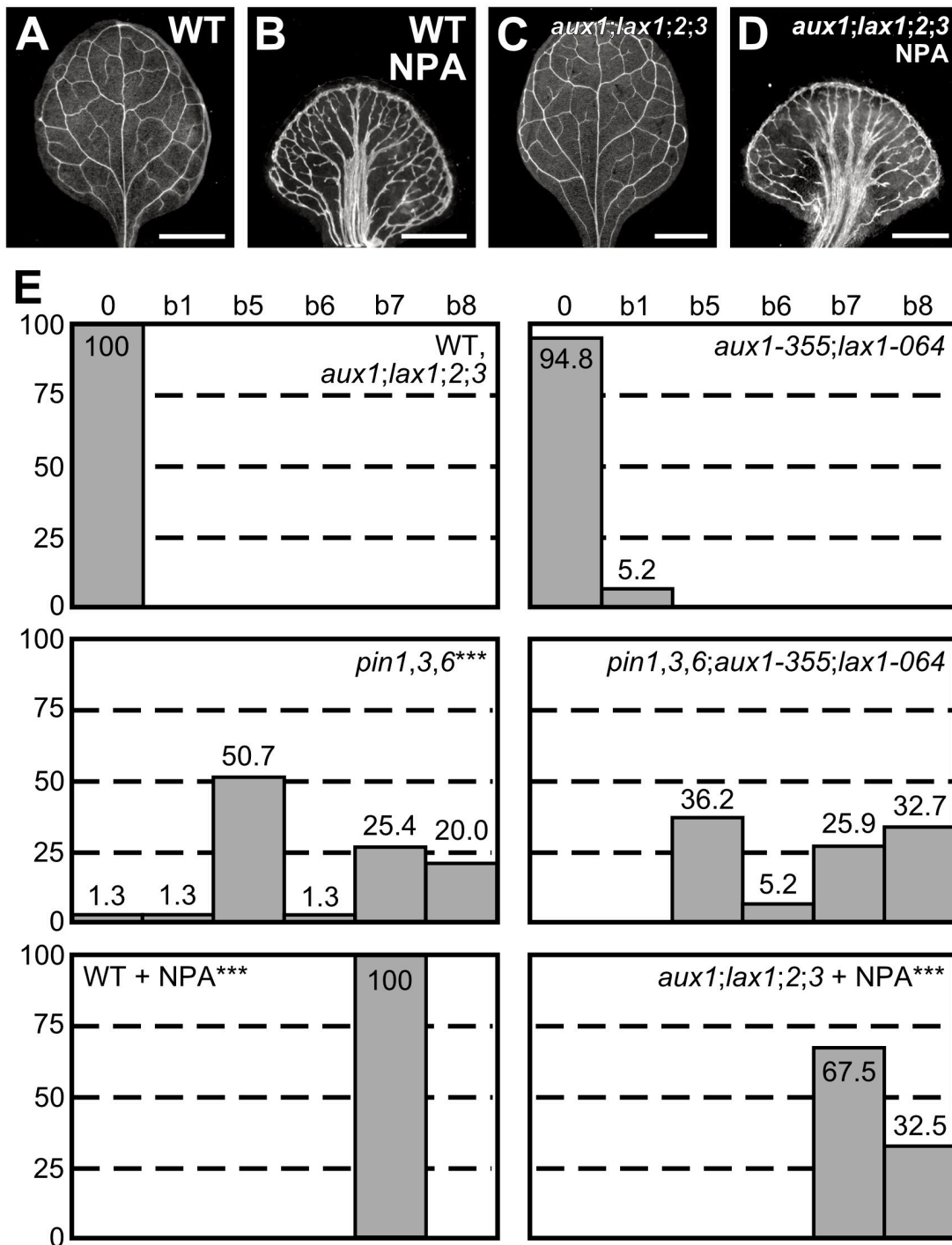


Figure 2.11. Contribution of AUX1/LAX genes to vein patterning. (A–D) Dark-field illumination of mature first leaves. Top right: genotype and treatment. (E) Percentages of leaves in phenotype classes (defined in Figures 2.2, 2.4, 2.7 and 2.9). Difference between

pin1-1,3,6 and WT, between NPA-grown WT and WT and between NPA-grown *aux1-21;lax1;2;3* and NPA-grown WT was significant at $P < 0.001$ (***) by Kruskal-Wallis and Mann-Whitney test with Bonferroni correction. Sample population sizes: WT, 53; *aux1-21;lax1;2;3*, 60; *aux1-355;lax1-064*, 77; *pin1-1,3,6*, 75; *pin1-1,3,6;aux1-355;lax1-064*, 58; NPA-grown WT, 46; NPA-grown *aux1-21;lax1;2;3*, 40. Bars: (A–D) 1 mm.

question, we tested whether vein pattern defects resulting from simultaneous loss of function of *PIN1*, *PIN3* and *PIN6* or induced in WT by 100 μ M NPA, which phenocopies simultaneous mutation of all the *PIN* genes with vein patterning function (Figure 2.7), were enhanced by simultaneous mutation of *AUX1* and *LAX1* — the two *AUX1/LAX* genes that most contribute to shoot organ patterning (Bainbridge et al., 2008) — or of all *AUX1/LAX* genes, respectively.

The embryos derived from the self-fertilization of *PIN1, pin3, PIN6/pin1, pin3, pin6; aux1/aux1; lax1/lax1* were viable (Table 2.9) and developed into seedlings (Table 2.10). The spectrum of vein pattern phenotypes of *pin1,3,6; aux1; lax1* was no different from that of *pin1,3,6* and the vein pattern defects induced in *aux1; lax1; 2;3* by NPA were no different from those induced in WT by NPA (Fig. 2.11B,D,E), suggesting no vein-patterning function of *AUX1/LAX* genes in conditions of extremely reduced auxin transport. On the other hand, simultaneous mutation of *AUX1* and *LAX1* in the *pin1,3,6* background shifted the distribution of *pin1,3,6* cotyledon pattern phenotypes toward stronger classes (Figure 2.4), and NPA induced leaf fusion in *aux1; lax1; 2;3* but not in WT (Fig. 2.11E), suggesting that *AUX1/LAX*-mediated auxin influx and *PIN*-dependent, NPA-sensitive auxin transport have overlapping functions in cotyledon and leaf separation and that — consistent with previous observations (Reinhardt et al., 2003; Bainbridge et al., 2008) *AUX1/LAX*-mediated auxin influx contributes to maintaining cotyledon and leaves separate in conditions of reduced auxin transport. Nevertheless, loss of *PIN*- and *AUX1/LAX*-mediated auxin transport fails to phenocopy the vein pattern defects of *gn*.

2.2.8 Genetic interaction between *GN* and *PIN* genes

The vein pattern defects of *gn* are not the sole result of loss of *PIN*-dependent auxin transport (Figure 2.2; Figure 2.7; Figure 2.8); however, they could be the result of abnormal polarity of *PIN*-mediated auxin transport induced by defects in coordination of *PIN* polar localization. Were that so, the vein pattern defects of *gn* would depend on *PIN* genes, and therefore the vein pattern defects of *gn; pin* mutants would resemble those of *pin* mutants; we tested whether that were so.

Table 2.9. Embryo viability of *toz*, *mp*, *pin1,3,6* and *pin1,3,6;aux1;lax1*

Genotype of self-fertilized parent	Proportion of viable embryos in siliques of self-fertilized parent (no. of non-aborted seeds / total no. of seeds)	Percentage of viable seeds in siliques of self-fertilized parent
<i>TOZ/toz-1</i>	185/244***	75.8
<i>MP/mp^{G12}</i>	220/220	100
<i>PIN1/pin1-1,pin3/pin3,PIN6/pin6</i>	259/261***	99.2
<i>PIN1/pin1-1,pin3/pin3,PIN6/pin6;aux1/aux1-355;lax1/lax1-064</i>	280/282***	99.3

Difference between negative control for completely penetrant embryo lethality (*mp^{G12}*) and positive control for completely penetrant embryo lethality (*toz-1*), between *pin1-1,3,6* and *toz-1* and between *pin1-1,3,6;aux1-355;lax1-064* and *toz-1* was significant at $P < 0.001$ (***) by Kruskal-Wallis and Mann-Whitney test with Bonferroni correction. Difference between *pin1-1,3,6* and *mp^{G12}* and between *pin1-1,3,6;aux1-355;lax1-064* and *mp^{G12}* was not significant by Kruskal-Wallis and Mann-Whitney test with Bonferroni correction. Linkage in *cis* between *pin1-1* and *pin6* in *PIN1/pin1-1,pin3/pin3,PIN6/pin6* and *PIN1/pin1-1,pin3/pin3,PIN6/pin6;aux1/aux1-355;lax1/lax1-064* was confirmed by phenotyping the progeny of the self-fertilized plants used for the embryo viability analysis for the presence of seedlings with cup-shaped cotyledons, which are characteristic of *pin1,6* double homozygous mutant (Sawchuk et al., 2013).

Table 2.10. Embryo viability of *pin1,3,6* and *pin1,3,6;aux1;lax1*

Genotype of self-fertilized parent	Proportion of embryo-viable mutants in progeny of self-fertilized parent (no. of mutant seedlings / total no. of seedlings)	Percentage of embryo-viable mutants in progeny of self-fertilized parent
<i>PIN1/pin1-1,pin3/pin3,PIN6/pin6</i>	87/390	22.3
<i>PIN1/pin1-1,pin3/pin3,PIN6/pin6;aux1/aux1-355;lax1/lax1-064</i>	109/489	22.3

Difference between observed and theoretical frequency distributions of embryo-viable mutants in the progeny of self-fertilized heterozygous parents was not significant by Pearson's chi-squared (χ^2) goodness-of-fit test ($\alpha=0.05$, dF=1). Genotype of the mutants seedlings of both *PIN1/pin1-1,pin3/pin3,PIN6/pin6* and *PIN1/pin1-1,pin3/pin3,PIN6/pin6;aux1/aux1-355;lax1/lax1-064* was confirmed by genotyping all mutant seedlings for *pin1-1* and *pin6* mutation.

We first tested what the phenotype were of the quintuple mutant between the strong allele *gn-13* (Figure 2.2) and mutation in *PIN1*, *PIN3*, *PIN4* and *PIN7* — i.e. the *PM-PIN* genes with vein patterning function (Figure 2.4).

Consistent with previous observations (Mayer et al., 1993; Shevell et al., 1994), in *gn* seedlings hypocotyl and root were replaced by a basal peg and the cotyledons were most frequently fused (Fig. 2.12A,C; Fig 2.13B; Fig. 2.14A,B). As shown above (Fig 2.5A,B; Fig 2.6A,H), *pin1,3;4;7* seedlings had hypocotyl, short root and a single cotyledon, or two — either separate or fused — cotyledons (Fig. 2.12A,B; Fig 2.13C,D; Fig. 2.14B).

gn;pin1,3;4;7 embryos were viable (Table 2.11). A novel phenotype segregated in approximately one-sixteenth of the progeny of plants homozygous for *pin3*, *pin4* and *pin7* and heterozygous for *pin1* and *gn* — no different from the one-sixteenth frequency expected for the *gn;pin1,3;4;7* homozygous mutants by Pearson's chi-squared (χ^2) goodness-of-fit test (Table 2.12). We genotyped 10 of the seedlings with the novel mutant phenotype and found they were *gn;pin1,3;4;7* homozygous mutants. *gn;pin1,3;4;7* seedlings had hypocotyl, no root and the cotyledons were fused (Fig. 2.12A,D; Fig 2.13E; Fig. 2.14B).

WT cotyledons had a I-shaped midvein and three or four loops (Fig. 2.15A,B,K). All the veins of *pin1,3;4;7* cotyledons were thick, and all *pin1,3;4;7* cotyledons had three or four loops (Fig. 2.15C,D). In *pin1,3;4;7* cotyledons, the proximal end of the first loops joined the midvein more basally than in WT, and minor veins branched from midvein and loops (Fig. 2.15C,D,K). Approximately 60% of *pin1,3;4;7* cotyledons had an I-shaped midvein, while the remaining ~40% of them had a Y-shaped midvein (Fig. 2.15C,D,K).

Consistent with previous observations (Mayer et al., 1993; Shevell et al., 1994), in ~70% of *gn* cotyledons short stretches of vascular elements connected the proximal side of a central, shapeless cluster of seemingly randomly oriented vascular elements with the basal part of the cotyledon, while vascular differentiation was limited to a central, shapeless vascular cluster in the remaining ~30% of *gn* cotyledons (Fig. 2.15F,G,K). The vein pattern defects of *gn;pin1,3;4;7* cotyledons were no different from those of *gn* cotyledons (Fig. 2.15H,K), suggesting that the vein pattern phenotype of *gn* cotyledons is epistatic to that of *pin1,3;4;7*

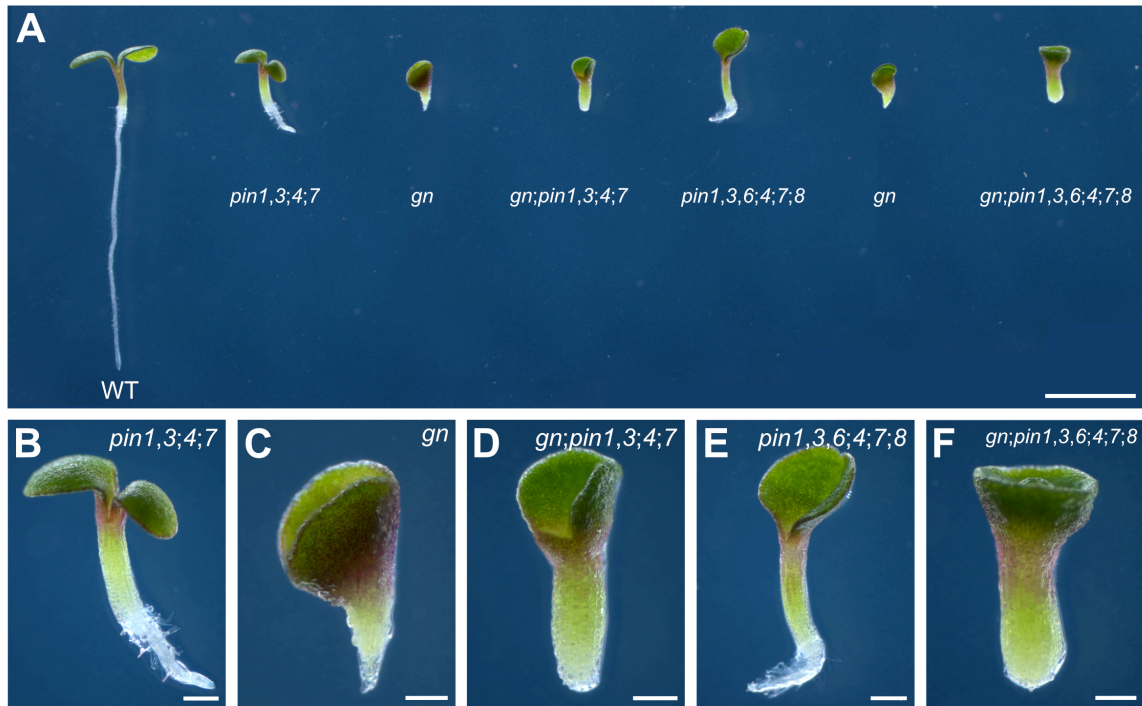


Figure 2.12. *pin* and *gn* mutant seedlings. (A–F) Dark-field illumination composite of 3-day-old seedlings. (A) Overview. Because the seedling lineup was wider than the stereomicroscope’s field of view, overlapping images of parts of the lineup were acquired and combined to reconstruct the original lineup. (B–F) Details. Genotypes below respective seedlings (A) or top right (B–F). Bars: (A) 2 mm; (B–F,) 0.25 mm.

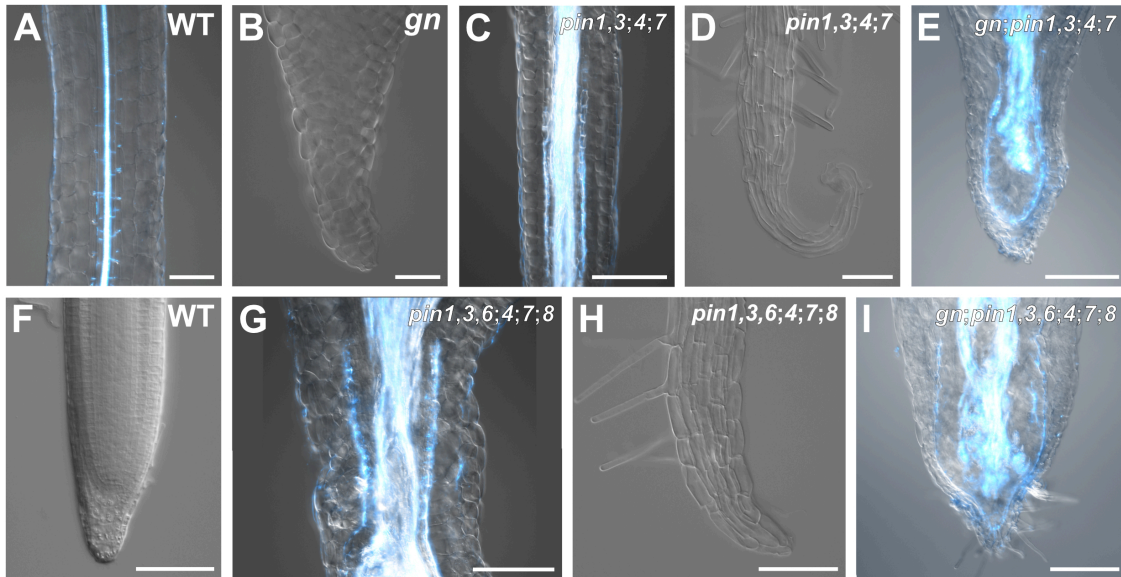


Figure 2.13. Seedling axes of *pin* and *gn* mutants. (A–I) Overlay of dark-field (false-colored in cyan) and differential-interference-contrast illumination of 4- (WT), 3- (*gn*) or 7- (all other genotypes) day-old seedlings. Top right: genotype. (A,C,G) Hypocotyl. (B) Basal peg (Berleth and Jurgens, 1993). (D,F,H) Root. (E,I) Hypocotyl/root. Bars: (A,B,D,F,H) 100 μm ; (C,E,I,G) 250 μm .

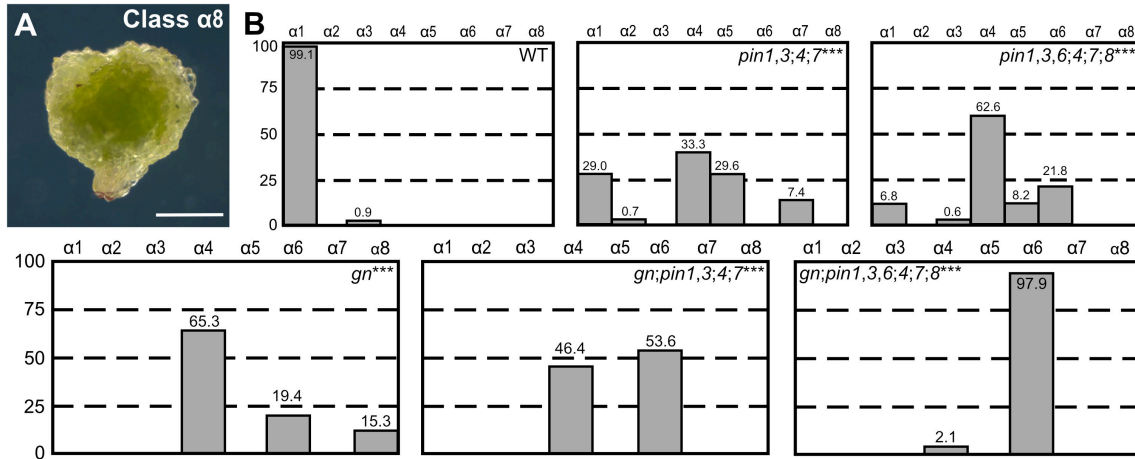


Figure 2.14. Cotyledon patterns of *pin* and *gn* mutants. (A) Dark-field illumination of a 5-day-old seedling illustrating phenotype class $\alpha 8$ (heart-shaped seedling). (B) Percentages of seedlings in phenotype classes (classes $\alpha 1$ – $\alpha 7$ defined in Figure 2.6). Difference between *pin1-1,3,4;7* and WT, between *pin1-1,3,6,4,7;8* and WT, between *gn-13* and WT, between *gn-13;pin1-1,3,4;7* and *pin1-1,3,4;7* and between *gn-13;pin1-1,3,6,4,7;8* and *pin1-1,3,6,4,7;8* was significant at $P < 0.001$ (***) by Kruskal-Wallis and Mann-Whitney test with Bonferroni correction. Sample population sizes: WT, 111; *pin1-1,3,4;7*, 135; *pin1-1,3,6,4,7;8*, 147; *gn-13*, 72; *gn-13;pin1-1,3,4;7*, 84; *gn-13;pin1-1,3,6,4,7;8*, 93. Bar: (A) 0.5 mm.

Table 2.11. Embryo viability of *axr1;axl*, *tir1;afb2*, *gn;pin1,3,4;7* and *gn;pin1,3,6,4;7;8*

Genotype of self-fertilized parent	Proportion of viable embryos in siliques of self-fertilized parent (no. of non-aborted seeds / total no. of seeds)	Percentage of viable seeds in siliques of self-fertilized parent
<i>AXR1/axr1-12;AXL/axl</i>	900/978	92
<i>TIR1/tir1;AFB2/afb2</i>	777/781***	99.5
<i>GN/gn-13;PIN1/pin1-1,pin3/pin3;pin4/pin4;pin7/pin7</i>	482/484***	99.6
<i>GN/gn-13;PIN1/pin1-1,pin3/pin3,pin6/pin6;pin4/pin4;pin7/pin7;pin8/pin8</i>	571/575***	99.3

Difference between negative control for completely penetrant embryo lethality (*tir1;afb2*) and positive control for completely penetrant embryo lethality (*axr1-12;axl*), between *gn;pin1-1,3,4;7* and *axr1-12;axl* and between *gn;pin1-1,3,6,4;7;8* and *axr1-12;axl* was significant at $P < 0.001$ (***) by Kruskal-Wallis and Mann-Whitney test with Bonferroni correction. Difference between *gn;pin1-1,3,4;7* and *tir1;afb2* and between *gn;pin1-1,3,6,4;7;8* and *tir1;afb2* was not significant by Kruskal-Wallis and Mann-Whitney test with Bonferroni correction.

Table 2.12. Embryo viability of *gn;pin1,3,4;7* and *gn;pin1,3,6,4;7;8*

Genotype of self-fertilized parent	Proportion of embryo-viable mutants in progeny of self-fertilized parent (no. of mutant seedlings / total no. of seedlings)	Percentage of embryo-viable mutants in progeny of self-fertilized parent
<i>GN/gn-13;PIN1/pin1-1,pin3/pin3,pin4/pin4,pin7/pin7</i>	256/3624	7.1
<i>GN/gn-13;PIN1/pin1-1,pin3/pin3,pin6/pin6,pin4/pin4,pin7/pin7,pin8/pin8</i>	222/3231	6.9

Difference between observed and theoretical frequency distributions of embryo-viable mutants in the progeny of self-fertilized heterozygous parents was not significant by Pearson's chi-squared (χ^2) goodness-of-fit test ($\alpha=0.05$, dF=1).

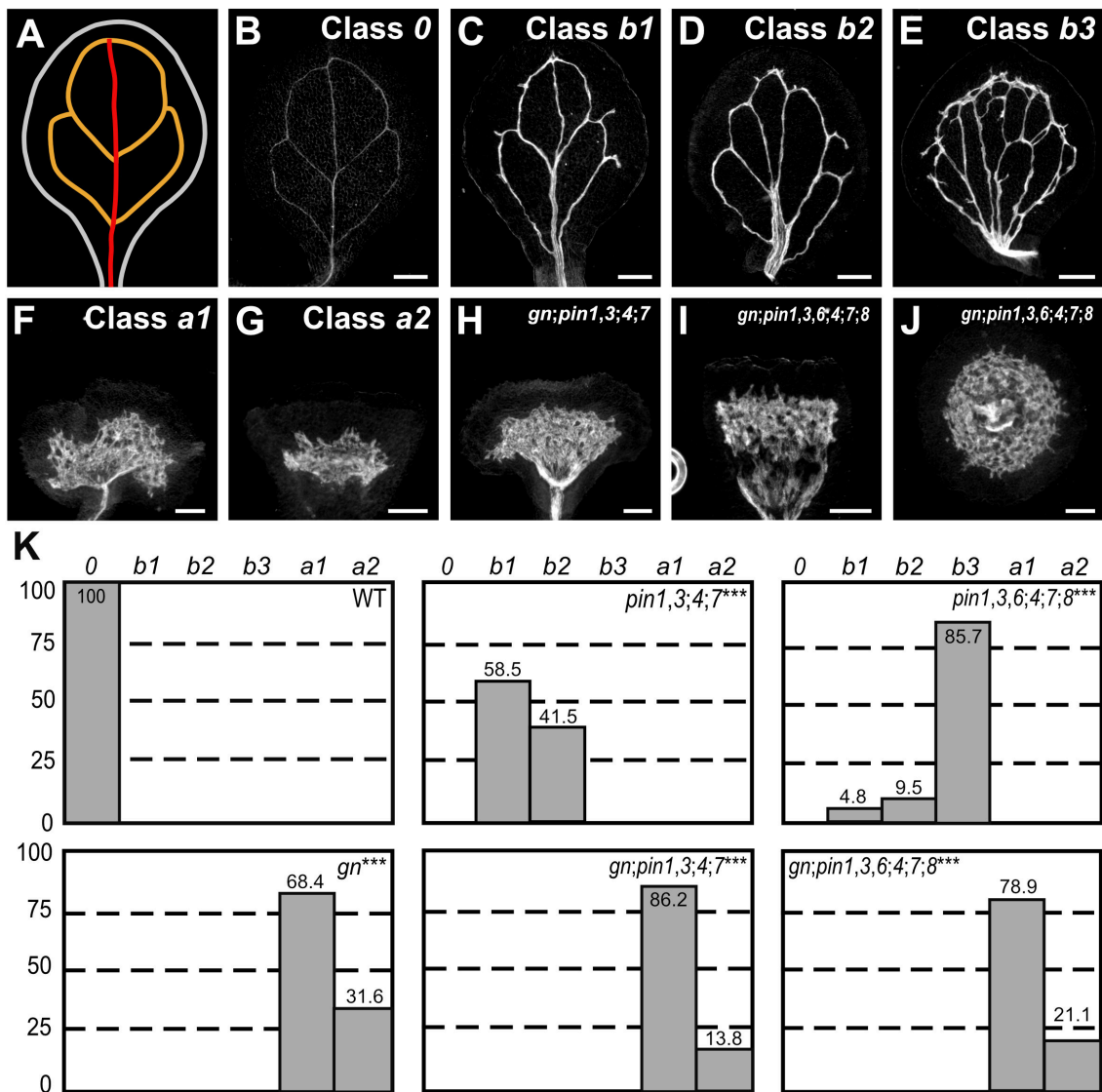


Figure 2.15. Cotyledon vein patterns of *pin* and *gn* mutants. (A,B) Vein pattern of WT mature cotyledon. In (A): red, midvein; orange, vein loops. (B–J) Dark-field illumination of mature cotyledons. Top right: phenotype class or genotype. (B–G) Phenotype classes: class 0, I-shaped midvein and three or four loops (B); class *b1*, I-shaped midvein, thick veins and minor veins (C); class *b2*, Y-shaped midvein, thick veins and minor veins (D); class *b3*, thick veins, loops joining midvein at base of cotyledon and apically thickened vein-network outline (E); class *a1*, shapeless vascular cluster with short stretches of vascular elements connecting cluster to base of cotyledon (F); class *a2*, shapeless vascular cluster (G). (H–J) Dark-field illumination of mature cotyledons of *gn-13;pin1-1,3,4,7* (class *a1*) (H) or *gn-*

13;pin1-1,3,6;4;7;8 (class *a1*) (I, side view; J, top view). (K) Percentages of cotyledons in phenotype classes. Difference between *pin1-1,3;4;7* and WT, between *pin1-1,3,6;4;7;8* and WT, between *gn-13* and WT, between *gn-13;pin1-1,3;4;7* and *pin1-1,3;4;7* and between *gn-13;pin1-1,3,6;4;7;8* and *pin1-1,3,6;4;7;8* was significant at $P < 0.001$ (***) by Kruskal-Wallis and Mann-Whitney test with Bonferroni correction. Sample population sizes: WT, 52; *pin1-1,3;4;7*, 65; *pin1-1,3,6;4;7;8*, 63; *gn-13*, 57; *gn-13;pin1-1,3;4;7*, 65; *gn-13;pin1-1,3,6;4;7;8*, 57. Bars: (B–J) 0.25 mm.

cotyledons. Likewise, the vein pattern defects of *gn;pin1,3,4;7* leaves were no different from those of *gn* leaves (Fig. 2.16A,B,E), suggesting that the vein pattern phenotype of *gn* leaves is epistatic to that of *pin1,3,4;7* leaves.

We next tested what the phenotype were of the septuple mutant between the strong allele *gn-13* (Figure 2.2) and mutation in all the *PIN* genes with vein patterning function (Figure 2.7).

As shown above (Fig 2.5A,D; Fig 2.6A,H), *pin1,3,6,4;7;8* seedlings had hypocotyl, short root and a single cotyledon or two fused cotyledons (Fig. 2.12A,E; Fig 2.13G,H; Fig. 2.14B).

gn;pin1,3,6,4;7;8 embryos were viable (Table 2.11). A phenotype similar to that of *gn;pin1,3,4;7* segregated in approximately one-sixteenth of the progeny of plants homozygous for *pin3*, *pin4*, *pin6*, *pin7* and *pin8* and heterozygous for *pin1* and *gn* — no different from the one-sixteenth frequency expected for the *gn;pin1,3,6,4;7;8* homozygous mutants by Pearson's χ^2 goodness-of-fit test (Table 2.12). We genotyped 10 of the seedlings with the novel mutant phenotype and found they were *gn;pin1,3,6,4;7;8* homozygous mutants. Like *gn;pin1,3,4;7* seedlings, *gn;pin1,3,6,4;7;8* seedlings had hypocotyl and no root, but unlike *gn;pin1,3,4;7* seedlings ~90% of *gn;pin1,3,6,4;7;8* seedlings had completely fused cup-shaped cotyledons (Fig. 2.12A,F; Fig 2.13I; Fig. 2.14B).

The vein pattern defects of *pin1,3,6,4;7;8* cotyledons were similar to those of *pin1,3,4;7* cotyledons, but in ~85% of *pin1,3,6,4;7;8* cotyledons the loops joined the midvein at the base of the cotyledon and the top half of the vein network outline was thick (Fig. 2.15C–E,K). The vein pattern defects of *gn;pin1,3,6,4;7;8* cotyledons were no different from those of *gn* cotyledons (Fig. 2.15I–K), suggesting that the vein pattern phenotype of *gn* cotyledons is epistatic to that of *pin1,3,6,4;7;8* cotyledons. Likewise, the vein pattern defects of *gn;pin1,3,6,4;7;8* leaves were no different from those of *gn* leaves (Fig. 2.16C,E), suggesting that the vein pattern phenotype of *gn* leaves is epistatic to that of *pin1,3,6,4;7;8* leaves.

Finally, 100 μ M NPA, which phenocopies loss of *PIN*-dependent vein-patterning function (Figure 2.8), failed to induce additional vein pattern defects in *gn* leaves (Fig. 2.16D,E). In conclusion, our results suggest that the vein pattern defects of *gn* are not the result of either

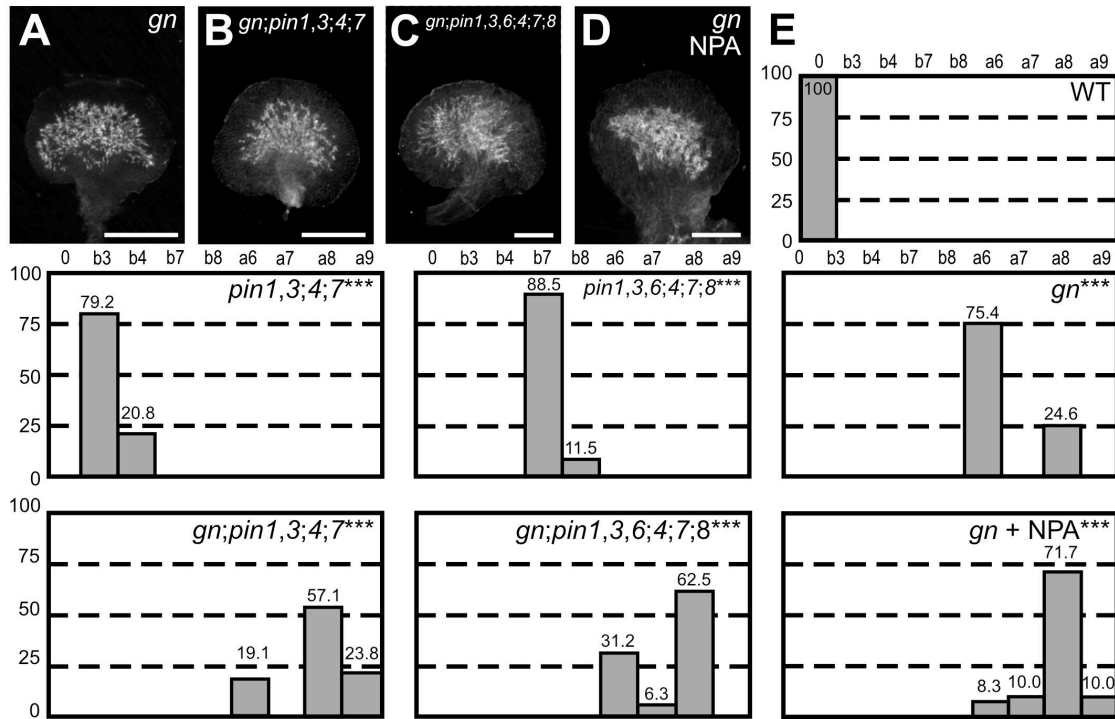


Figure 2.16. Genetic Interaction Between *GN* and *PIN* Genes. (A–D) Dark-field illumination of mature first leaves. Top right: genotype and treatment. (E) Percentages of leaves in phenotype classes (defined in Figures 2–4). Difference between *pin1-1,3,4,7* and WT, between *pin1-1,3,6,4,7,8* and WT, between *gn* and WT, between *gn-13;pin1-1,3,4,7* and *pin1-1,3,4,7*, between *gn-13;pin1-1,3,6,4,7,8* and *pin1-1,3,6,4,7,8* and between NPA-grown *gn-13* and *pin1-1,3,6,4,7,8* was significant at $P < 0.001$ (***) by Kruskal-Wallis and Mann-Whitney test with Bonferroni correction. Sample population sizes: WT, 63; *pin1-1,3,4,7*, 53; *pin1-1,3,6,4,7,8*, 52; *gn-13*, 69; *gn-13;pin1-1,3,4,7*, 21; *gn-13;pin1-1,3,6,4,7,8*, 15; NPA-grown *gn-13*, 60. Bars: (A–D) 0.5 mm.

the sole loss of PIN-mediated auxin transport or the sole abnormal polarity of PIN-mediated auxin transport induced by defects in coordination of PIN polar localization.

2.2.9 Response of *pin* leaves to auxin application

The uniform vein-pattern phenotype of *pin1,3,6;4;7;8* was phenocopied by growth of WT in the presence of high concentration of NPA (Figure 2.8). Moreover, the vein-pattern phenotype of *pin1,3,6;4;7;8* was unchanged by NPA treatment, and the NPA-induced vein-pattern phenocopy of *pin1,3,6;4;7;8* was unchanged by mutation in any other known intercellular auxin-transporter (Figure 2.9; Figure 2.11). These observations suggest that the function of known intercellular auxin-transporters in vein patterning is dispensable in the absence of the auxin transport activity of PIN1, PIN3, PIN4, PIN6, PIN7 and PIN8. Because auxin transport is thought to be essential for auxin-induced vascular-strand formation (reviewed in (Sachs, 1981; Berleth et al., 2000; Aloni, 2010; Sawchuk and Scarpella, 2013)), we tested whether auxin induced vein formation in *pin1,3,6;4;7;8* and consequently whether veins were formed by an auxin-dependent mechanism in *pin1,3,6;4;7;8*. To address this question, we applied lanolin paste containing 1% of the natural auxin indole-3-acetic acid (IAA) to one side of developing leaves of WT and *pin1,3,6;4;7;8* and recorded tissue response in mature leaves. Consistent with previous reports (Scarpella et al., 2006; Sawchuk et al., 2007), IAA induced formation of extra veins in ~70% of WT leaves (27/38) (Fig. 2.17A,B), while ~30% of WT leaves (9/38) failed to respond to IAA application.

The effects of IAA on *pin1,3,6;4;7;8* leaves were variable. In 40% of the leaves (28/70), IAA induced formation of extra veins (Fig. 2.17C,D). In ~60% of the leaves in which IAA induced formation of extra veins (17/28), IAA also induced tissue outgrowth of varied shape (Fig. 2.17E,F). In 30% of *pin1,3,6;4;7;8* leaves (21/70), IAA induced tissue outgrowth but failed to induce formation of extra veins in the leaf; however, in nearly 80% of the *pin1,3,6;4;7;8* leaves in which IAA induced tissue outgrowth [$30/(17+21)=30/38$], IAA also induced formation of vascular strands in the outgrowth (Fig. 2.17E,F). Finally, as in WT, 30% of *pin1,3,6;4;7;8* leaves (21/70) failed to respond to IAA application in any noticeable way.

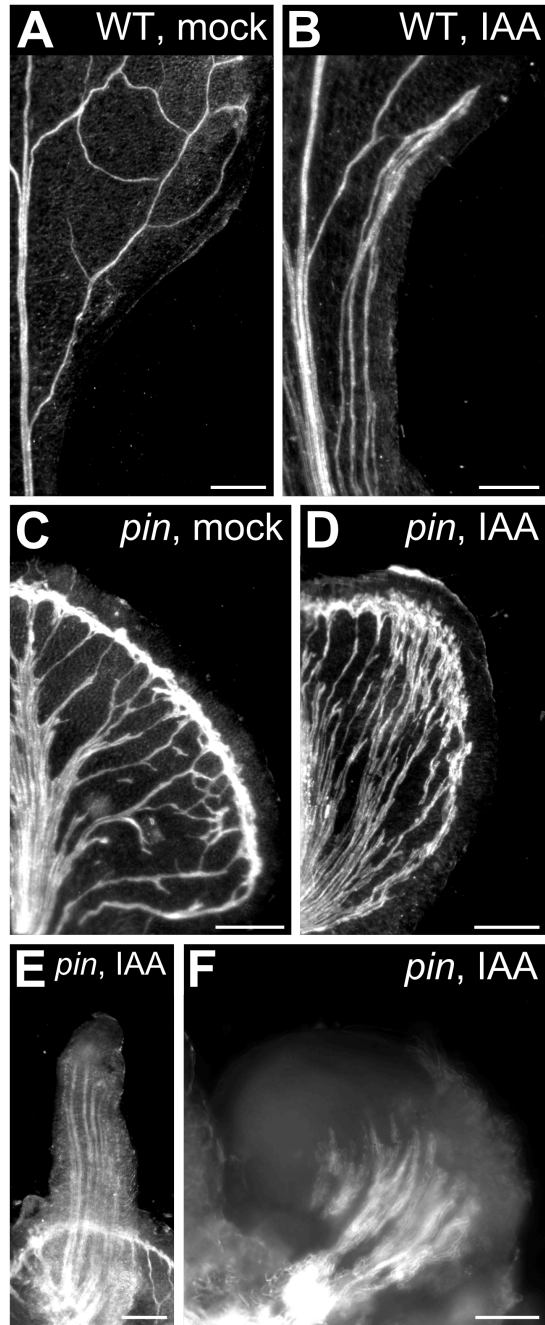


Figure 2.17. Response of *pin* leaves to auxin application. (A–F) Top right: genotype and treatment. Dark-field illumination of mature first leaves of WT (A,B) or *pin1-1,3,6;4;7;8* (C–F) at side of application of lanolin paste (A,C) or lanolin paste containing 1% IAA (B,D–F). Bars: (A) 0.5 mm; (B–E) 0.25 mm; (F) 0.1 mm.

We conclude that *pin1,3,6;4;7;8* leaves respond to vein-formation-inducing auxin signals and consequently that veins are formed by an auxin-dependent mechanism in the absence of PIN-mediated auxin transport.

2.2.10 Contribution of auxin signaling to vein patterning

Leaves of *pin1,3,6;4;7;8* respond to vein-formation-inducing auxin signals (Figure 2.17), suggesting that the residual vein-patterning activity in those leaves may be provided by an auxin-dependent mechanism. We therefore tested what the contribution of auxin signaling to vein patterning were in the absence of *PIN*-dependent vein patterning activity.

To address this question, we used mutants in *AUXIN-RESISTANT1 (AXR1)*, which lack a required post-translational modification of the auxin receptor complex (reviewed in (Calderon-Villalobos et al., 2010; Schwechheimer, 2018)); double mutants in *TRANSPORT INHIBITOR RESPONSE1 (TIR1)* and *AUXIN SIGNALING F-BOX2 (AFB2)*, which lack the two auxin receptors that most contribute to auxin signaling (Dharmasiri et al., 2005); and phenylboronic acid (PBA), which inhibits auxin signaling (Matthes and Torres-Ruiz, 2016).

The embryos of *axr1* and *tir1;afb2* were viable (Table 2.13). In ~40–65% of the leaves of *axr1*, of *tir1;afb2* and of WT grown in the presence of 10 μ M PBA — as in leaves of the *gn-18*, *gn^{fwr}* and *gn^{B/E}* weak *gn* alleles (Figure 2.2) — loops were open (Fig 2.18A,B,H). Furthermore, in ~20–50% of the leaves of *axr1*, of *tir1;afb2* and of WT grown in the presence of 10 μ M PBA — again as in leaves of the *gn-18*, *gn^{fwr}* and *gn^{B/E}* weak *gn* alleles (Figure 2.2) — veins were fragmented (Fig 2.18A,B,H).

We next tested whether PBA, mutation of *AXR1* or simultaneous mutation of *TIR1* and *AFB2* enhanced the vein pattern defects induced by NPA, which phenocopies loss of *PIN*-dependent vein-patterning activity (Figure 2.8). Approximately 3-25% of the leaves of NPA-grown *axr1*, NPA-grown *tir1;afb2* and NPA- and PBA-grown WT resembled those of NPA-grown WT or of *pin1,3,6;4;7;8* (Fig 2.18C,H). However, ~25-50% of the leaves of NPA-grown *axr1*, NPA-grown *tir1;afb2* and NPA- and PBA-grown WT resembled those of the *gn^{R5}* intermediate allele: veins were thicker, the vein network was denser and its outline was jagged because of narrow clusters of vascular

Table 2.13. Embryo viability of WT, *axr1* and *tir1;afb2*

Genotype of self-fertilized parent	Proportion of viable embryos in siliques of self-fertilized parent (no. of non-aborted seeds / total no. of seeds)	Percentage of viable seeds in siliques of self-fertilized parent
WT	408/412	99
<i>axr1-3</i>	391/403	97
<i>tir1;afb2</i>	300/303	99

Difference between *axr1-3* and WT and between *tir1;afb2* and WT was not significant by Kruskal-Wallis and Mann-Whitney test with Bonferroni correction.

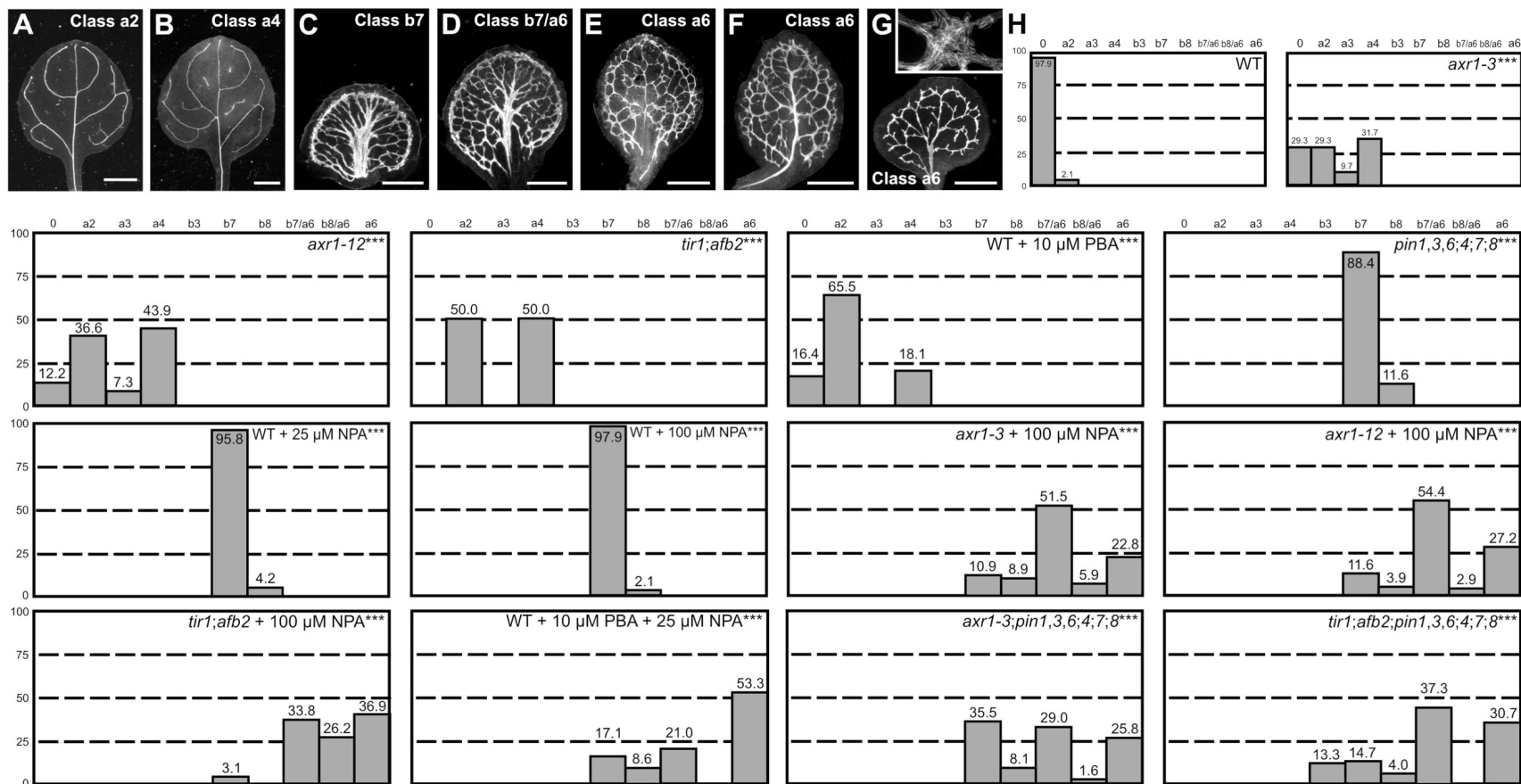


Figure 2.18. Contribution of auxin signaling to vein patterning. (A–G) Dark-field illumination of mature leaves illustrating phenotype classes (A–F, top right; G, bottom left): class a2 (*axr1-3*; A); class a4 (*tir1;afb2*; B); class b7 (NPA-grown WT; C); class b7/a6, wide midvein, more lateral-veins, dense network of thick veins and conspicuous marginal vein (NPA-grown *axr1-12*; D); class b8/a6, fused leaves with wide midvein, more lateral-veins, dense network of thick veins and conspicuous marginal vein (not shown);

class a6 (E: PBA- and NPA-grown WT; F: NPA-grown *tir1;afb2*; G: *tir1;afb2;pin1-1,3,6;4;7;8*); inset in (G) illustrates cluster of seemingly randomly oriented vascular elements. (H) Percentages of leaves in phenotype classes (Classes 0, a2, a3, a4, a6, b7 and b8 defined in Figures 2.2, 2.4 and 2.7). Difference between *axr1-3* and WT, between *axr1-12* and WT, between *tir1;afb2* and WT, between PBA-grown WT and WT, between *pin1-1,3,6;4;7;8* and WT, between NPA-grown WT and WT, between NPA-grown *axr1-3* and NPA-grown WT, between NPA-grown *axr1-12* and NPA-grown WT, between NPA-grown *tir1;afb2* and NPA-grown WT, between PBA- and NPA-grown WT and NPA-grown WT, between *axr1-3;pin1-1,3,6;4;7;8* and *pin1-1,3,6;4;7;8* and between *tir1;afb2;pin1-1,3,6;4;7;8* and *pin1-1,3,6;4;7;8* was significant at $P < 0.001$ (***) by Kruskal-Wallis and Mann-Whitney test with Bonferroni correction. Sample population sizes: WT, 47; *axr1-3*, 41; *axr1-12*, 41; *tir1;afb2*, 42; PBA-grown WT, 58; *pin1-1,3,6;4;7;8*, 63; NPA-grown WT, 48 (25 μ M) or 146 (100 μ M); NPA-grown *axr1-3*, 101; NPA-grown *axr1-12*, 103; NPA-grown *tir1;afb2*, 65; PBA- and NPA-grown WT, 105; *axr1-3;pin1-1,3,6;4;7;8*, 62; *tir1;afb2;pin1-1,3,6;4;7;8*, 75. Bars: (A,B) 1 mm; (C–E) 0.75 mm (F,G) 0.5 mm.

elements that were oriented perpendicular to the leaf margin and that were laterally connected by veins or that, in the most severe cases, were aligned in seemingly random orientations (Figure 2.2; Fig 2.18E,F,H; Fig 2.18G, inset). Finally, ~20-60% of the leaves of NPA-grown *axr1*, NPA-grown *tir1;afb2* and NPA- and PBA-grown WT had features intermediate between those of NPA-grown WT or of *pin1,3,6;4;7;8* and those of intermediate *gn* alleles (Fig 2.18D,H).

We next tested whether the spectrum of vein pattern defects of NPA-grown *axr1* and *tir1;afb2* were recapitulated by *axr1;pin1,3,6;4;7;8* and *tir1;afb2;pin1,3,6;4;7;8*.

axr1;pin1,3,6;4;7;8 embryos were viable (Table 2.14) and developed into seedlings (Table 2.15) that resembled *pin1,3,6;4;7;8* seedlings (Figure 2.19; Figure 2.20). Also *tir1;afb2;pin1,3,6;4;7;8* embryos were viable (Table 2.14), but they developed into seedlings (Table 2.15) whose cotyledon pattern defects were more severe than those of *pin1,3,6;4;7;8* seedlings (Figure 2.20; Figure 2.21) and whose root was replaced by a basal peg (Fig. 2.21C), as in strong *gn* alleles (Mayer et al., 1993) (Fig. 2.13B). Nevertheless, the spectrum of vein pattern defects of *axr1;pin1,3,6;4;7;8* and *tir1;afb2;pin1,3,6;4;7;8* was no different from that of NPA-grown *axr1* and NPA-grown *tir1;afb2* (Fig 2.18C–H).

These observations suggest that the residual vein-patterning activity in *pin1,3,6;4;7;8* is provided, at least in part, by AXR1- and TIR1/AFB2-mediated auxin signaling. Because reduction of AXR1- and TIR1/AFB2-mediated auxin signaling synthetically enhanced vein pattern defects resulting from loss of *PIN*-dependent vein-patterning function, we conclude that *PIN*-mediated auxin transport and AXR1- and TIR1/AFB2-mediated auxin signaling provide overlapping functions in vein patterning. Finally, the similarity between the vein pattern defects of NPA-grown *axr1* and *tir1;afb2*, of NPA- and PBA-grown WT and of *axr1;pin1,3,6;4;7;8* and *tir1;afb2;pin1,3,6;4;7;8*, on the one hand, and those of the *gn*^{R5} intermediate allele, on the other, suggests that the vein pattern defects of *gn* are caused by simultaneous defects in auxin transport and signaling.

Table 2.14. Embryo viability of *toz*, *mp*, *pin1,3,6;4;7;8*, *pin1,3,6;4;7;8;axr1*, *pin1,3,6;4;7;8;tir1;afb2*

Genotype of self-fertilized parent	Proportion of viable embryos in siliques of self-fertilized parent (no. of non-aborted seeds / total no. of seeds)	Percentage of viable seeds in siliques of self-fertilized parent
<i>TOZ/toz-1</i>	190/239	79.5
<i>MP/mp^{G12}</i>	261/262 ^{***}	99.6
<i>PIN1/pin1-1,pin3/pin3,pin6/pin6;pin4/pin4;pin7/pin7;pin8/pin8</i>	243/244 ^{***}	99.6
<i>PIN1/pin1-1,pin3/pin3,pin6/pin6;pin4/pin4;pin7/pin7;pin8/pin8;axr1/axr1-3</i>	240/248 ^{***}	96.8
<i>PIN1/pin1-1,pin3/pin3,pin6/pin6;pin4/pin4;pin7/pin7;pin8/pin8;tir1/tir1;afb2/afb2</i>	473/475 ^{***}	99.6

Difference between negative control for completely penetrant embryo lethality (*mp^{G12}*) and positive control for completely penetrant embryo lethality (*toz-1*), between *pin1-1,3,6;4;7;8* and *toz-1*, between *pin1-1,3,6;4;7;8;axr1-3* and *toz-1* and between *pin1-1,3,6;4;7;8;tir1;afb2* and *toz-1* was significant at $P < 0.001$ (***) by Kruskal-Wallis and Mann-Whitney test with Bonferroni correction. Difference between *pin1-1,3,6;4;7;8* and *mp^{G12}*, between *pin1-1,3,6;4;7;8;axr1-3* and *mp^{G12}* and between *pin1-1,3,6;4;7;8;tir1;afb2* and *mp^{G12}* was not significant by Kruskal-Wallis and Mann-Whitney test with Bonferroni correction.

Table 2.15. Embryo viability of *pin1,3,6;4;7;8;axr1* and *pin1,3,6;4;7;8;tir1;afb2*

Genotype of self-fertilized parent	Proportion of embryo-viable mutants in progeny of self-fertilized parent (no. of mutant seedlings / total no. of seedlings)	Percentage of embryo-viable mutants in progeny of self-fertilized parent
<i>PIN1/pin1-1, pin3/pin3, pin6/pin6; pin4/pin4; pin7/pin7; pin8/pin8; axr1/axr1-3</i>	66/277	23.8
<i>PIN1/pin1-1, pin3/pin3, pin6/pin6; pin4/pin4; pin7/pin7; pin8/pin8; tir1/tir1; afb2/afb2</i>	77/324	23.8

Difference between observed and theoretical frequency distributions of embryo-viable mutants in the progeny of self-fertilized heterozygous parents was not significant by Pearson's chi-squared (χ^2) goodness-of-fit test ($\alpha=0.05$, dF=1).

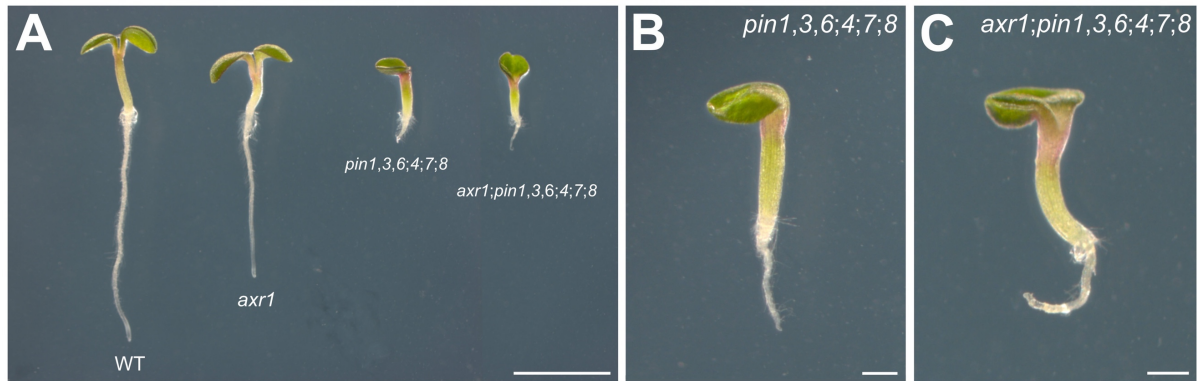


Figure 2.19. *pin* and *axr1* mutant seedlings. (A,B) Dark-field illumination composite of 3-day-old seedlings; genotypes below respective seedlings (A) or top right (B). (A) Overview. (B) Details. Bars: (A) 2 mm; (B) 0.5 mm.

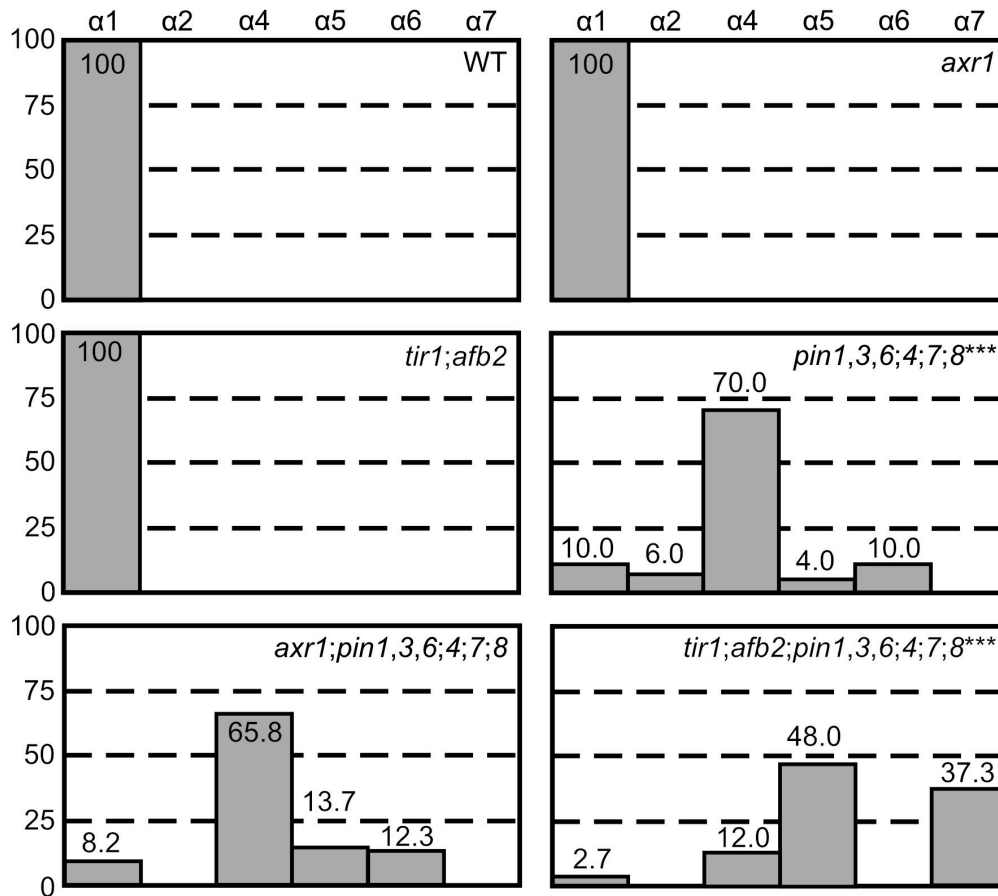


Figure 2.20. Cotyledon patterns of *pin*, *axr1* and *tir1;afb2* mutants. Percentages of seedlings in phenotype classes (defined in Figure 2.6). Difference between *pin1-1,3,6;4;7;8* and WT and between *tir1;afb2;pin1-1,3,6;4;7;8* and *pin1-1,3,6;4;7;8* was significant at $P < 0.001$ (***) by Kruskal-Wallis and Mann-Whitney test with Bonferroni correction. Sample population sizes: WT, 59; *axr1-3*, 49; *tir1;afb2*, 44; *pin1-1,3,6;4;7;8*, 50; *axr1-3;pin1-1,3,6;4;7;8*, 146; *tir1;afb2;pin1-1,3,6;4;7;8*, 75.



Figure 2.21. *pin* and *tir1;afb2* mutant seedlings. (A–C) Dark-field (A,B) or differential-interference-contrast (C) illumination of 3-day-old seedlings; genotypes below respective seedlings (A) or top right (B,C). (A) Overview. (B) Detail. (C) Basal peg (Berleth and Jurgens, 1993). Bars: (A) 2 mm; (B) 0.5 mm; (C) 0.1 mm.

2.2.11 Contribution of *GN* to auxin signaling

Were the vein pattern defects of *gn* not only the result of abnormal polarity or loss of PIN-mediated auxin transport but that of defects in auxin signaling, the vein pattern defects of *gn* might be associated with reduced auxin response and the reduced auxin response of *gn* would be recapitulated by NPA-grown *axr1*; we tested whether that were so.

To address this question, we imaged expression of the auxin response reporter DR5rev::nYFP (Heisler et al., 2005; Sawchuk et al., 2013) in developing first-leaves of WT, *pin1,3,6;4;7;8*, NPA-grown WT, *axr1*, *gn* and NPA-grown *axr1*.

As previously shown (Sawchuk et al., 2013; Verna et al., 2015), strong DR5rev::nYFP expression was mainly associated with developing veins in WT (Fig 2.22A). In *pin1,3,6;4;7;8* and NPA-grown WT, DR5rev::nYFP expression was weaker and mainly confined to areas near the margin of the leaf (Fig 2.22B–E). DR5rev::nYFP expression was weaker also in *axr1* but was still associated with developing veins (Fig 2.22F,G). Finally, in both *gn* and NPA-grown *axr1*, DR5rev::nYFP expression was much weaker and scattered across large areas of the leaf (Fig 2.22H–K), suggesting that the vein pattern defects of *gn* are associated with reduced auxin response and that the reduced auxin response of *gn* is recapitulated by NPA-grown *axr1*.

Were the vein pattern defects of *gn* caused by simultaneous defects in auxin transport and signaling and did *GN* control auxin signaling as it controls auxin transport, the vein pattern defects of *gn;axr1* should resemble those of *gn*, just as the vein pattern defects of *gn;pin1,3;4;7* and *gn;pin1,3,6;4;7;8* resemble those of *gn*; we tested whether that were so.

gn;axr1 embryos were viable (Table 2.16) and developed into seedlings (Table 2.17) that resembled *gn* seedlings (Figure 2.23; Figure 2.24), and the vein pattern defects of *gn;axr1* were no different from those of *gn* (Fig 2.25A–C), suggesting that the phenotype of *gn* is epistatic to that of *axr1*.

We conclude that the vein pattern defects of *gn* are caused by simultaneous defects in auxin transport and signaling and that *GN* controls both auxin signaling and auxin transport.

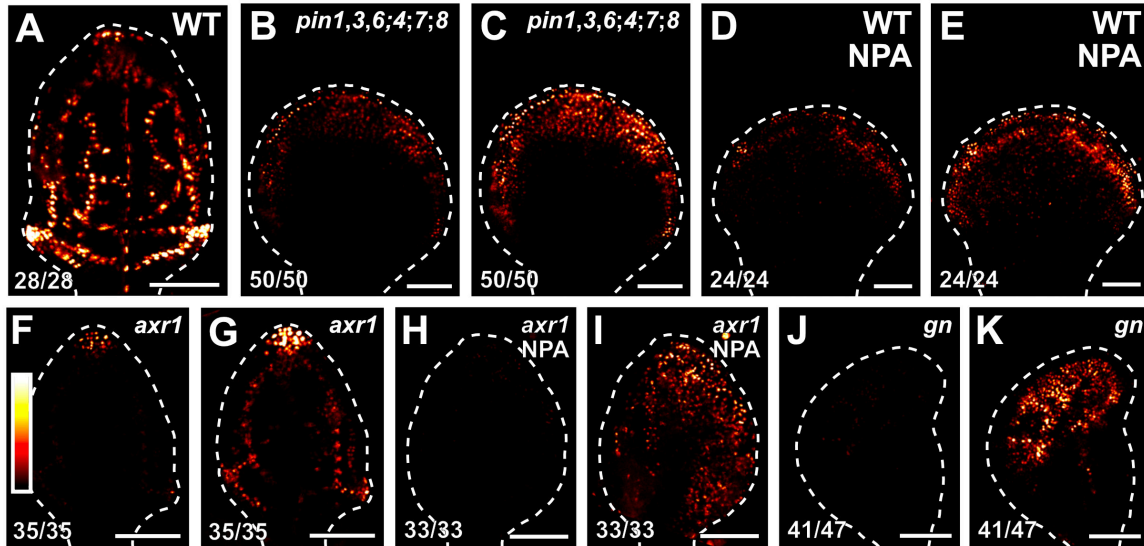


Figure 2.22. Auxin response in developing leaves. (A–K) Confocal laser scanning microscopy; first leaves 4 (A,D,E), 5 (B,C,F–I) or 6 (J,K) days after germination. DR5rev::nYFP expression; look-up table (ramp in F) visualizes expression levels. Top right: genotype and treatment. Bottom left: reproducibility index. Dashed white line delineates leaf outline. Images in A,B,D,F,H,J were taken at identical settings. Images in A,C,E,G,I,K were taken by matching signal intensity to detector’s input range (~5% saturated pixels). Bars: (A–K) 100 μ m.

Table 2.16. Embryo viability of *toz*, *mp*, *gn* and *gn;axr1*

Genotype of self-fertilized parent	Proportion of viable embryos in siliques of self-fertilized parent (no. of non-aborted seeds / total no. of seeds)	Percentage of viable seeds in siliques of self-fertilized parent
<i>TOZ/toz-1</i>	206/259	79.5
<i>MP/mp^{G12}</i>	243/247***	98.4
<i>GN/gn-13</i>	248/252***	98.4
<i>GN/gn-13;axr1/axr1-3</i>	264/270***	97.8
<i>GN/gn-13;axr1/axr1-12</i>	214/224***	95.6

Difference between negative control for completely penetrant embryo lethality (*mp^{G12}*) and positive control for completely penetrant embryo lethality (*toz-1*), between *gn-13* and *toz-1*, between *gn-13;axr1-3* and *toz-1* and between *gn-13;axr1-12* and *toz-1* was significant at $P < 0.001$ (***) by Kruskal-Wallis and Mann-Whitney test with Bonferroni correction. Difference between *gn-13* and *mp^{G12}*, between *gn-13;axr1-3* and *mp^{G12}* and between *gn-13;axr1-12* and *mp^{G12}* was not significant by Kruskal-Wallis and Mann-Whitney test with Bonferroni correction.

Table 2.17. Embryo viability of *gn* and *gn;axr1*

Genotype of self-fertilized parent	Proportion of embryo-viable mutants in progeny of self-fertilized parent (no. of mutant seedlings / total no. of seedlings)	Percentage of embryo-viable mutants in progeny of self-fertilized parent
<i>GN/gn-13</i>	101/411	24.6
<i>GN/gn1-13;axr1-3</i>	74/321	23.0
<i>GN/gn1-13;axr1-12</i>	70/276	25.4

Difference between observed and theoretical frequency distributions of embryo-viable mutants in the progeny of self-fertilized heterozygous parents was not significant by Pearson's chi-squared (χ^2) goodness-of-fit test ($\alpha=0.05$, dF=1).

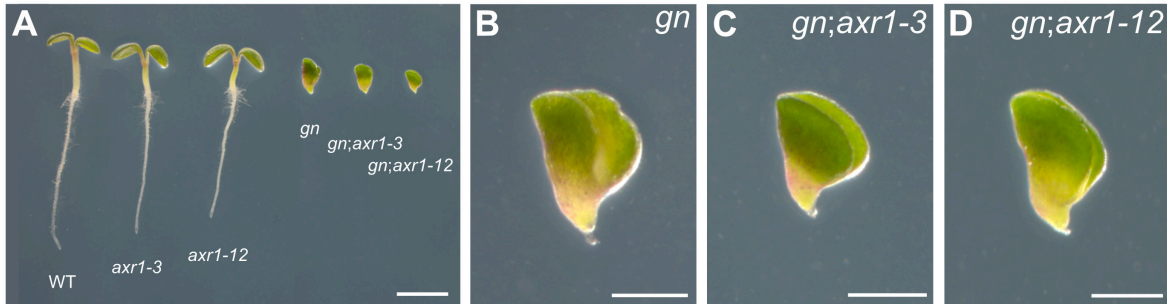


Figure 2.23. *gn* and *axr1* mutant seedlings. (A–C) Dark-field illumination composite of 3-day-old seedlings; genotypes below respective seedlings (A) or top right (B,C). (A) Overview. Because the seedling lineup was wider than the stereomicroscope’s field of view, overlapping images of parts of the lineup were acquired and combined to reconstruct the original lineup. (B,C) Details. Bars: (A) 2 mm; (B,C) 0.5 mm.

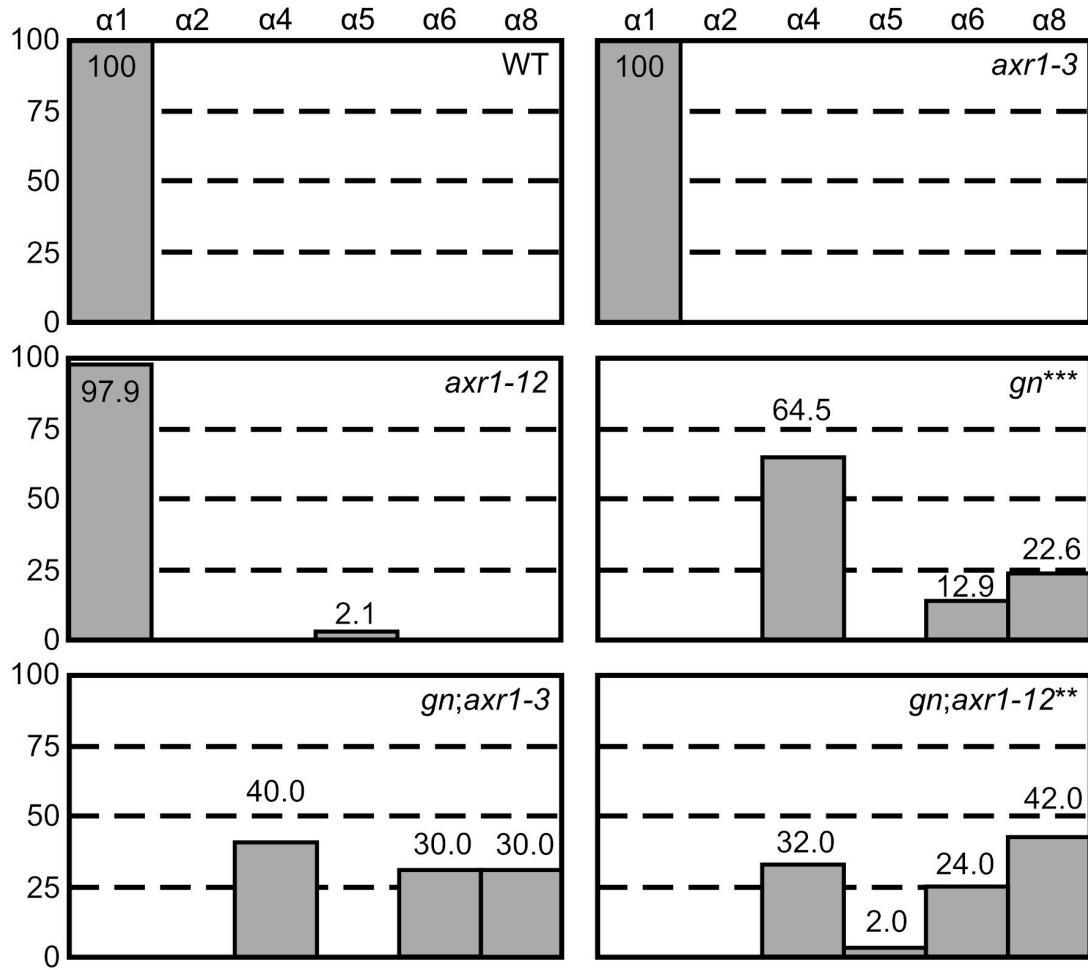


Figure 2.24. Cotyledon patterns of *gn* and *axr1* mutants. Percentages of seedlings in phenotype classes (defined in Figure 2.6). Difference between *gn-13* and WT was significant at $P < 0.001$ (***) and between *gn-13;axr1-12* and *gn-13* was significant at $P < 0.01$ (**) by Kruskal-Wallis and Mann-Whitney test with Bonferroni correction. Sample population sizes: WT, 86; *axr1-3*, 87; *axr1-12*, 47; *gn-13*, 62; *gn-13;axr1-3*, 70; *gn-13;axr1-12*, 50.

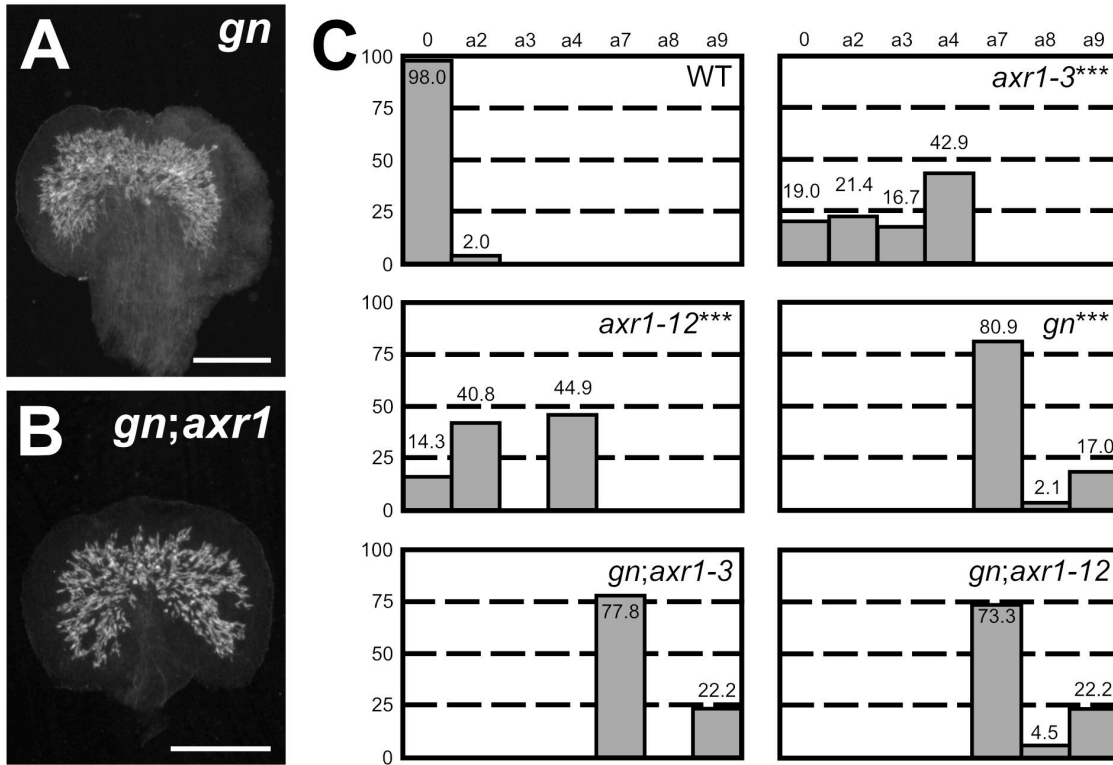


Figure 2.25. Genetic interaction between *GN* and *AXR1*. (A,B) Dark-field illumination of mature first leaves. Top right: genotype. (C) Percentages of leaves in phenotype classes (defined in Figures 2.2, 2.4 and 2.7). Difference between *axr1-3* and WT, between *axr1-12* and WT and between *gn-13* and WT was significant at $P < 0.001$ (***) by Kruskal-Wallis and Mann-Whitney test with Bonferroni correction. Sample population sizes: WT, 49; *axr1-3*, 42; *axr1-12*, 49; *gn-13*, 47; *gn-13;axr1-3*, 45; *gn-13;axr1-12*, 45. Bars: (A,B) 0.75 mm.

2.2.12 Contribution of auxin transport and signaling to coordination of tissue cell polarity during vein formation

The vein pattern defects of *gn* are caused by simultaneous defects in auxin transport and signaling. We finally tested whether simultaneous defects in auxin transport and signaling recapitulated *gn* defects in coordination of tissue cell polarity.

To address this question, we imaged cellular localization of PIN1::PIN1:GFP expression during first-leaf development in WT, *tir1;afb2*, NPA-grown WT, NPA-grown *tir1;afb2* and *gn^{van7}*.

Consistent with previous reports (Benkova et al., 2003; Reinhardt et al., 2003; Heisler et al., 2005; Scarpella et al., 2006; Wenzel et al., 2007; Bayer et al., 2009; Sawchuk et al., 2013; Marcos and Berleth, 2014; Verna et al., 2015), and as shown above (Fig 2.1P,T), in the cells of the second loop at early stages of its development in WT leaves, PIN1::PIN1:GFP expression was mainly localized to the basal side of the PM, toward the midvein; in the inner cells flanking the developing loop, PIN1::PIN1:GFP expression was mainly localized to the side of the PM facing the developing loop; and in the inner cells further away from the developing loop, PIN1::PIN1:GFP expression was localized isotropically, or nearly so, at the PM (Fig 2.26B). At later stages of second-loop development, by which time PIN1::PIN1:GFP expression had become restricted to the sole, elongated cells of the developing loop, PIN1::PIN1:GFP expression was localized to the basal side of the PM, toward the midvein (Fig 2.26H). We observed a similar pattern of localization of PIN1::PIN1:GFP expression in *tir1;afb2*, but in this background stages of second-loop development comparable to those in WT appeared at later stages of leaf development, and nearly 70% (24/35) of second loops failed to connect to the first loop (Fig 2.26C,I).

Consistent with previous reports (Scarpella et al., 2006; Wenzel et al., 2007), PIN1::PIN1:GFP expression domains were broader at early stages of development of the tissue that in NPA-grown WT corresponds to that from which the second loop forms in WT; PIN1::PIN1:GFP expression was localized isotropically, or nearly so, at the PM in the outermost inner cells but was mainly localized to the basal side of the PM in the innermost

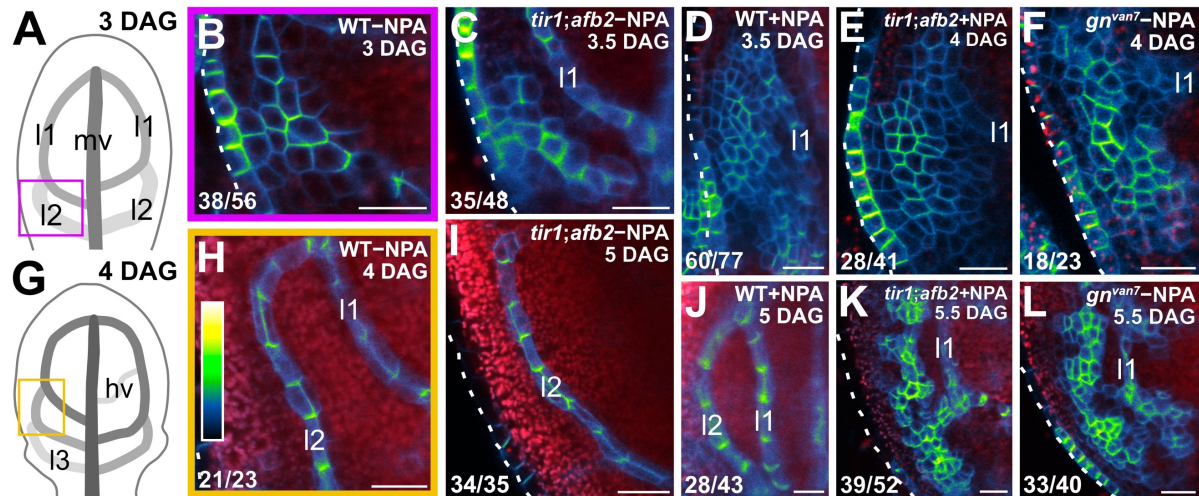


Figure 2.26. Contribution of auxin transport and signaling to coordination of tissue cell polarity during vein formation. (A,G) Increasingly darker grays depict progressively later stages of vein development. Boxes illustrate positions of closeups in B and H, respectively. hv: minor vein; l1, l2 and l3: first, second and third loops; mv: midvein. (B–F,H–L) Confocal laser scanning microscopy. First leaves. Top right: genotype, treatment and leaf age in days after germination (DAG). Dashed white line delineates leaf outline. Bottom left: reproducibility index. PIN1::PIN1:GFP expression; look-up table (ramp in H) visualizes expression levels. Red: autofluorescence. Bars: (B–F,H–L) 20 μm.

inner cells (Fig 2.26D). At later stages of second-loop development in NPA-grown WT, by which time PIN1::PIN1:GFP expression had become restricted to the sole, elongated cells of the developing loop, PIN1::PIN1:GFP expression was localized to the basal side of the PM (Fig 2.26J).

As in NPA-grown WT, in both *gn^{van7}* and NPA-grown *tir1;afb2* PIN1::PIN1:GFP expression domains were broader at early stages of development of the tissue that corresponds to that from which the second loop forms in WT, but PIN1::PIN1:GFP was expressed more heterogeneously in *gn^{van7}* and NPA-grown *tir1;afb2* than in NPA-grown WT (Fig 2.26E,F). Nevertheless, as in NPA-grown WT, in both *gn^{van7}* and NPA-grown *tir1;afb2* PIN1::PIN1:GFP expression remained localized isotropically, or nearly so, at the PM, except in cells near the edge of higher-expression domains; in those cells, localization of PIN1::PIN1:GFP expression at the PM was weakly polar, but such weak cell polarities pointed in seemingly random directions (Fig 2.26E,F). At later stages of second-loop development of both *gn^{van7}* and NPA-grown *tir1;afb2*, heterogeneity of PIN1::PIN1:GFP expression had become more pronounced, and PIN1::PIN1:GFP expression had become restricted to narrow clusters of cells; in those cells, localization of PIN1::PIN1:GFP expression at the PM was weakly polar, but such weak cell polarities still pointed in seemingly random directions (Fig 2.26K,L).

In conclusion, simultaneous defects in auxin transport and signaling recapitulate *gn* defects in coordination of PIN1 polar localization, suggesting not only that the vein pattern defects of *gn* are caused by simultaneous defects in auxin transport and signaling, but that simultaneous defects in auxin transport and signaling recapitulate *gn* defects in coordination of tissue cell polarity during vein formation.

2.3 Discussion

The current hypothesis of how auxin coordinates tissue cell polarity to induce polar-vein-formation proposes that GN controls the cellular localization of PIN1 and other PIN proteins; the resulting cell-to-cell, polar transport of auxin would coordinate tissue cell polarity and

control polar developmental processes such as vein formation (reviewed in, e.g., (Berleth et al., 2000; Richter et al., 2010; Nakamura et al., 2012; Linh et al., 2018)).

Contrary to predictions of the hypothesis, we find that auxin-induced polar-vein-formation occurs in the absence of PIN proteins or any known intercellular auxin transporter; that auxin-transport-independent vein-patterning activity relies on auxin signaling; and that a GN-dependent signal that coordinates tissue cell polarity to induce polar-vein-formation acts upstream of both auxin transport and signaling (Fig. 2.27).

2.3.1 Control of vein patterning by carrier-mediated polar auxin-transport

Overwhelming experimental evidence places polar auxin transport at the core of the mechanism that defines sites of vein formation (reviewed in (Sachs, 1981; Sachs, 1991a; Berleth et al., 2000; Sachs, 2000; Sawchuk and Scarpella, 2013)). The polarity of auxin transport is determined by the asymmetric localization of efflux carriers of the PIN family at the PM of auxin-transporting cells (Wisniewska et al., 2006). Therefore, loss of function of all the PM-PIN proteins should lead to loss of reproducible vein-pattern features or even, in the most extreme case, to the inability to form veins. Neither prediction is, however, supported by evidence: mutants in all the *PM-PIN* genes with vein patterning function — *PIN1*, *PIN3*, *PIN4* and *PIN7* — or in all the *PM-PIN* genes — *PIN1–PIN4* and *PIN7* — form veins, and these veins are arranged in reproducible, albeit abnormal, patterns. The most parsimonious account for the discrepancy between the observed and expected mutant defects is that vein patterning is controlled by additional, PM-PIN-independent auxin-transport pathways.

The existence of PM-PIN-independent auxin-transport pathways with vein patterning function can also be inferred from the discrepancy between the vein pattern defects of *pin1,3;4;7*, or of *pin1,3;2;4;7*, and those induced by NPA, which is thought to be a specific inhibitor of carrier-mediated cellular auxin-efflux (Cande and Ray, 1976; Sussman and Goldsmith, 1981; Petrasek et al., 2003; Dhonukshe et al., 2008). The vein pattern defects of WT grown in the presence of NPA are more severe than those of *pin1,3;4;7* or *pin1,3;2;4;7*, suggesting the existence of an NPA-sensitive auxin-transport pathway with vein patterning

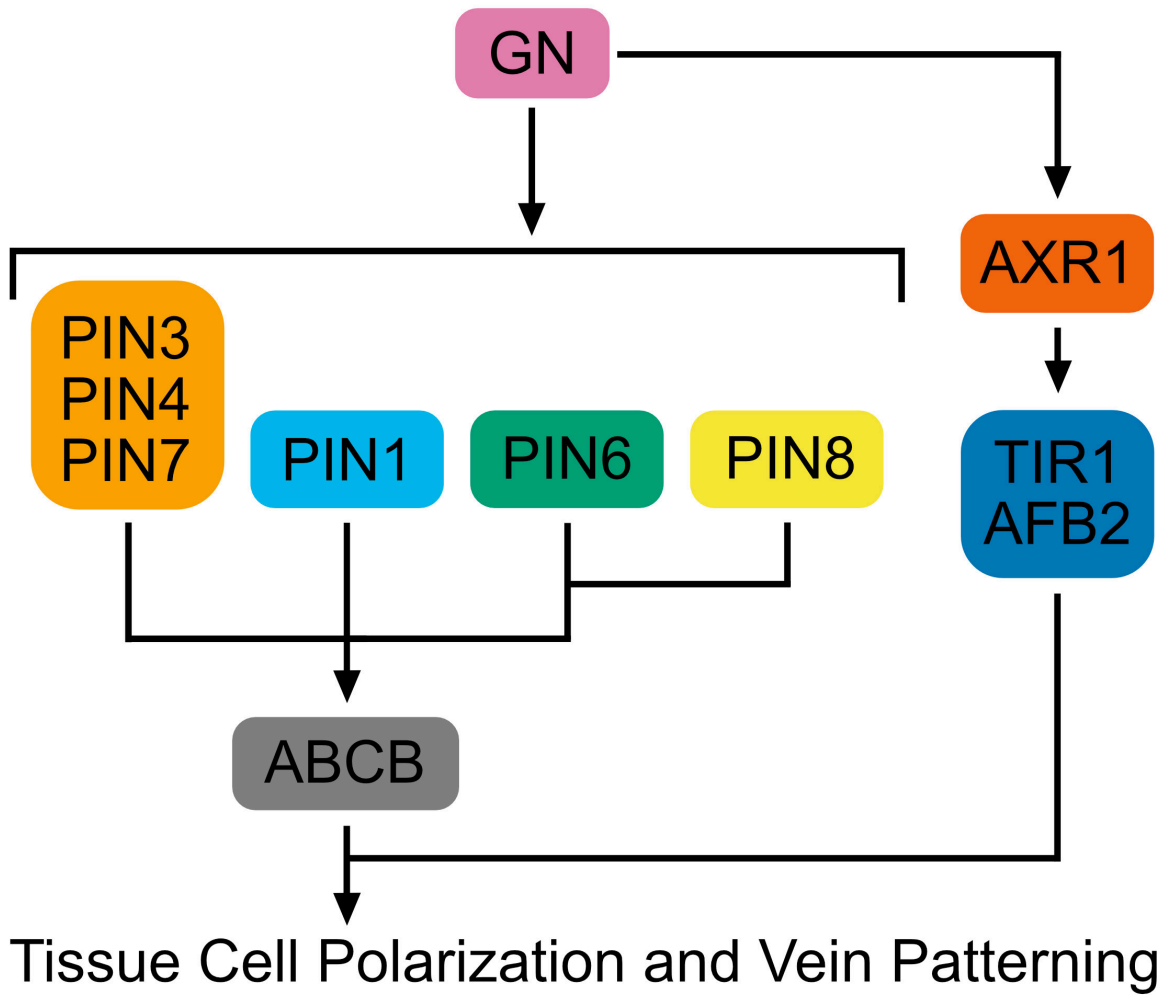


Figure 2.27. Interpretation summary. Genetic interaction network controlling tissue cell polarization and vein patterning. Arrows indicate positive effects.

function in addition to that controlled by PM-PIN proteins, a suggestion that is supported by the observation that growth in the presence of NPA enhances the vein pattern defects of *pin1,3,4;7* to match those induced in WT by NPA.

Such PM-PIN-independent NPA-sensitive auxin-transport pathway with vein patterning function depends on the activity of the ER-PIN proteins PIN6 and PIN8, as inferred from the identity of the vein pattern defects induced in WT by NPA and those of *pin1,3,6;4;7;8*, and from the inability of NPA to induce further defects in *pin1,3,6;4;7;8*. Moreover, that NPA-grown WT phenocopies *pin1,3,6;4;7;8*, that no further defects can be induced in *pin1,3,6;4;7;8* by NPA, and that the vein patterns of *pin1,3,6;4;7;8* and NPA-grown WT fall into the same single phenotype-class suggest the absence of NPA-sensitive vein-patterning activity beyond that provided by PIN1, PIN3, PIN4, PIN6, PIN7 and PIN8, and hence the existence of NPA-insensitive vein-patterning pathways. It is of course possible that PIN6 and PIN8 are partially localized to the PM, and PM-localization of PIN5 and PIN6 has indeed been reported (Ganguly et al., 2014; Bennett et al., 2016; Simon et al., 2016; Ditengou et al., 2018); most important, however, that would not argue against the existence of NPA-insensitive vein patterning pathways, which is a logical conclusion, not a hypothesis.

These NPA-insensitive vein-patterning pathways are unlikely to be mediated by known intercellular auxin transporters — the AUX1/LAX influx carriers (Yang et al., 2006; Swarup et al., 2008; Peret et al., 2012) and the ABCB efflux carriers (Geisler et al., 2005; Bouchard et al., 2006; Petrasek et al., 2006) — as their mutation fails to enhance the vein pattern defects of *pin1,3,6* and of the NPA-induced phenocopy of *pin1,3,6;4;7;8*. Though it remains unexplored whether the NPA-insensitive vein-patterning pathways depend on the function of the PIN-LIKES intracellular auxin-transporters (Barbez et al., 2012), and though we cannot rule out the existence of unknown auxin transporters, it is unlikely that the NPA-insensitive vein-patterning pathways depend on NPA-insensitive carrier-mediated auxin-transport because as little as 10 μ M NPA (one-tenth of the concentration we used) is sufficient to inhibit carrier-mediated polar auxin-transport completely in tissue segments (Okada et al., 1991; Kaneda et al., 2011). Whatever the molecular nature of the NPA-insensitive vein-patterning pathways, they do contribute to the polar propagation of the inductive auxin

signal: application of auxin to *pin1,3,6;4;7;8* leaves, just as to WT leaves, induces the formation of veins that connect the applied auxin to the pre-existing vasculature basal to the site of auxin application.

2.3.2 Control of vein patterning by auxin signaling

The residual NPA-insensitive auxin-dependent vein-patterning activity of *pin1,3,6;4;7;8* relies, at least in part, on the signal transduction mediated by the TIR1/AFB auxin receptors and their post-translational regulator AXR1. Loss of *AXR1* or of *TIR1* and *AFB2*, the two auxin receptors that most contribute to auxin signaling (Dharmasiri et al., 2005), or growth in the presence of the auxin signaling inhibitor PBA (Matthes and Torres-Ruiz, 2016), induces entirely new vein-pattern defects in *pin1,3,6;4;7;8* or in its NPA-induced phenocopy, defects never observed in *pin1,3,6;4;7;8* or NPA-grown WT: in the more-severely affected leaves of *axr1;pin1,3,6;4;7;8*, *tir1;afb2;pin1,3,6;4;7;8*, NPA-grown *axr1*, NPA-grown *tir1;afb2* and NPA- and PBA-grown WT, the end-to-end alignment of vascular elements oriented with their axis along the axis of the vein is often replaced by the clustered differentiation of abnormally oriented vascular elements. Not only are these defects never observed in *pin1,3,6;4;7;8* or NPA-grown WT, but they are more severe than the predicted sum of the defects of *pin1,3,6;4;7;8* or NPA-grown WT, on the one hand, and of *axr1*, *tir1;afb2* or PBA-grown WT, on the other. These observations are particularly interesting because genetic analysis of auxin signaling components has so far implicated auxin signaling only in the differentiation of normally patterned veins (Przemeck et al., 1996; Hardtke and Berleth, 1998; Hardtke et al., 2004; Alonso-Peral et al., 2006; Candela et al., 2007; Esteve-Bruna et al., 2013). Instead, the mutual synthetic enhancement between the vein pattern defects caused by reduced auxin signaling and those caused by reduced auxin transport suggests non-homologous redundancy of auxin signaling and auxin transport in vein patterning, a conclusion which is consistent with observations in the shoot apical meristem (Schuetz et al., 2008). Unlike in the shoot apical meristem, however, in the leaf such redundancy is unequal: whereas auxin transport is required for vein patterning even in the presence of normal auxin signaling, the vein patterning activity of auxin signaling is only exposed in conditions of compromised auxin transport.

How auxin signaling, inherently non-directional (Leyser, 2018), could contribute to the polar propagation of the inductive auxin signal in the absence of carrier-mediated polar auxin-transport is unclear. One possibility is that auxin signaling promotes the passive diffusion of auxin through the tissue by controlling, for example, the proton gradient across the PM (Fendrych et al., 2016). However, it is difficult to conceive how auxin diffusion through a specific side of the PM would positively feed back on the ability of auxin to diffuse through that specific side of the PM — a positive feedback that would be required to drain neighboring cells from auxin and thus to form veins, i.e. channels of preferential auxin movement (Sachs, 1969).

One other possibility is that auxin signaling promotes the facilitated diffusion of auxin through the plasmodesmata intercellular channels, a possibility that had previously been suggested (Mitchison, 1980) and that has recently received some experimental support (Han et al., 2014). Here, how auxin movement through a specific side of the PM could positively feed back on the ability of the cell to move auxin through that specific side of the PM is conceivable (e.g., (Cieslak et al., 2015)), but no experimental evidence exists of such feedback or that auxin movement through plasmodesmata controls vein patterning.

Yet another possibility is that auxin signaling activates an unknown mobile signal. Such signal need not be chemical and alternatives, for example a mechanical signal, have been suggested (Couder et al., 2002; Laguna et al., 2008; Corson et al., 2009; Lee et al., 2014) and have been implicated in other auxin-driven processes (e.g., (Hamant et al., 2008; Heisler et al., 2010; Peaucelle et al., 2011; Nakayama et al., 2012; Braybrook and Peaucelle, 2013)). However, whether a mechanical signal controls vein patterning remains to be tested.

2.3.3 A tissue-cell-polarizing signal upstream of auxin transport and signaling

The vein pattern defects of leaves in which both transport and transduction of the auxin signal are compromised are never observed in leaves in which either process is; yet those defects are not unprecedented: they are observed — though in more extreme form — in leaves of *gn* mutants, suggesting that *GN* controls both transport and transduction of the auxin signal during vein patterning.

That *GN* controls PM-PIN-mediated auxin transport during vein patterning is also suggested by the very limited or altogether missing restriction of PIN1 expression domains and coordination of PIN1 polar localization during *gn* leaf development, which is consistent with observations in embryos and roots (Steinmann et al., 1999; Kleine-Vehn et al., 2008). However, if failure to coordinate the polarization of the localization of PIN1 — and possibly other PM-PIN proteins — were the sole cause of the vein pattern defects of *gn*, these defects would be dependent on *PM-PIN* function and would therefore be masked by those of *pin1,3,4,7* in the *gn;pin1,3,4,7* mutant. The epistasis of the vein pattern defects of *gn* to those of *pin1,3,4,7* instead suggests that the vein pattern defects of *gn* are independent of PM-PIN function, and therefore that they are not the sole result of loss or abnormal polarity of PM-PIN-mediated auxin transport, and that *GN* acts upstream of *PM-PIN* genes in vein patterning. Moreover, the epistasis of the vein pattern defects of *gn* to those of *pin1,3,6,4,7,8* and the inability of *NPA*, which phenocopies the vein pattern defects of *pin1,3,6,4,7,8*, to induce additional defects in *gn* suggest that the vein pattern defects of *gn* are independent of all the *PIN* genes with vein patterning function, and therefore that they are not the sole result of loss or abnormal polarity of PIN-mediated auxin transport, and that *GN* acts upstream of all the *PIN* genes in vein patterning. Whereas mechanisms by which *GN* may control PM-PIN-mediated auxin transport have been suggested (e.g., (Richter et al., 2010; Luschnig and Vert, 2014; Naramoto et al., 2014)), it is unclear how *GN* could control auxin transport mediated by the ER-localized PIN6 and PIN8; it is possible, however, that such control is mediated by *GN* function in ER-Golgi trafficking (Richter et al., 2007; Teh and Moore, 2007; Nakano et al., 2009).

These observations suggest that the function of *GN* in coordination of tissue cell polarity and vein patterning entails more than the regulation of PIN-mediated auxin transport, a conclusion which is consistent with functions of *GN* that do not seem to be related to auxin transport or mediated by *PIN* genes (Shevell et al., 2000; Fischer et al., 2006; Irani et al., 2012; Nielsen et al., 2012; Moriwaki et al., 2014).

The auxin-transport-, *PIN*-independent functions of *GN* in coordination of tissue cell polarity and vein patterning are, at least in part, provided by TIR1/AFB2- and AXR1-mediated auxin

signaling. This conclusion is suggested by the ability of simultaneous reduction in auxin transport and signaling to phenocopy defects in coordination of tissue cell polarity, auxin response and vein patterning of *gn*; it is also supported by the epistasis of the vein pattern defects of *gn* to those of *axr1*, which is consistent with genetic analysis placing *GN* upstream of auxin signaling in the formation of apical-basal polarity in the embryo (Mayer et al., 1993).

Though it is unclear how *GN* controls auxin signaling during vein patterning, the most parsimonious account is that *GN* controls the coordinated localization of proteins produced in response to auxin signaling. Auxin signaling has indeed been shown to control the production of proteins that are polarly localized at the plasma membrane of root cells (e.g., (Scacchi et al., 2009; Scacchi et al., 2010; Yoshida et al., 2019)), and at least some of these proteins act synergistically with PIN-mediated auxin transport in the root (e.g., (Marhava et al., 2018)); however, it remains to be tested whether such proteins have vein patterning activity, whether their localization is controlled by *GN* and whether they mediate *GN* function in auxin signaling during vein patterning.

Alternatively, because cell wall composition and properties are abnormal in *gn* (Shevell et al., 2000), *GN* could control the production, propagation or interpretation of a mechanical signal that has been proposed to be upstream of both auxin signaling and transport in the shoot apical meristem (Heisler et al., 2010; Nakayama et al., 2012); however, whether a mechanical signal controls vein patterning and whether such signal acts downstream of *GN* remains to be tested.

Irrespective of the mechanism of action, our results reveal a synergism between auxin transport and signaling and their unsuspected control by *GN* in the coordination of cell polarity during vein patterning, a control whose logic is unprecedented in multicellular organisms.

2.4 Materials & Methods

2.4.1 Notation

In agreement with (Crittenden et al., 1996), linked genes or mutations (<2,500 kb apart, which in *Arabidopsis* corresponds, on average, to ~10 cM (Lukowitz et al., 2000)) are separated by a comma, unlinked ones by a semicolon and homologous chromosomes by a slash.

2.4.2. Plants

Origin and nature of lines, genotyping strategies and oligonucleotide sequences are in Tables 2.1, 2.18 and 2.19. Seeds were sterilized and sown as in (Sawchuk et al., 2008). Stratified seeds were germinated and seedlings were grown at 22°C under continuous fluorescent light (~80 $\mu\text{mol m}^{-2} \text{s}^{-1}$). Plants were grown at 25°C under fluorescent light (~110 $\mu\text{mol m}^{-2} \text{s}^{-1}$) in a 16-h-light/8-h-dark cycle. Plants were transformed and representative lines were selected as in (Sawchuk et al., 2008).

2.4.3 Chemicals

N-1-naphthylphthalamic acid and phenylboronic acid were dissolved in dimethyl sulfoxide and water, respectively; dissolved chemicals were added to growth medium just before sowing. Indole-3-acetic acid was dissolved in melted (55°C) lanolin; the IAA-lanolin paste was applied to first leaves 4 days after germination and was reapplied weekly.

2.4.4 RT-PCR

Total RNA was extracted as in (Chomczynski and Sacchi, 1987) from 4-day-old seedlings grown as in (Odat et al., 2014). RT-PCR was performed (25 cycles) as in (Odat et al., 2014) with the “GN_qFb” and “GN_qRb” oligonucleotides (Table S19), and with the “ROC1 F” and “ROC1 R” oligonucleotides (Beeckman et al., 2002) (Table S19).

2.4.5 Imaging

Developing leaves were mounted and imaged as in (Sawchuk et al., 2013), except that emission was collected from ~2.5- μ m-thick optical slices. Light paths are in Table 2.20. Mature leaves were fixed in 3 : 1 or 6 : 1 ethanol : acetic acid, rehydrated in 70% ethanol and water, cleared briefly (few seconds to few minutes) — when necessary — in 0.4 M sodium hydroxide, washed in water, mounted in 80% glycerol or in 1 : 2 : 8 or 1 : 3 : 8 water : glycerol : chloral hydrate and imaged as in (Odat et al., 2014). Grayscaled RGB color images were turned into 8-bit images, look-up-tables were applied, and brightness and contrast were adjusted by linear stretching of the histogram in the Fiji distribution (Schindelin et al., 2012) of ImageJ (Schneider et al., 2012; Schindelin et al., 2015; Rueden et al., 2017).

Table 2.18. Genotyping strategies

Line	Strategy
<i>gn-13</i>	<i>GN</i> : ‘SALK_045424 gn LP’ and ‘SALK_045424 gn RP’; <i>gn</i> : ‘SALK_045424 gn RP’ and ‘LBb1.3’
<i>gn-18</i>	<i>GN</i> : ‘Salk026031 LP gnp close’ and ‘Salk026031 RP gnp close’; <i>gn</i> : ‘Salk026031 RP gnp close’ and ‘LBb1.3’
<i>fwr (gn^{fwr})</i>	‘FWR for’ and ‘FWR REV2’; <i>EcoRI</i>
<i>van7/emb30-7 (gn^{van7})</i>	‘van7 Hpa1 FP’ and ‘van7 Hpa1 RP’; <i>HpaI</i>
<i>pin1-1</i>	‘pin1-1 F’ and ‘pin1-1 R’; <i>TatI</i>
<i>pin1-134</i>	‘pin1-1 F’ and ‘pin1-134 R mse-I’; <i>MseI</i>
<i>pin3-3</i>	‘pin3-3 F’ and ‘pin3-3 R’; <i>StyI</i>
<i>pin4-2</i>	<i>PIN4</i> : ‘PIN4 forw geno II’ and ‘PIN4en rev Ikram’; <i>pin4</i> : ‘PIN4en rev Ikram’ and ‘en primer’
<i>pin7^{En}</i>	<i>PIN7</i> : ‘PIN7en forw Ikram’ and ‘PIN7en rev’; <i>pin7</i> : ‘PIN7en rev Ikram II’ and ‘en primer’
<i>eir1-1 (pin2)</i>	‘eir1-1 F’ and ‘eir1-1 R’; <i>BseLI</i>
<i>pin6</i>	<i>PIN6</i> : ‘PIN6 spm F’ and ‘PIN6 spm R’; <i>pin6</i> : ‘PIN6 spm F’ and ‘Spm32’
<i>pin8-1</i>	<i>PIN8</i> : ‘SALK_107965 LP’ and ‘SALK_107965 RP’; <i>pin8</i> : ‘SALK_107965 RP’ and ‘LBb1.3’
<i>pgp1-100 (abcb1)</i>	<i>ABCB1</i> : ‘SALK_083649 pgp1-100 LP’ and ‘SALK_083649 pgp1-100 RP’; <i>abcb1</i> : ‘SALK_083649 pgp1-100 RP’ and ‘LBb1.3’
<i>mdr1-101 (abcb19)</i>	<i>ABCB19</i> : ‘SALK_033455 atmdr1-101 LP’ and ‘SALK_033455 atmdr1-101 RP’; <i>abcb19</i> : ‘SALK_033455 atmdr1-101 RP’ and ‘LBb1.3’

<i>ucu2-4 (twd1)</i>	<i>UCU2</i> : ‘SALK_012836 twd1 LP’ and ‘SALK_012836 twd1 RP’; <i>ucu2</i> : ‘SALK_012836 twd1 RP’ and ‘LBb1.3’
<i>aux1-21</i>	‘aux1-21 Fwd’ and ‘aux1-21 Rev’; <i>ApaLI</i>
<i>lax1</i>	<i>LAX1</i> : ‘lax1 Fwd’ and ‘lax1 WT Rev’; <i>lax1</i> : ‘lax1 fwd’ and ‘lax123 mutant Rev’
<i>lax2-1</i>	<i>LAX2</i> : ‘lax2 Fwd’ and ‘lax2 WT Rev’; <i>lax2</i> : ‘lax2 fwd’ and ‘lax123 mutant Rev’
<i>lax3</i>	<i>LAX3</i> : ‘lax3 Fwd’ and ‘lax3 WT Rev’; <i>lax3</i> : ‘lax3 fwd’ and ‘dSpm5’
<i>aux1-355</i>	<i>AUX1</i> : ‘SALK_020355 LP (aux1)’ and ‘SALK_020355 RP (aux1)’; <i>aux1</i> : ‘SALK_020355 RP (aux1)’ and ‘LBb1.3’
<i>lax1-064</i>	<i>LAX1</i> : ‘SALK_071064 lax1 LP’ and ‘SALK_071064 lax1 RP’; <i>lax1</i> : ‘SALK_071064 lax1 RP’ and ‘LBb1.3’
<i>axr1-3</i>	‘AXR1-Acc1’ and ‘AXR1-15’; <i>Sall</i>
<i>axr1-12</i>	‘axr1-12 forw’ and ‘axr1-12 rev’; <i>DraI</i>
<i>axl</i>	<i>AXL</i> : ‘AXL SAIL LP’ and ‘AXL SAIL RP’; <i>axl</i> : ‘AXL SAIL RP’ and ‘LB3’
<i>tir1-1</i>	‘tir1-1F2’ and ‘tir1-1R2’, <i>BsaI</i>
<i>afb2-3</i>	<i>AFB2</i> : ‘AFB2+F’ and ‘AFB2-TR’; <i>afb2</i> : ‘pROK-LB’ and ‘AFB2-TR’

Table 2.19. Oligonucleotide sequences

Name	Sequence (5' to 3')
SALK_045424 gn LP	TGATCCAAATCACTGGGTTTC
SALK_045424 gn RP	AGCTGAAGATAGGGAATTCGC
LBb1.3	ATTTTGCCGATTTCGGAAC
Salk026031 LP gnp close	TGAAAGAGACATGTCCTTCGG
Salk026031 RP gnp close	GACACGTCTCGCTAAATCTCG
FWR for	AAGAGCCAAGATCACAGCCTACTG
FWR REV2	GAGAGCACGCGCAAGCTGCAACAAG
van7 Hpa1 FP	ATCCGTGCCCTTGATCTAATGGGAG
van7 Hpa1 RP	CACTTTTCTTAGTCCTTGAACAAGCGTTAA
GN Fwd NotI	TCTGCGGCCGCTCTAGAGGTGTGTATGATAATG
GN Rev NotI	TTTGC GGCCGCTCTAGAAATCGAAATCCGTCTC
fwr-mutagenesis F	GCTTGC GCGTGCTCTCATTGGGC
fwr-mutagenesis R	TGCAACAAAAATTCAGCTTGTAGAACTTGCTTTCG
pin1-1 F	ATGATTACGGCGGGCGGACTTCTA
pin1-1 R	TTCCGACCACCACCAGAAGCC
pin1-134 R mse-I	CTCAGCTTCAGTTTCCAAAGGTTG
pin3-3 F	GGAGCTCAAACGGGTCACCCG
pin3-3 R	GCTGGATGAGCTACAGCTATATTC
PIN4 forw geno II	GTCCGACTCCACGGCCTTC
PIN4en rev Ikram	ATCTTCTTCTTCACCTTCCACTCT
en primer	GAGCGTCGGTCCCCACACTTCTATAC
PIN7en forw Ikram	CCTAACGGTTTCCACACTCA
PIN7en rev	TAGCTCTTTAGGGTTTAGCTC
PIN7en rev Ikram II	GGTTTAGCTCTGCTGTGGAGTT
eir1-1 F	TTGTTGATCATTTTACCTGGGACA
eir1-1 R	GGTTGCAATGCCATAAATAGAC
PIN6 spm F	CATAACGAAGCTAACTAAGGGGTAATCTC

PIN6 spm R	GGAGTTCAAAGAGGAATAGTAGCAGAG
Spm32	TACGAATAAGAGCGTCCATTTTAGAGTG
SALK_107965 LP	TGAAAGACATTTTGATGGCATC
SALK_107965 RP	CCAAATCAAGCTTTGCAAGAC
SALK_083649 pgp1-100 LP	GAAGACTGCGACAAGGACAAG
SALK_083649 pgp1-100 RP	GCAAGAGCGATGTTGAAGAAC
SALK_033455 atmdr1-101 LP	GCAATTGCAATTCTCTGCTTC
SALK_033455 atmdr1-101 RP	CTCAGGCAATTGCTCAAGTTC
SALK_012836 twd1 LP	GTGAAGCTGAGGTCTTGGATG
SALK_012836 twd1 RP	TATGGCCTGAAACAGCAAACC
aux1-21 Fwd	CTGGAAAGCACTAGGACTCGC
aux1-21 Rev	AAGCGGCGAAGAAACGATACAG
lax1 Fwd	ATATGGTTGCAGGTGGCACA
lax1 WT Rev	GTAACCGGCAAAGCTGCA
lax123 mutant Rev	AAGCACGACGGCTGTAGAATAG
lax2 Fwd	ATGGAGAACGGTGAGAAAGCAGC
lax2 WT Rev	CGCAGAAGGCAGCGTTAGCG
lax3 Fwd	TACTTCACCGGAGCCACCA
lax3 WT Rev	TGATTGGTCCGAAAAGG
dSpm5	CGGGATCCGACACTCTTTAATTAAGTACTGCACTC
SALK_020355 LP (aux1)	GGCTCCCGTAAAATAAAGCAC
SALK_020355 RP (aux1)	AATTATCGTTGGTTTCAGGTGG
SALK_071064 lax1 LP	CAATAGTAGTCTCCGGGGAGG
SALK_071064 lax1 RP	ACAACACAAGCTTGGTTGGAC
AXR1-Acc1	AAACCAACTTAACGTTTGCATGTCG

AXR1-15	TCTCATATGTA CTTTTCTCGTCCTCTTCAC
axr1-12 forw	CCGAGCAGCATCCCAAAC
axr1-12 rev	GTTGGCAGCAAATCTGTCCG
AXL SAIL LP	TGGACTTACTGGGTTTGTTCG
AXL SAIL RP	CAAACCTTGAGTGCTGCTACC
LB3	TAGCATCTGAATTTTCATAACCAATCTCGATACAC
SALK_045424 gn LP	TGATCCAAATCACTGGGTTTC
SALK_045424 gn RP	AGCTGAAGATAGGGAATTCGC
tir1-1F2	AGCGACGGTGATTAGGAGG
tir1-1R2	CAGGAACAACGCAGCAAAA
AFB2+F	TTCTCCTTCGATCATTGTCAAC
AFB2-TR	TAGCGGCAATAGAGGCAAGA
pROK-LB	GGAACCACCATCAAACAGGA
GN_qFb	ACTTGTCAACAGAGCTGGTAGC
GN_qRb	GCTGCAAACCATCGAAAGAATC
ROC1 F	CAAACCTCTTCTTCAGTCTGATAGAGA
ROC1 R	GAGTGCTCATTTCCTTATTTCTGGTAG

Table 2.20. Light paths

Fluorophore	Laser	Wavelength (nm)	Main dichroic beam splitter	First secondary dichroic beam splitter	Second secondary dichroic beam splitter	Emission filter (detector)
YFP	Ar	514	HFT 405/514/594	NFT 595	NFT 515	BP 520-555 IR (PMT3)
GFP; Autofluorescence	Ar	488	HFT 405/488/594	NFT 545	NFT 490 (PMT3); Plate (META)	BP 505-530 (PMT3); 550-574 (META)
GFP	Ar	488	HFT 405/488/594	NFT 545	NFT 490	BP 505-530 (PMT3)

Chapter 3: Identification of new auxin-signaling-dependent regulators of vein patterning

3.1 Introduction

Most multicellular organisms transport signals and nutrients by means of tissue networks such as the vascular system of mammalian embryos and the vein network of plant leaves. How these networks are formed is thus a key question in biology. In animals, the formation of tissue networks is often driven by cell movements (Ciruna et al., 2006; Yin et al., 2008); by contrast, plant cells cannot move because of a wall that holds them in place. Therefore, plants form tissue networks by a mechanism that is entirely different from that by which animals form tissue networks.

How plants form vein networks in their leaves is unclear; however, auxin is so far the only known molecule that can induce vein formation in plant tissues (reviewed in (Sachs, 1981; Berleth et al., 2000; Sawchuk and Scarpella, 2013)). This unique property of auxin seems to depend on its polar transport through plant tissues (Thompson and Jacobs, 1966). Indeed, auxin is primarily synthesized in immature apical organs, such as leaf and flower primordia, and is transported basally to the roots through the vascular strands (Went, 1928; Thimann and Skoog, 1934; Avery, 1935; Wangermann, 1974). The resulting apical-basal transport of auxin seems to depend on the polar localization of auxin transporters of the PIN-FORMED (PIN) family to the basal plasma-membrane of auxin-transporting cells (Wisniewska et al., 2006).

How plants coordinate PIN polarity between auxin-transporting cells is unclear, but for the past 20 years the prevailing hypothesis has been that GNOM (GN) — a guanine-nucleotide exchange factor for ADP-ribosylation factors that regulates vesicle formation in membrane trafficking — controls the cellular localization of PIN proteins; the resulting cell-to-cell, polar transport of auxin would coordinate PIN polarity between auxin-transporting cells and control polar developmental processes such as vein formation (reviewed in, e.g., (Berleth et al., 2000; Richter et al., 2010; Nakamura et al., 2012; Linh et al., 2018)). Contrary to

predictions of this hypothesis, however, vein-formation has recently been shown to occur in the absence of PIN proteins or any known intercellular auxin transporter: it turns out that auxin-transport-independent vein patterning relies on auxin signaling and that GN controls both auxin transport and signaling to induce vein formation (Chapter 2).

Whereas mechanisms by which GN may control PIN polarity and derived polar auxin transport have been suggested (reviewed in (Richter et al., 2010; Luschnig and Vert, 2014); see also (Naramoto et al., 2014) and references therein), it is unclear how GN could control auxin signaling, which takes place in the nucleus and is inherently non-directional (reviewed in (Leyser, 2018)). The most parsimonious account is that auxin signaling leads to the production of proteins which control vein patterning and whose localization is controlled by GN. These proteins, if existing, would be expressed at lower levels in plants in which both auxin transport and auxin signal transduction are inhibited than in plants in which only auxin transport is inhibited. Here we leveraged this expectation and tested, by means of a combination of gene expression screen and molecular genetic analysis, the hypothesis that auxin signaling leads to the production of proteins which control vein patterning synergistically with auxin transport and whose localization is controlled by GN.

3.2 Results and Discussion

3.2.1 A gene expression screen for auxin signaling targets that control vein patterning synergistically with auxin transport

To test the hypothesis that auxin signaling leads to the production of proteins which control vein patterning synergistically with auxin transport and whose localization is controlled by GN, we screened for genes whose expression is lower in plants in which both auxin transport and auxin signaling are inhibited than in plants in which only auxin transport is inhibited.

To identify such genes, we first sequenced RNA from (1) 4-day-old leaves of the double mutant *transport inhibitor response1;auxin signaling f-box2* (*tir1;afb2*), which lacks the two auxin receptors that most contribute to auxin signaling (Dharmasiri et al., 2005), grown in the presence of 100 μ M N-1-naphthylphthalamic acid (NPA), which inhibits auxin transport (Morgan and Söding, 1958), and of WT grown in the presence of 100 μ M NPA; and (2) 4-

day-old leaves of WT grown in the presence of 25 μ M NPA and 10 μ M phenylboronic acid (PBA), which inhibits auxin signaling (Matthes and Torres-Ruiz, 2016), and of WT grown in the presence of 25 μ M NPA. We found (1) 21,823 genes that were expressed in both NPA-grown *tir1;afb2* and NPA-grown WT; and (2) 21,629 genes that were expressed in both PBA- and NPA-grown WT and NPA-grown WT (Figure 3.1).

We next tested for which genes expression was (1) ≥ 1.5 -fold lower in NPA-grown *tir1;afb2* than in NPA-grown WT and (2) ≥ 1.5 -fold lower in PBA- and NPA-grown WT than in NPA-grown WT. We found (1) 2,188 genes whose expression was ≥ 1.5 -fold lower in NPA-grown *tir1;afb2* than in NPA-grown WT and (2) 4,548 genes whose expression was ≥ 1.5 -fold lower in PBA- and NPA-grown WT than in NPA-grown WT (Figure 3.1).

We expect genes encoding proteins which control vein patterning synergistically with auxin transport, whose expression is controlled by auxin signaling, and whose localization is controlled by GN, to be co-expressed with *GN*, *PINI*, which encodes the only auxin transporter with nonredundant functions in vein patterning (Sawchuk et al., 2013) (Chapter 2), or *MONOPTEROS* (*MP*), which encodes the auxin signaling component that most contributes to auxin-signaling-dependent vein patterning (Przemeck et al., 1996; Hardtke et al., 2004; Esteve-Bruna et al., 2013) (Chapter 2). Therefore, by means of the Expression Angler tool (Austin et al., 2016), we identified the top 50 genes that are co-expressed with *GN*, *PINI* or *MP*. Next, we tested for which of these 147 genes expression was (1) ≥ 1.5 -fold lower in NPA-grown *tir1;afb2* than in NPA-grown WT and (2) ≥ 1.5 -fold lower in PBA- and NPA-grown WT than in NPA-grown WT. We found (1) 27 genes that are co-expressed with *GN*, *PINI* or *MP* and whose expression was ≥ 1.5 -fold lower in NPA-grown *tir1;afb2* than in NPA-grown WT and (2) 67 genes that are co-expressed with *GN*, *PINI* or *MP* and whose expression was ≥ 1.5 -fold lower in PBA- and NPA-grown WT than in NPA-grown WT (Figure 3.1).

Next, we tested for which of the genes that are co-expressed with *GN*, *PINI* or *MP* expression was both ≥ 1.5 -fold lower in NPA-grown *tir1;afb2* than in NPA-grown WT and ≥ 1.5 -fold lower in PBA- and NPA-grown WT than in NPA-grown WT; we found 22 such genes (Figure 3.1).



Figure 3.1. Flowchart of screen for auxin signaling targets that control vein patterning synergistically with auxin transport. Proportional Venn diagrams of number of genes expressed in the indicated genotypes and treatments.

Because GN regulates protein trafficking to the plasma membrane (reviewed in (Richter et al., 2010; Luschnig and Vert, 2014); see also (Naramoto et al., 2014) and references therein), we expect genes encoding proteins which control vein patterning synergistically with auxin transport, whose expression is controlled by auxin signaling, and whose localization is controlled by GN to encode plasma-membrane-integral or secreted proteins. Therefore, by means of the SUBA4 tool (Hooper et al., 2017), we tested which of the 22 genes that are co-expressed with *GN*, *PINI* or *MP*, and whose expression was both ≥ 1.5 -fold lower in NPA-grown *tir1;afb2* than in NPA-grown WT and ≥ 1.5 -fold lower in PBA- and NPA-grown WT than in NPA-grown WT encoded proteins that are predicted to be localized to the plasma membrane or to be secreted to the extracellular space; we found eight such genes (Table 3.1).

3.2.2 Contribution of auxin signaling targets to vein patterning

Eight genes are co-expressed with *GN*, *PINI* or *MP*; their expression is lower in plants in which both auxin transport and auxin signaling are inhibited than in plants in which only auxin transport is inhibited; and they encode proteins that are predicted to be localized to the plasma membrane or to be secreted to the extracellular space (Table 3.1). Of these eight genes, one is *PINI*, one encodes a hydrolase, one a transmembrane protein, and five for leucine-rich-repeat receptor-like protein kinases (LRR-RLKs); we focused on three of these five LRR-RLKs, SCRAMBLED/STRUBBELIG (SCM/SUB; SCM hereafter) (Chevalier et al., 2005; Kwak et al., 2005), ERECTA (ER) (Torii et al., 1996) and ER-LIKE2 (ERL2) (Shpak et al., 2004), and on the PHLOEM INTERCALATED WITH XYLEM/TRACHEARY ELEMENT DIFFERENTIATION INHIBITORY FACTOR (TDIF) RECEPTOR (PXY/TDR; PXY hereafter) (AT5G61480) LRR-RLK, which is also a target of auxin signaling and has been shown to control vascular patterning in stem and hypocotyl (Fisher and Turner, 2007; Hirakawa et al., 2008; Suer et al., 2011). Were these genes mediating auxin signaling functions in vein patterning, their mutants would have vein patterning defects similar to those of auxin signaling mutants; we tested whether that were so. WT Arabidopsis (*Arabidopsis thaliana* (L.) Heynh) grown under normal conditions forms separate leaves whose vein patterns are defined by at least four reproducible features (Chapter 2) (Telfer and Poethig, 1994; Nelson and Dengler,

Table 3.1. Genes that are co-expressed with *GN*, *PIN1* or *MP*, whose expression was both ≥ 1.5 -fold lower in NPA-grown *tir1;afb2* than in NPA-grown WT and ≥ 1.5 -fold lower in PBA- and NPA-grown WT than in NPA-grown WT, and which encoded proteins that are predicted to be localized to the plasma membrane or to be secreted to the extracellular space.

Locus ID	Annotation	Predicted localization	Expression fold difference between NPA-grown <i>tir1;afb2</i> and NPA-grown WT; expression fold difference between PBA/ NPA-grown WT and NPA-grown WT
AT1G02690	IMPA-6 (Importin alpha isoform 6)	Nucleus	1.6; 1.9
AT1G07790	HTB1 (Histone superfamily protein)	Nucleus	1.7; 1.8
AT1G11130	SCRAMBLED/STRUBBELLIG (leucine-rich-repeat receptor-like kinase)	Plasma membrane	1.9; 1.6
AT1G19850	ARF5/MP (Transcriptional factor B3 family protein / auxin-responsive factor AUX/IAA-related)	Nucleus	2.6; 2.6
AT1G26540	Agenet domain-containing protein	Nucleus	1.8; 2.4
AT1G32190	Alpha/beta-hydrolase	Extracellular, plasma membrane	1.5; 1.8
AT1G33940	Serine/Threonine Kinase ULK-4 like protein	Nucleus	1.8; 1.5
AT1G57820	ORTH2/VIM1 (Zinc finger family protein)	Nucleus	1.7; 1.7
AT1G72670	iqd8 (IQ-domain 8)	Nucleus	1.6; 1.5
AT1G73590	PIN-FORMED1 (auxin efflux carrier)	Plasma membrane	1.9; 1.6

AT1G77470	EMB2810 / RFC3 / RFC5 (Replication factor C subunit 3)	Nucleus	1.5; 1.6
AT2G16270	Transmembrane protein	Nucleus	1.6; 1.9
AT2G26330	ERECTA (leucine-rich-repeat receptor-like kinase)	Plasma membrane	3.6; 3.1
AT2G34710	ATHB 14 (Homeobox-leucine zipper family protein)	Nucleus	1.5; 2.0
AT3G02640	Transmembrane protein	Plasma membrane	1.7; 1.5
AT3G21100	RNA-binding family protein	Nucleus	1.5; 1.9
AT3G61830	ARF18 (Auxin response factor 18)	Nucleus	1.5; 1.5
AT5G07180	ERECTA-LIKE2 (leucine-rich-repeat receptor-like kinase)	Plasma membrane	1.5; 2.9
AT5G48650	Nuclear transport factor 2 (NTF2) family protein with RNA binding domain	Nucleus	1.5; 1.8
AT5G51560	Leucine-rich-repeat receptor-like kinase	Plasma membrane	2.0; 1.7
AT5G51600	ATMAP65-3 (Microtubule associated family protein)	Cytosol	1.5; 1.5
AT5G62710	Leucine-rich-repeat receptor-like kinase	Plasma membrane	1.5; 2.0

1997; Kinsman and Pyke, 1998; Candela et al., 1999; Mattsson et al., 1999; Sieburth, 1999; Steynen and Schultz, 2003; Sawchuk et al., 2013; Verna et al., 2015) (Fig. 3.2A,E): (1) a narrow I-shaped midvein that runs the length of the leaf; (2) lateral veins that branch from the midvein and join distal veins to form closed loops; (3) minor veins that branch from midvein and loops and either end freely or join other veins; (4) minor veins and loops that curve near the leaf margin, lending a scalloped outline to the vein network.

Vein patterns of *tir1;afb2* and PBA-grown WT deviate from those of WT in two respects: (1) closed loops were often replaced by open loops, i.e. loops that contact the midvein or other loops at only one of their two ends, and (2) veins were often replaced by “vein fragments”, i.e. stretches of vascular elements that fail to contact other stretches of vascular elements at either one of their two ends (Chapter 2).

The vein patterns of *er* and *erl2* were no different from those of WT (Fig. 3.2E). By contrast, and as in *tir1;afb2* and PBA-grown WT (Chapter 2), in ~5–45% of the leaves of *er;erl2*, *scm* and *pxy* loops were open, midveins were Y-shaped and veins were fragmented (Fig. 3.2B–E). Furthermore, the vein pattern defects of *scm* were changed by mutation in *SUB RECEPTOR FAMILY3* (*SRF3*), one of the two *SCM*-related genes (Eyüboğlu et al., 2007; Kwak and Schiefelbein, 2007), though not by mutation in *SRF1*, the other *SCM*-related gene (Fig. 3.2E).

In conclusion, our results suggest that *ER* and *ERL2* (redundantly with each other), *SCM*, *SRF3* (redundantly with *SCM*) and *PXY* mediate auxin signaling functions in vein patterning.

3.2.3 Interaction between auxin signaling targets and auxin transport in vein patterning

ER and *ERL2* (redundantly with each other), *SCM* and *PXY* may mediate auxin signaling functions in vein patterning (Figure 3.2). Were these genes also controlling vein patterning synergistically with auxin transport, the vein pattern defects of their mutants would be enhanced by growth on NPA, which phenocopies loss of auxin-transport-dependent vein patterning activity (Chapter 2); we tested whether that were so.

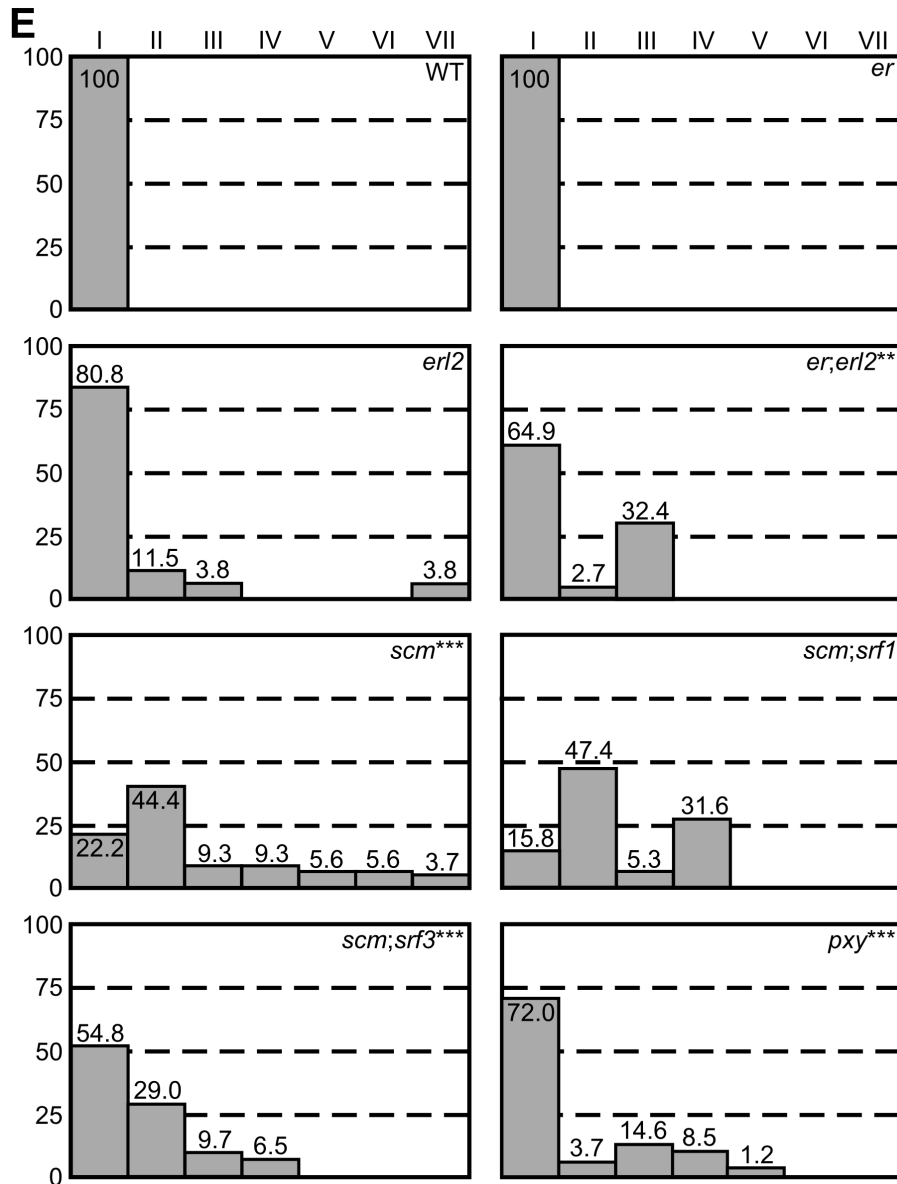
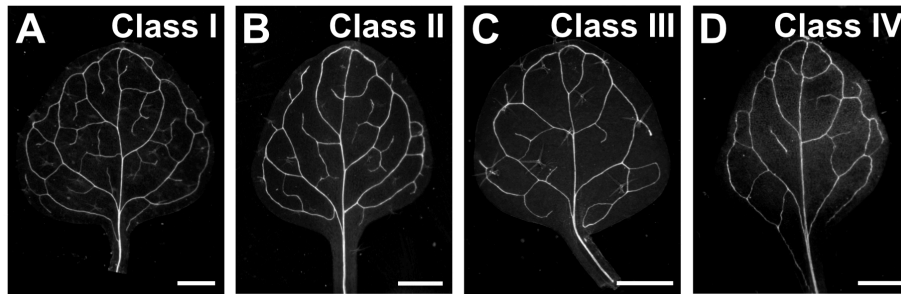


Figure 3.2. Contribution of auxin signaling targets to vein patterning. (A-D) Dark-field illumination of mature first leaves illustrating phenotype classes (top right): class I, narrow I-shaped midvein and scalloped vein-network outline (A); class II, open vein-network outline

(B); class III, Y-shaped midvein and scalloped vein-network outline (C); class IV, narrow I-shaped midvein and fragmented vein network (D); class V, Y-shaped midvein and open vein-network outline (not shown); class VI, fragmented vein network and open vein-network outline (not shown); class VII, Y-shaped midvein, fragmented vein network and open vein-network outline (not shown). (E) Percentages of leaves in phenotype classes. Difference between *er;erl2* and WT was significant at $P < 0.01$ (**), and between *scm* and WT, between *scm;srf3* and *scm* and between *pxy* and WT was significant at $P < 0.001$ (***) by Kruskal-Wallis and Mann-Whitney test with Bonferroni correction. Sample population sizes: WT, 32; *er*, 34; *erl2*, 52; *er;erl2*, 37; *scm*, 54; *scm;srf1*, 19; *scm;srf3*, 31; *pxy*, 35. Bars: (A–C) 0.5 mm; (D) 1 mm.

Consistent with previous reports (Mattsson et al., 1999; Sieburth, 1999) (Chapter 2), NPA only rarely induced leaf fusion but reproducibly induced characteristic vein-pattern defects in WT: (1) the vein network comprised more lateral veins; (2) lateral veins failed to join midvein but ran parallel to it to form a wide midvein; (3) lateral veins ended in a marginal vein that closely paralleled the leaf margin, lending a smooth outline to the vein network; (4) veins were thicker (Fig. 3.3A,C).

The vein pattern defects induced by NPA in *er*, *erl2*, *er;erl2* and *pxy* were no different from those induced by NPA in WT (Fig. 3.3C).

By contrast, the vein patterns of NPA-grown *scm* were intermediate between those of *scm* and of NPA-grown WT (Fig. 3.3B,C), suggesting that *scm* is, at least partially, insensitive to NPA.

In conclusion, the vein pattern defects of *er*, *erl2*, *er;erl2*, *scm* and *pxy* failed to be enhanced by growth on NPA, suggesting that the respective genes do not control vein patterning synergistically with auxin transport; however, it is possible that such synergistic function is masked by functional redundancy among those genes or with other members of their respective families.

3.2.4 PXY redundancy in vein patterning

The vein pattern defects of *pxy* fail to be enhanced by growth on NPA (Figure 3.3), suggesting that *PXY* does not control vein patterning synergistically with auxin transport; however, it is possible that such synergism is masked by redundant functions provided by *PXY*-related genes; we tested whether that were so.

To address this question, we reasoned that overexpression of the PXY ligands CLAVATA3/EMBRYO SURROUNDING REGION-RELATED (CLE) 41/44 and CLE42 (Hirakawa et al., 2008; Etchells and Turner, 2010) in the *pxy* background would lead to the defects that overexpression of CLE41, CLE42 and CLE44 induces in WT (Strabala et al., 2006; Etchells and Turner, 2010) only if these ligands were also perceived by PXY-related receptors.

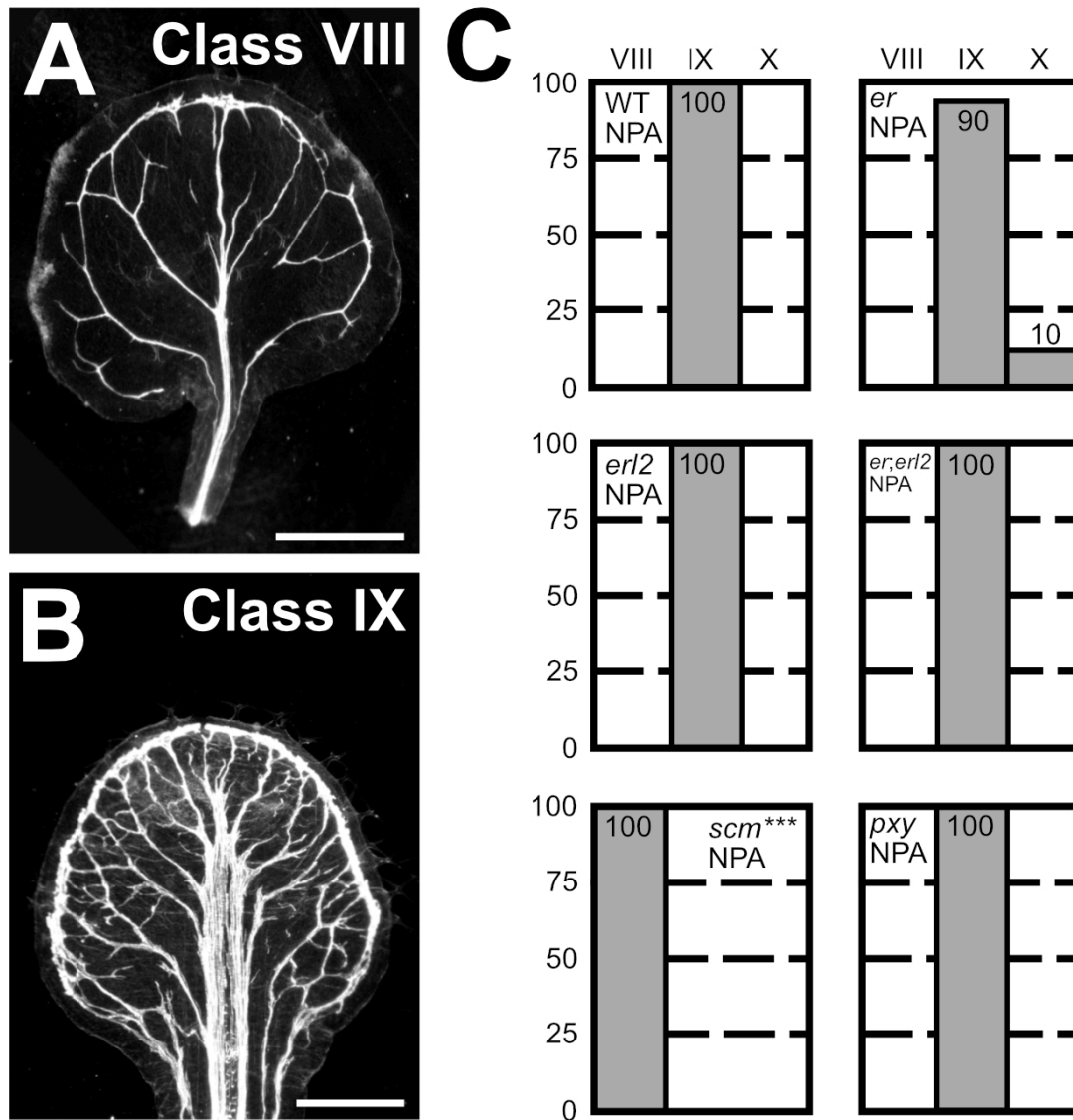


Figure 3.3. Contribution of auxin signaling targets and auxin transport to vein patterning. (A,B) Dark-field illumination of mature first leaves illustrating phenotype classes (top right): class VIII, narrow midvein and apically thickened marginal vein (A); class IX, wide midvein, more lateral-veins and conspicuous marginal vein (B); class X, fused leaves with wide midvein, more lateral-veins and conspicuous marginal vein (not shown). (C) Percentages of leaves in phenotype classes. Difference between NPA-grown *scm* and NPA-grown WT was significant at $P < 0.001$ (***) by Kruskal-Wallis and Mann-Whitney test with Bonferroni correction. Sample population sizes: NPA-grown WT, 34; NPA-grown *er*, 30; NPA-grown *erl2*, 22; NPA-grown *er;erl2*, 23; NPA-grown *scm*, 25; NPA-grown *pxy*, 34. Bars: (A,B) 1 mm.

A similar approach had been used to identify TDR/PXY as the TDIF/CLE41/44 receptor: *tdr/pxy* turned out to be the only mutant that was resistant to the effects of TDIF/CLE41/44 application (Hirakawa et al., 2008). Therefore, we overexpressed *CLE41*, *CLE42* and *CLE44* in the *pxy* background by the broadly active *MP*, *RIBOSOMAL PROTEIN S5A* (RPS5A) and *UBIQUITIN10* (*UBQ10*) promoters (Weijers et al., 2001; Donner et al., 2009; Sawchuk et al., 2013). We then compared vein patterns of mature leaves of *pxy*, *MP::CLE41;pxy*, *RPS5A::CLE41;pxy*, *UBQ10::CLE41;pxy*, *MP::CLE42;pxy*, *RPS5A::CLE42;pxy*, *UBQ10::CLE42;pxy*, *MP::CLE44;pxy*, *RPS5A::CLE44;pxy* and *UBQ10::CLE44;pxy*. In addition, we overexpressed in the *pxy* background *CLE43*, which is related to *CLE41*, *CLE42* and *CLE44* (Ito et al., 2006; Strabala et al., 2006; Whitford et al., 2008), and analyzed vein patterns of mature leaves of *MP::CLE43;pxy* and *UBQ10::CLE43;pxy*.

Because the vein patterns of all transgenics except *UBQ10::CLE41;pxy*, *RPS5A::CLE42;pxy* and *MP::CLE44;pxy* were no different from those of *pxy* (Figure 3.4), it is unlikely that the vein pattern defects of *pxy* failed to be enhanced by growth on NPA because of redundant functions provided by *PXY*-related genes; rather, our results suggest that *PXY* and related genes do not control vein patterning synergistically with auxin transport.

3.2.5 Conclusions and prospects

We sought to identify targets of auxin signaling which control vein patterning synergistically with auxin transport and whose localization is controlled by GN.

We have identified four auxin-signaling-dependent genes that control vein patterning: *ER* and *ERL2* (redundantly with each other), *SCM* and *PXY*. Though our results suggest that none of these genes seem to control vein patterning synergistically with auxin transport, it is possible that such synergism is masked by functional redundancy among these genes or, at least for *ER*, *ERL2* and *SCM*, with other members of their respective families. This may especially be so for *SCM*, which functions redundantly with the related *SRF3* in vein patterning, and whose mutant is, at least partially, insensitive to auxin transport inhibition, a feature shared with, for example, *tir1* (Ruegger et al., 1997). In the future, it would be interesting to generate high-order mutants in *ER*, *ERL2* and related genes, and in *SCM*, *SRF3*

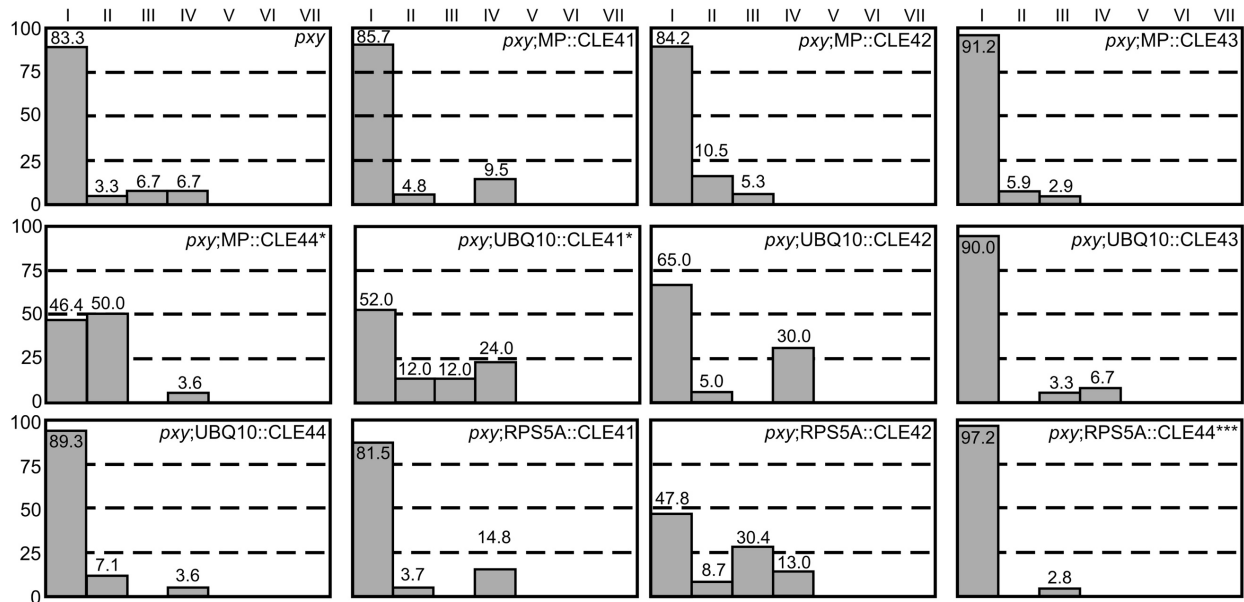


Figure 3.4. *PXY* redundancy to vein patterning. Percentages of leaves in phenotype classes (defined in Fig. 3.2). Difference between *pxy;RPS5A::Cle44* and *pxy* was significant at $P < 0.001$ (***) and difference between *pxy;MP::Cle44* and *pxy*, between *pxy;UBQ10::Cle41* and *pxy* was significant at $P < 0.05$ (*) by Kruskal-Wallis and Mann-Whitney test with Bonferroni correction. Sample population sizes: *pxy*, 30; *pxy;MP::Cle41*, 21; *pxy;MP::Cle42*, 19; *pxy;MP::Cle43*, 34; *pxy;MP::Cle44*, 28; *pxy;UBQ10::Cle41*, 25; *pxy;UBQ10::Cle42*, 20; *pxy;UBQ10::Cle43*, 30; *pxy;UBQ10::Cle44*, 28; *pxy;RPS5A::Cle41*, 27; *pxy;RPS5A::Cle42*, 23; *pxy;RPS5A::Cle44*, 36;

and related genes, analyze their vein patterns, and test whether their vein pattern defects are enhanced by growth in the presence of auxin transport inhibitors.

ER, ERL2, SCM and PXY are predicted to localize to the plasma membrane, but clear evidence of such localization is only available for SCM (Kwak and Schiefelbein, 2008; Yadav et al., 2008) and TDR/PXY (Hirakawa et al., 2008). In the future, it would be interesting to test whether ER and ERL2 indeed localize to the plasma membrane and whether the localization of ER, ERL2, SCM and PXY depends on GN.

3.3 Materials & Methods

3.3.1 Plants

Origin and nature of lines, genotyping strategies and oligonucleotide sequences are Table 3.2, Table 3.3 and Table 3.4, respectively. Seeds were sterilized and sown as in (Sawchuk et al. 2008). Stratified seeds were germinated, and seedlings were grown at 22°C under continuous fluorescent light ($\sim 80 \mu\text{mol m}^{-2} \text{s}^{-1}$). Plants were grown at 25°C under fluorescent light ($\sim 110 \mu\text{mol m}^{-2} \text{s}^{-1}$) in a 16-h-light/8-h-dark cycle. Plants were transformed and representative lines were selected as in (Sawchuk et al., 2008).

3.3.2 Imaging

Mature leaves were fixed in 6 : 1 ethanol : acetic acid, rehydrated in 70% ethanol and in water, cleared briefly (few seconds to few minutes) in 0.4 M sodium hydroxide, washed in water and mounted in 1 : 3 : 8 water : glycerol : chloral hydrate. Mounted leaves were imaged as in (Odat et al. 2014). Image brightness and contrast were adjusted by linear stretching of the histogram in the Fiji distribution (Schindelin et al., 2012) of ImageJ (Schindelin et al., 2015; Rueden et al., 2017; Schneider et al., 2012).

3.3.3 RNA isolation and sequencing

Total RNA was extracted as in (Chomczynski and Sacchi, 1987) from 4-day-old leaves of seedlings grown in half-strength Murashige and Skoog salts, 15 g l⁻¹ sucrose, 0.5 g l⁻¹ MES,

pH 5.7, at 23°C under continuous light ($\sim 80 \mu\text{mol m}^{-2} \text{s}^{-1}$) on a rotary shaker at 50 rpm. DNA was removed with Invitrogen's TURBO DNA-free TM kit, and RNA quality was evaluated with an RNA 6000 Nano chip on an Agilent 2100 Bioanalyzer. RNA samples were delivered to the service provider BGI (Shenzen, China), where it was sequenced using a BGISEQ instrument, with a single-end, 50 bp protocol.

3.3.4 Gene expression analysis

Clean reads, from which primers and low-quality bases had been trimmed, were delivered by the service provider as fastq files. Analysis was done by Dr. M. K. Deyholos (University of British Columbia). The fastq files were uploaded to NCBI SRA (PRJNA432269) and were mapped to the Arabidopsis reference genome (Lamesch et al., 2012, TAIR10 Release, <https://phytozome.jgi.doe.gov/>) using HISAT2 (Kim et al., 2015) with default parameters. The resulting SAM files were sorted using samtools (view -Su , sort) (Li et al., 2009), and the sorted output, along with the current Arabidopsis genome annotation (TAIR10 Release downloaded from <https://phytozome.jgi.doe.gov> in .gff3 format) were used as input for the StringTie assembler (Pertea et al., 2016), and differential gene expression was calculated using cuffdiff (Trapnell et al., 2012).

Table 3.2. Origin and nature of lines.

Line	Origin/Nature
<i>er-105</i>	ABRC; (Torii et al., 1996)
<i>erl2-1</i>	ABRC; (Shpak et al., 2004)
<i>er-105;erl2-1</i>	(Shpak et al., 2004)
<i>pxy-3</i>	ABRC; (Fisher et al., 2007)
<i>scm-2</i>	ABRC; (Kwak et al., 2005)
<i>tir1-1;afb2-3</i>	(Savaldi-Goldstein et al., 2008)
UBQ10:: <i>CLE41</i>	Transcriptional fusion of <i>UBQ10</i> (AT4G05320; -1516 to -1; primers: ‘UBQ10 HindIII Forw’ and ‘UBQ10 SmaI Rev’) to the sequence encoding <i>CLE41</i> (AT3G24770; primers ‘CLE41 Kpn1 FP’ and ‘CLE41 BamH1 RP’)
UBQ10:: <i>CLE42</i>	Transcriptional fusion of <i>UBQ10</i> (AT4G05320; -1516 to -1; primers: ‘UBQ10 HindIII Forw’ and ‘UBQ10 SmaI Rev’) to the sequence encoding <i>CLE42</i> (AT2G34925; primers ‘CLE42 Kpn1 FP’ and ‘CLE42 BamH1 RP’)
UBQ10:: <i>CLE43</i>	Transcriptional fusion of <i>UBQ10</i> (AT4G05320; -1516 to -1; primers: ‘UBQ10 HindIII Forw’ and ‘UBQ10 SmaI Rev’) to the sequence encoding <i>CLE43</i> (AT1G25425; primers ‘CLE43 KPN1 Fwd’ and ‘CLE43 BAMH1 Rev’)
UBQ10:: <i>CLE44</i>	Transcriptional fusion of <i>UBQ10</i> (AT4G05320; -1516 to -1; primers: ‘UBQ10 HindIII Forw’ and ‘UBQ10 SmaI Rev’) to the sequence encoding <i>CLE44</i> (AT4G13195; primers ‘CLE44 KPN1 Fwd’ and ‘CLE44 BAMH1 Rev’)
MP:: <i>CLE41</i>	Transcriptional fusion of <i>MP</i> (AT1G18950; -3281 to -1; primers: ‘MP Sall Fwd’ and ‘MP BamHI Rev’) to the sequence encoding <i>CLE41</i> (AT3G24770; primers ‘CLE41 BamH1 FP’ and ‘CLE41 Kpn1 RP’)
MP:: <i>CLE42</i>	Transcriptional fusion of <i>MP</i> (AT1G18950; -3281 to -1; primers: ‘MP Sall Fwd’ and ‘MP BamHI Rev’) to the sequence encoding <i>CLE42</i> (AT2G34925; primers ‘CLE42 BamH1 FP’ and ‘CLE42 Kpn1 RP’)

MP::CLE43	Transcriptional fusion of <i>MP</i> (AT1G18950; -3281 to -1; primers: ‘MP Sall Fwd’ and ‘MP BamHI Rev’) to the sequence encoding <i>CLE43</i> (AT1G25425; primers ‘CLE43 BAMH1 Fwd’ and ‘CLE43 KPN1 Rev’)
MP::CLE44	Transcriptional fusion of <i>MP</i> (AT1G18950; -3281 to -1; primers: ‘MP Sall Fwd’ and ‘MP BamHI Rev’) to the sequence encoding <i>CLE44</i> (AT4G13195; primers ‘CLE44 BAMH1 Fwd’ and ‘CLE44 KPN1 Rev’)
RPS5A::CLE41	Transcriptional fusion of <i>RPS5A</i> (AT3G11940; -2236 to -1; primers: ‘RPS5A SmaI Forw’ and ‘RPS5A SmaI Rev’) to the sequence encoding <i>CLE41</i> (AT3G24770; primers ‘CLE41 BamH1 FP’ and ‘CLE41 BamH1 RP’)
RPS5A::CLE42	Transcriptional fusion of <i>RPS5A</i> (AT3G11940; -2236 to -1; primers: ‘RPS5A SmaI Forw’ and ‘RPS5A SmaI Rev’) to the sequence encoding <i>CLE42</i> (AT2G34925; primers ‘CLE42 BamH1 FP’ and ‘CLE42 BamH1 RP’)
RPS5A::CLE44	Transcriptional fusion of <i>RPS5A</i> (AT3G11940; -2236 to -1; primers: ‘RPS5A SmaI Forw’ and ‘RPS5A SmaI Rev’) to the sequence encoding <i>CLE44</i> (AT4G13195; primers ‘CLE44 BAMH1 Fwd’ and ‘CLE44 BAMH1 Rev’)

Table 3.3. Genotyping strategies.

Line	Strategy
<i>erl2-1</i>	<i>ERL2</i> : ‘erl 2- 1 erl2g2166’ and ‘erl 2-1 ertj3182’; <i>erl2-1</i> : ‘erl 1- 2 JL202’ and ‘erl2-1 ertj3182’
<i>pxy-3</i>	<i>PXY</i> : ‘SEQ. P_ SALK_ 026128 LP’ and ‘SEQ. P_ SALK_ 026128 RP’; <i>pxy-3</i> : ‘LBb1.3’ and ‘SEQ. P_ SALK_ 026128 RP’
<i>scm-2</i>	<i>SCM</i> : ‘scm-2 SALK_ 086357 LP’ and ‘scm-2 SALK_ 086357 RP’; <i>scm-2</i> : ‘LBb1.3’ and ‘scm-2 SALK_ 086357 RP’
<i>tir1-1</i>	‘tir1-1F2’ and ‘tir1-1R2’; <i>BsaI</i>
<i>afb2-3</i>	<i>AFB2</i> : ‘AFB2+F’ and ‘AFB2-TR’; <i>afb2-3</i> : ‘pROK-LB’ and ‘AFB2-TR’

Table 3.4. Oligonucleotide sequences.

Name	Sequence (5' to 3')
UBQ10 HindIII Forw	CTCAAGCTTTCCCATGTTTCTCGTCTGTC
UBQ10 SmaI Rev	CGACCCGGGCTGTTAATCAGAAAACTCAG
CLE 41 Kpn1 FP	GTCGGTACCATGGCAACATCAAATGAC
CLE 41 BamH1 RP	GCTGGATCCCTAGTTGGAAATAGGGTTTGGAC
CLE 42 Kpn1 FP	CGTGGTACCATGAGATCTCCTCACATCACC
CLE 42 BamH1 RP	GACGGATCCCTACCTATTGGAGATGG
CLE 43 KPN1 Fwd	GGCGGTACCATGGGTTGTCGAGATATTCTGTTG
CLE 43 BAMH1 Rev	CGAGGATCCCTAGTTATGAAGGCGATCCGG
CLE 44 KPN1 Fwd	GCGGGTACCATGGCAACTACAATTGATCAAACCAG
CLE 44 BAMH1 Rev	GCGGGATCCTCAGTTGGAGATAGGGTTTGGACC
MP SalI Fwd	TAGGGATCCACAGAGAGATTTTTCAATGTTCTG
MP BamHI Rev	TATGTCGACCCCGGGTTAATCAGTATTATTAC
CLE 41 BamH1 FP	GCTGGATCCATGGCAACATCAAATG
CLE 41 Kpn1 RP	GCGGGTACCCTAGTTGGAAATAGGGTTTGGACC
CLE 42 BamH1 FP	GTCGGATCCATGAGATCTCCTCACATCACCA
CLE 42 Kpn1 RP	GGCGGTACCCTACCTATTGGAGATGGGATTT
CLE 43 BAMH1 Fwd	GCGGGATCCATGGGTTGTCGAGATATTCTGTTG
CLE 43 KPN1 Rev	GCCGGTACCCTAGTTATGAAGGCGATCCGG
CLE 44 BAMH1 Fwd	GCGGGATCCATGGCAACTACAATTGATCAAACCAG
CLE 44 KPN1 Rev	GCGGGTACCTCAGTTGGAGATAGGGTTTGGACC
RPS5A SmaI Forw	ATACCCGGAGCAGGAGATCTATCAGTG
RPS5A SmaI Rev	ATACCCGGGGGCTGTGGTGAGAGAAAC
erl 2- 1 erl2g2166	GCCTATTCCACCAATACTTG

erl 2-1 ertj3182	ACAAATCTGAGAGAGTTAATGCAAAGCAG
erl 1- 2 JL202	CATTTTATAATAACGCTGCGGACATCTAC
SEQ. P_ SALK_026128 LP	CCCCACACAAAACCATAATG
SEQ. P_ SALK_026128 RP	AAAAATCGAGAAGCTTGAGGG
scm-2 SALK_086357 LP	G TTCCTGTGAGCTTGTTGTCC
scm-2 SALK_086357 RP	TATCACTTTGGGAGCACCATC
LBb1.3	ATTTTGCCGATTTCGGAAC
tir1-1F2	AGCGACGGTGATTAGGAGG
tir1-1R2	CAGGAACAACGCAGCAAAA
AFB2+F	TTCTCCTTCGATCATTGTCAAC
AFB2-TR	TAGCGGCAATAGAGGCAAGA
pROK-LB	GGAACCACCATCAAACAGGA

Chapter 4: GAL4/GFP enhancer-trap lines for identification and manipulation of cells and tissues in developing Arabidopsis leaves

4.1 Introduction

The ability to unambiguously identify cells and tissues at different stages of their development and to selectively manipulate their properties is key to our understanding of developmental processes. Both means can most efficiently be acquired through a single GAL4 system (Brand and Perrimon, 1993). In the original system or one of its variations, a minimal promoter in a construct randomly inserted in a genome responds to neighboring regulatory elements and activates the expression of a gene — included in the same construct — encoding a variant of the GAL4 transcription factor of yeast; the same construct also includes a GAL4-responsive, UAS-driven lacZ, GUS or GFP, which reports GAL4 expression. Independent, wild-type-looking lines, in which the construct is inserted in different genomic locations, are selected that reproducibly express GAL4/reporter in cell-, tissue- or stage-specific patterns, and can thus be used to identify those cells, tissues or stages and to drive GAL4-responsive cell-, tissue- or stage-specific expression in wild-type or, by crossing, in mutants and transgenics (e.g., (Halder et al., 1995; Ito et al., 1997)).

The first implementation of the GAL4 system in Arabidopsis (*Arabidopsis thaliana* (L.) Heynh) was the Haseloff collection of GAL4/GFP enhancer-trap lines, in which an endoplasmic-reticulum-localized GFP (erGFP) responds to the activity of a fusion between the GAL4 DNA-binding domain and the activating domain of the Viral Protein 16 of *Herpes simplex* (Haseloff, 1999). The Haseloff collection is still the most extensively used GAL4 system in Arabidopsis (e.g., (Sabatini et al., 1999; Weijers et al., 2003; Laplaze et al., 2005; Sawchuk et al., 2007; Gardner et al., 2009; Wenzel et al., 2012)), even though it is in the C24 background. This can be problematic because the phenotype of hybrids between C24 and Columbia-0 (Col-0), generally considered the reference genotype in Arabidopsis (Koornneef and Meinke, 2010), is different from that of either parent (e.g., (Groszmann et al., 2014; Kawanabe et al., 2016; Zhang et al., 2016)); the use of GAL4/GFP enhancer-trap lines in the C24 background to investigate processes in the Col-0 background thus imposes the burden of

ad-hoc and laborious generation of proper control backgrounds. Therefore, most desirable is the generation and characterization of GAL4/GFP enhancer-trap collections in the Col-0 background. Two such collections have been reported: the Berleth collection, which has been used to identify lines that express GAL4/GFP in vascular tissues (Ckurshumova et al., 2009), and the Poethig collection, which has been used to identify lines that express GAL4/GFP in stomata (Gardner et al., 2009).

Here we screened the Poethig collection and provide a set of lines for the specific labeling of cells and tissues during leaf development, and we show that these lines can be used to address key questions in plant developmental biology.

4.2 Results and discussion

To identify enhancer-trap lines in the Columbia background of Arabidopsis with reproducible GAL4-driven GFP expression in developing leaves, we screened the collection generated and donated by Scott Poethig to the Arabidopsis Biological Resource Center. We screened 312 lines for GFP expression in developing leaves; 29 lines satisfied this criterion (Table 4.1). In 10 of these 29 lines, GFP was expressed in specific cells or tissues; nine of these 10 lines grew normally (Table 4.1). We imaged GFP expression in first leaves of these nine lines from 2 to 5 days after germination (DAG).

The development of Arabidopsis leaves has been described previously (Pyke et al., 1991; Telfer and Poethig, 1994; Larkin et al., 1996; Kinsman and Pyke, 1998; Candela et al., 1999; Donnelly et al., 1999; Mattsson et al., 1999; Kang and Dengler, 2002; Mattsson et al., 2003; Kang and Dengler, 2004; Scarpella et al., 2004). Briefly, at 2 DAG the first leaf is recognizable as a cylindrical primordium with a midvein at its center (Fig. 4.1A). By 2.5 DAG, the primordium has elongated along the apical-basal axis and has expanded laterally (Fig. 4.1B). By 3 DAG, the first loops of veins (“first loops”) have formed (Fig. 4.1C). By 4 DAG, a lamina and a petiole have become recognizable, second loops have formed, and minor veins have started to form in the top half of the lamina (Fig. 4.1D). By 5 DAG, lateral outgrowths (“teeth” or hydathodes) have become recognizable in the bottom quarter of the lamina, third loops have formed, and minor vein formation has started to

Table 4.1. Origin and nature of lines.

ABRC stock no.	Donor stock no.	Expression in developing leaves	Tissue- and/or stage-specific expression	Wild-type looking
CS24240	E53	N		
CS24241	E306	N		
CS24242	E337	N		
CS24243	E362	N		
CS24244	E456	N		
CS24245	E513	N		
CS24246	E652	N		
CS24247	E751	N		
CS24248	E788	N		
CS24249	E829	N		
CS24250	E1012	N		
CS24251	E1075	N		
CS24252	E1195	N		
CS24253	E1247	N		
CS24254	E1287	N		
CS24255	E1324	N		
CS24256	E1332	Y	N	
CS24257	E2042	N		
CS24258	E2065	N		
CS24259	E2072	N		
CS24260	E2119	N		
CS24262	E2168	N		
CS24264	E2242	N		
CS24265	E2263	N		
CS24266	E2271	N		
CS24267	E2306	N		
CS24269	E3191	N		
CS24270	E3597	N		
CS24271	E3604	N		
CS24272	E4259	Y	Y	Y
CS65892	E2331	Y	Y	Y
CS65893	E2023	N		
CS67882	suo-1	N		
CS70001	E1	N		

CS70002	E3	N		
CS70003	E63	N		
CS70004	E66	N		
CS70005	E74	Y	N	
CS70006	E829	N		
CS70007	E100	Y	Y	Y
CS70008	E103	N		
CS70009	E105	N		
CS70010	E107	N		
CS70011	E135	N		
CS70012	E144	N		
CS70013	E183	N		
CS70014	E191	N		
CS70015	E226	N		
CS70016	E227	Y	N	
CS70017	E230	N		
CS70018	E232	N		
CS70019	E242	N		
CS70020	E244	N		
CS70021	E254	N		
CS70022	E259	Y	N	
CS70023	E268	N		
CS70024	E280	N		
CS70025	E292	N		
CS70026	E314	N		
CS70027	E325	N		
CS70028	E336	N		
CS70029	E340	Y	N	
CS70030	E361	N		
CS70031	E387	N		
CS70032	E434	N		
CS70033	E457	N		
CS70034	E461	N		
CS70035	E462	N		
CS70036	E464	N		
CS70037	E470	N		
CS70038	E491	N		
CS70039	E555-1	N		

CS70040	E555-2	N		
CS70041	E556	N		
CS70042	E583	N		
CS70043	E655	N		
CS70044	E657	Y	N	
CS70045	E658	N		
CS70046	E668	N		
CS70047	E698	N		
CS70048	E700	N		
CS70049	E719	N		
CS70050	E744	N		
CS70051	E771	N		
CS70052	E790	N		
CS70053	E835	N		
CS70054	E838	N		
CS70055	E861	Y	Y	Y
CS70056	E864	N		
CS70057	E876	N		
CS70058	E884	N		
CS70059	E892	N		
CS70060	E894	N		
CS70061	E903	N		
CS70062	E910	N		
CS70063	E912	N		
CS70065	E939	N		
CS70066	E940	N		
CS70067	E945	N		
CS70068	E951	N		
CS70069	E992	N		
CS70070	E994	N		
CS70071	E1049	N		
CS70072	E1092	N		
CS70073	E1100	N		
CS70074	E1127	N		
CS70075	E1128	N		
CS70076	E1130	N		
CS70077	E1155	N		
CS70078	E1161	N		

CS70079	E1176	N		
CS70080	E1222	N		
CS70081	E1223	N		
CS70082	E1237	N		
CS70083	E1238	N		
CS70084	E1250	N		
CS70085	E1252	N		
CS70086	E1271	N		
CS70087	E1289	Y	N	
CS70088	E1304	N		
CS70089	E1322	N		
CS70090	E1325	N		
CS70091	E1331	N		
CS70092	E1341	N		
CS70093	E1344	N		
CS70094	E1356	N		
CS70095	E1361	N		
CS70096	E1362	N		
CS70097	E1370	N		
CS70098	E1387	N		
CS70099	E1388	N		
CS70100	E1395	N		
CS70101	E1396	N		
CS70102	E1405	N		
CS70103	E1416	N		
CS70104	E1439	N		
CS70105	E1439m	N		
CS70106	E1457	N		
CS70107	E1567	N		
CS70108	E1570	N		
CS70109	E1607	N		
CS70110	E1626	N		
CS70111	E1627	N		
CS70112	E1628	N		
CS70113	E1638	N		
CS70114	E1644	N		
CS70115	E1662	N		
CS70116	E1663	Y	N	

CS70117	E1665	N		
CS70118	E1678	N		
CS70119	E1684	N		
CS70120	E1689	N		
CS70121	E1691	N		
CS70122	E1701	N		
CS70123	E1728	N		
CS70125	E1751	N		
CS70126	E1765	N		
CS70127	E1767	N		
CS70128	E1785	N		
CS70129	E1786	N		
CS70130	E1797	N		
CS70131	E1801	N		
CS70132	E1809	N		
CS70133	E1815	N		
CS70134	E1817	N		
CS70135	E1818	N		
CS70136	E1819	N		
CS70137	E1825	N		
CS70138	E1828	N		
CS70139	E1832	N		
CS70140	E1833	N		
CS70141	E1853	N		
CS70142	E1868	N		
CS70143	E1950	N		
CS70144	E1998	N		
CS70145	E2034	N		
CS70146	E217	N		
CS70147	E562	N		
CS70148	E1001	N		
CS70149	E1368	N		
CS70150	E1690	N		
CS70151	E1704-1	N		
CS70152	E1704-3	N		
CS70153	E1715	N		
CS70154	E1723	N		
CS70155	E1735	N		

CS70156	E1935	N		
CS70157	E1967	N		
CS70158	E2014	N		
CS70159	E2057	N		
CS70160	E2207	N		
CS70161	E2406	N		
CS70162	E2408	Y	Y	Y
CS70163	E2410	N		
CS70164	E2415	N		
CS70165	E2425	N		
CS70166	E2425	N		
CS70167	E2441	N		
CS70168	E2443	N		
CS70169	E2448	N		
CS70170	E2491	N		
CS70171	E2502	N		
CS70172	E2513	N		
CS70173	E2563	N		
CS70174	E2609	N		
CS70175	E2633	N		
CS70176	E2676	N		
CS70177	E2692	Y	N	
CS70178	E2724	N		
CS70179	E2763	N		
CS70180	E2764	N		
CS70181	E2779	N		
CS70182	E2861	N		
CS70183	E2862	N		
CS70184	E2897	N		
CS70185	E2904	N		
CS70186	E2905	N		
CS70187	E2947	N		
CS70188	E2993	N		
CS70189	E3004	N		
CS70190	E3006	N		
CS70191	E3017	N		
CS70192	E3065	N		
CS70193	E3134	N		

CS70194	E3190	N		
CS70195	E3198	N		
CS70196	E3258	N		
CS70197	E3267	N		
CS70198	E3298	N		
CS70199	E3313	N		
CS70200	E3317	Y	Y	N
CS70201	E3430	N		
CS70202	E3459	N		
CS70203	E3462	N		
CS70204	E3474	N		
CS70205	E3478	N		
CS70206	E3501	N		
CS70207	E3505	N		
CS70208	E3530	N		
CS70209	E3531	N		
CS70210	E3598-1	N		
CS70211	E3598-2	N		
CS70212	E3637	N		
CS70213	E3642	N		
CS70214	E3655	Y	N	
CS70215	E3683	N		
CS70216	E3700	N		
CS70217	E3754	N		
CS70218	E3756	N		
CS70219	E3783	Y	N	
CS70220	E3806	N		
CS70221	E3816	N		
CS70222	E3826	N		
CS70223	E3876	N		
CS70224	E3879	N		
CS70225	E3880	N		
CS70226	E3885	Y	N	
CS70227	E3912	Y	Y	Y
CS70228	E3927	N		
CS70229	E3930	Y	N	
CS70230	E3963	N		
CS70231	E3980	N		

CS70232	E4009	N		
CS70233	E4028	Y	N	
CS70234	E4058	N		
CS70235	E4096	N		
CS70236	E4104	N		
CS70237	E4105	N		
CS70238	E4110	N		
CS70239	E4118	Y	N	
CS70240	E4129	N		
CS70241	E4148	N		
CS70242	E4150	N		
CS70243	E4151	N		
CS70244	E4162	N		
CS70245	E4223	N		
CS70246	E4247	N		
CS70247	E4256	N		
CS70248	E4272	N		
CS70249	E4285	N		
CS70250	E4295	Y	Y	Y
CS70251	E4350	N		
CS70252	E4396	N		
CS70253	E4411	N		
CS70254	E4423	N		
CS70255	E4491	N		
CS70256	E4506	Y	N	
CS70257	E4522	Y	N	
CS70258	E4583	N		
CS70259	E4589	N		
CS70260	E4633	N		
CS70261	E4680	N		
CS70262	E4695	N		
CS70263	E4715	N		
CS70264	E4716	Y	Y	Y
CS70265	E4722	Y	Y	YY
CS70266	E4751	N		
CS70267	E4791	N		
CS70268	E4801	N		
CS70269	E4811	N		

CS70270	E4812	N		
CS70271	E4820	N		
CS70272	E4856	Y	N	
CS70273	E4907	N		
CS70274	E4930	N		
CS70275	E4940	N		
CS70276	E4970	N		
CS70277	E5008	N		
CS70278	E5025	N		
CS70279	E5026	N		
CS70280	E5085	N		
CS70281	E5096	Y	N	

N, No; Y, Yes.

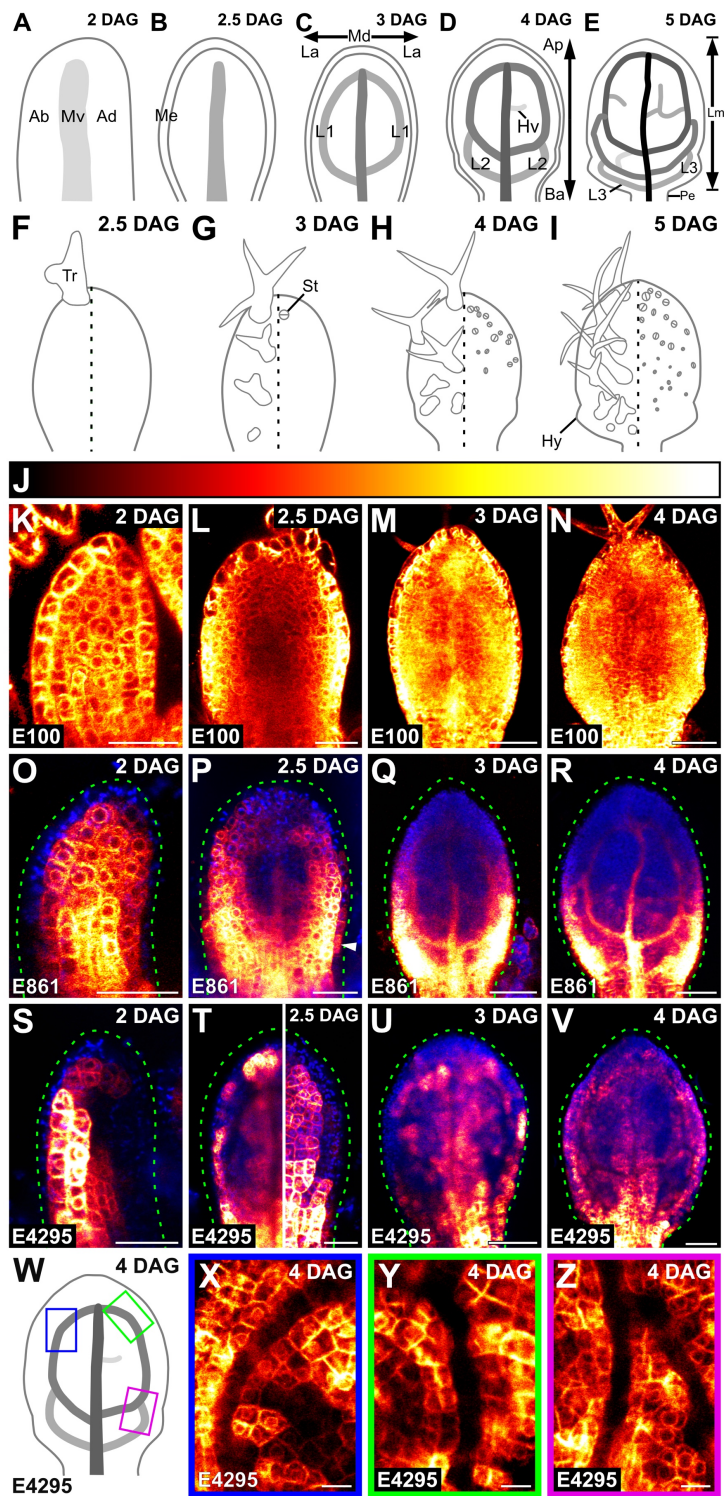


Figure 4.1. Expression of E100>>, E861>> and E4295>>erGFP in Arabidopsis leaf development. (A–Z) First leaves. Top right: leaf age in days after germination (DAG). (A–E) Development of leaf and veins; increasingly darker grays depict progressively later stages

of vein development. See text for details. (F–I) Development of trichomes and stomata in adaxial (left) or abaxial (right) epidermis. See text for details. Ab: abaxial; Ad: adaxial; Ap: apical; Ba: basal; Hv: minor vein; Hy: hydathode; L1, L2 and L3: first, second and third loop; La: lateral; Lm: Lamina; Md: median; Me: marginal epidermis; Mv: midvein; Pe: Petiole; St: stoma; Tr: trichome. (K–V,X–Z) Confocal laser scanning microscopy. Bottom left: genotype. Look-up table (ramp in J) visualizes erGFP expression levels. Blue: autofluorescence. Dashed green line delineates leaf outline. White arrowhead points to epidermal expression. (K–S,U,V,X–Z) Median view (abaxial side to the left in K,O,S). (T) Median (left) and abaxial subepidermal (right) views. (W) Increasingly darker grays depict progressively later stages of vein development. Boxes illustrate positions of closeups in X,Y and Z. See Table 4.2 for reproducibility of expression features. Bars: (K,L,O,P,S,T) 30 μm ; (M,N,Q,R,U,V) 60 μm ; (X–Z) 10 μm .

Table 4.2. Reproducibility of expression and pattern features

Figure	Panel	Reproducibility of expression or pattern features (No. leaves showing the displayed features / No. of analyzed leaves)	Assessed expression or pattern features
1	K	15/18	Ubiquitous
1	L	15/17	Ubiquitous
1	M	19/19	Ubiquitous
1	N	33/33	Ubiquitous
1	O	26/29	Inner cells
1	P	29/29	Veins in the top half of the primordium, inner cells in the basal half of the primordium
1	Q	31/31	Veins in the top half of the primordium, inner cells in the basal half of the primordium
1	R	19/19	Veins in the top half of the leaf, inner cells in the basal half of the leaf
1	S	16/19	Abaxial inner cells
1	T	34/36	Abaxial inner cells and middle tissue layer
1	U	24/25	Abaxial inner cells and middle tissue layer
1	V	34/34	Abaxial inner cells and middle tissue layer
1	X	14/14	Inner, non-vascular cells

1	Y	14/14	Inner, non-vascular cells
1	Z	14/14	Inner, non-vascular cells
2	A	22/28	Top third of adaxial epidermis and whole abaxial epidermis
2	B, left	22/23	Top three-quarters of epidermis, and trichomes
2	B, right	30/30	Whole epidermis
2	C, left	14/14	Top three-quarters of epidermis, and trichomes
2	C, right	15/15	Whole epidermis
2	D, left	16/16	Epidermis of whole lamina and petiole midline, and trichomes
2	D, right	18/18	Whole epidermis
2	E	16/16	Trichomes
2	F	17/18	Top three-quarters of marginal epidermis
2	G	14/14	Whole marginal epidermis
2	H	16/16	Whole marginal epidermis
2	I	59/59	All epidermal cells
2	J, left	42/42	All cells of marginal epidermis, except a few cells in top half of primordium
2	J, right	45/45	All epidermal cells
2	K, left	33/38	Bottom quarter and a few cells in top three-quarters of marginal epidermis
2	K, right	21/21	All epidermal cells, including stomata

2	L, left	31/31	Bottom quarter and a few cells in top three-quarters of marginal epidermis
2	L, right	21/21	All epidermal cells, including stomata
2	M	29/30	Absent
2	N	26/26	Top quarter of primordium
2	O	18/18	Top three-quarters of primordium
2	P	18/18	Whole leaf
2	Q	31/33	Absent
2	R	19/21	Top quarter of primordium
2	S	23/28	Top half of lamina
2	T	16/18	Top three-quarters of lamina
3	A	22/22	Midvein
3	B	30/30	Midvein
3	C	16/17	Midvein and first loop
3	D	34/48	Midvein, first and second loop
3	E	25/25	Absent
3	F	20/20	Midvein
3	G	27/37	Midvein and first loop
3	H	24/28	Midvein, first and second loop
4	A	32/46	Midvein, first and second loop
4	B	21/21	Shapeless vascular domains
4	C	ND	Narrow midvein and scalloped vein-network outline
4	D	19/20	Shapeless vascular cluster
4	E	16/23	Midvein, first and second loop
4	F	18/18	Broad vascular domain

4	G	21/21	Narrow midvein and scalloped vein-network outline
4	H	19/19	Broad vascular zone

ND, not determined.

spread toward the base of the lamina (Fig. 4.1E). Leaf hairs (trichomes) and pores (stomata) can be first recognized at the tip of 2.5- and 3-DAG primordia, respectively, and their formation spreads toward the base of the lamina during leaf development (Fig. 4.1F–I).

Consistent with previous observations (Huang et al., 2014), E100>>erGFP was expressed in all the cells of 2-, 2.5-, 3- and 4-DAG leaf primordia (Fig. 4.1K–N).

Consistent with previous observations (Krogan and Berleth, 2012), E861>>erGFP was expressed in all the inner cells of 2-DAG primordia, though more strongly in the innermost cells of the primordium (Fig. 4.1O). At 2.5 DAG, expression was activated in the lowermost epidermal cells of the primordium margin and persisted in all the inner cells of the bottom half of the primordium; in the top half of the primordium, weaker expression persisted in inner cells, except near the midvein, where by then it had been terminated (Fig. 4.1P). At 3 DAG, expression continued to persist in all the inner cells of the bottom half of the primordium, though expression was stronger in the areas where second loops would form; in the top half of the primordium, weaker expression had become restricted to the midvein, first loops and minor veins (Fig. 4.1Q). At 4 DAG, expression in the top half of the leaf remained restricted to the midvein, first loops and minor veins, and in the bottom half of the leaf it had declined in inner cells between the first loops and the developing second loops (Fig. 4.1R). In summary, E861>>erGFP was expressed ubiquitously at early stages of inner cell development; over time, however, expression became restricted to developing veins. As such, expression of E861>>erGFP closely resembles that of *MONOPTEROS* and *PIN-FORMED1*, which marks the gradual selection of vascular cells from within the leaf inner tissue (Scarpella et al., 2006; Wenzel et al., 2007).

E4295>>erGFP expression was restricted to inner cells in 2-, 2.5-, 3- and 4-DAG leaf primordia (Fig. 4.1S–V,X–Z). At 2 DAG, E4295>>erGFP was expressed almost exclusively in the inner cells of the abaxial side of the primordium (Fig. 4.1S), but by 2.5 DAG it had spread to the middle tissue layer (Fig. 4.1T), from which veins form (Stewart, 1978; Tilney-Bassett, 1986). Expression persisted in the inner cells of the abaxial side and of the middle tissue layer at 3 and 4 DAG (Fig. 4.1U,V). High-resolution images of the middle tissue layer showed that expression was excluded from developing veins (Fig. 4.1X–Z), suggesting that it

marks inner, non-vascular cells; therefore, expression of E4295>>erGFP closely resembles that of *LIGHT HARVESTING COMPLEX A6* and *SCARECROW-LIKE32* (Sawchuk et al., 2008; Gardiner et al., 2011).

At 2 DAG, E4259>>erGFP was expressed in the top third of the median adaxial epidermis and in the whole median abaxial epidermis, though expression was stronger in the top half of the primordium (Fig. 4.2A). By 2.5 DAG, strong expression had spread to the whole abaxial and to the top three-quarters of the marginal epidermis; expression had spread to the top three-quarters of the adaxial epidermis too, but it was stronger in the top half of the primordium (Fig. 4.2B,F). By 3 DAG, strong expression had spread to the top three-quarters of the adaxial epidermis and to the whole marginal epidermis, and persisted in the whole abaxial epidermis (Fig. 4.2C,G). By 4 DAG, expression persisted in the whole marginal epidermis, continued to persist in the whole abaxial epidermis, and had spread to the whole lamina and the petiole midline in the adaxial epidermis (Fig. 4.2D,H). At all analyzed stages, E4259>>erGFP was expressed in trichomes but was not expressed in mature stomata (Fig. 4.2B–H). In conclusion, expression of E4259>>erGFP closely resembles that of *ARABIDOPSIS THALIANA MERISTEM LAYER1* (Lu et al., 1996; Sessions et al., 1999), which marks epidermal cells and whose promoter is used to drive epidermis-specific expression (e.g., (Takada and Jürgens, 2007; Bilsborough et al., 2011; Kierzkowski et al., 2013)).

E4722>>erGFP was expressed in all the epidermal cells of the 2-DAG primordium, though more weakly at its tip (Fig. 4.2I). E4722>>erGFP was expressed in all the epidermal cells of the 2.5-DAG primordium too, except at its margin, where expression had been terminated in a few cells of its top half (Fig. 4.2J). By 3 DAG, expression persisted in all the epidermal cells, except at the primordium margin, where expression had been terminated in most of the cells of its top three-quarters (Fig. 4.2K). By 4 DAG, expression continued to persist in all the epidermal cells, except at the leaf margin, where expression had almost completely been terminated in the cells of its top three-quarters (Fig. 4.2L). Unlike E4259>>erGFP, E4722>>erGFP was expressed in stomata but was not expressed in trichomes (Fig. 4.2J–L).

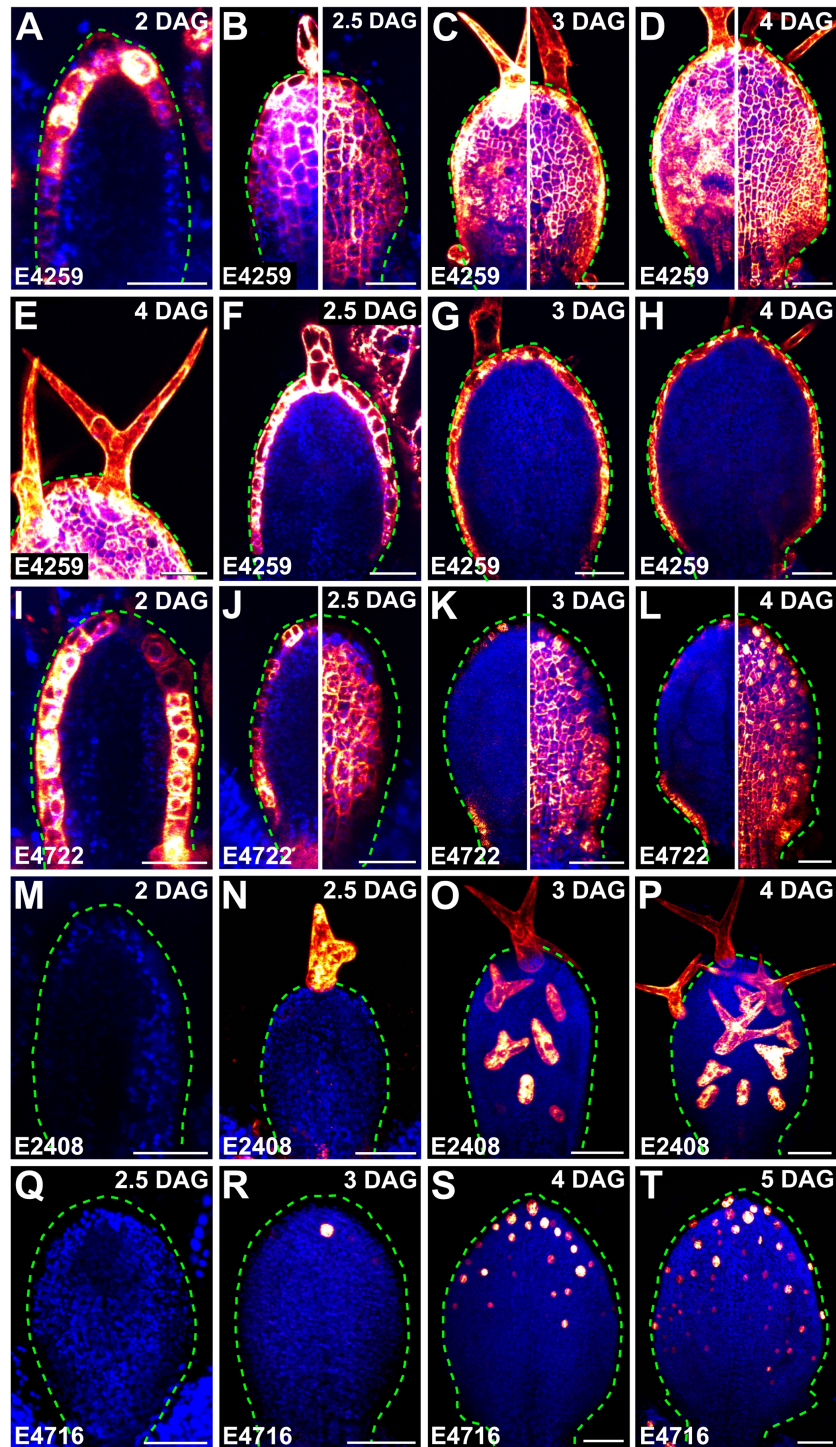


Figure 4.2. Expression of E4259>>, E4722>>, E2408>> and E4716>>erGFP in leaf development. (A–T) Confocal laser scanning microscopy. First leaves. Top right: leaf age in days after germination (DAG). Bottom left: genotype. Look-up table (ramp in Fig. 4.1J)

visualizes erGFP expression levels. Blue: autofluorescence. Dashed green line delineates leaf outline. (A,F–I,M) Median view (abaxial side to the left in A,I,M). (B–D) Adaxial (left) and abaxial (right) epidermal views. (E) Closeup of trichome in D, left. (J–L) Median (left) and abaxial epidermal (right) views. (N–P) Adaxial epidermal view. (Q–T) Abaxial epidermal view. See Table 4.2 for reproducibility of expression features. Bars: (A,B,F,I,J,M,N,Q) 30 μm ; (C,D,E,G,H,K,L,O,P,R,S,T) 60 μm .

At all analyzed stages, expression of E2408>>erGFP and E4716>>erGFP was restricted to trichomes and stomata, respectively.

E2408>>erGFP was first expressed in developing trichomes at the tip of 2.5-DAG primordia (Fig. 4.2M,N). By 3 DAG, E2408>>erGFP expression had spread to developing and mature trichomes in the top three-quarters of the primordium (Fig. 4.2O), and by 4 DAG to those in the whole lamina (Fig. 4.2P).

E4716>>erGFP was first expressed in stomata at the tip of 3-DAG primordia (Fig. 4.2Q,R). By 4 DAG, E4716>>erGFP expression had spread to the stomata in the top half of the lamina (Fig. 4.2S), and by 5 DAG to those in its top three-quarters (Fig. 4.2T).

At all analyzed stages, expression of E2331>>erGFP and E3912>>erGFP was restricted to developing veins.

E2331>>erGFP was expressed in both isodiametric and elongated cells of the midvein in 2- and 2.5-DAG primordia (Fig. 4.3A,B). By 3 DAG, it was expressed in first loops, and by 4 DAG in second loops and minor veins (Fig. 4.3C,D).

E3912>>erGFP was first expressed in the midvein of 3-DAG primordia (Fig. 4.3E,F). By 4 DAG, expression had spread to first loops, and by 5 DAG to second loops and minor veins (Fig. 4.3G,H).

These observations suggest that expression of E3912>>erGFP is initiated later than that of E2331>>erGFP during vein development. Furthermore, because the expression of E2331>>erGFP appears to be no different from that of the preprocambial markers ATHB8::nYFP, J1721>>erGFP and SHR::nYFP (Sawchuk et al., 2007; Donner et al., 2009; Gardiner et al., 2011), we suggest that E2331>>erGFP expression marks preprocambial stages of vein development, a conclusion that is consistent with E2331>>erGFP expression during embryogenesis (Gillmor et al., 2010). Finally, because E3912>>erGFP expression appears to be no different from that of the procambial marker Q0990>>erGFP in the C24 background (Sawchuk et al., 2007), we suggest that E3912>>erGFP expression marks procambial stages of vein development.

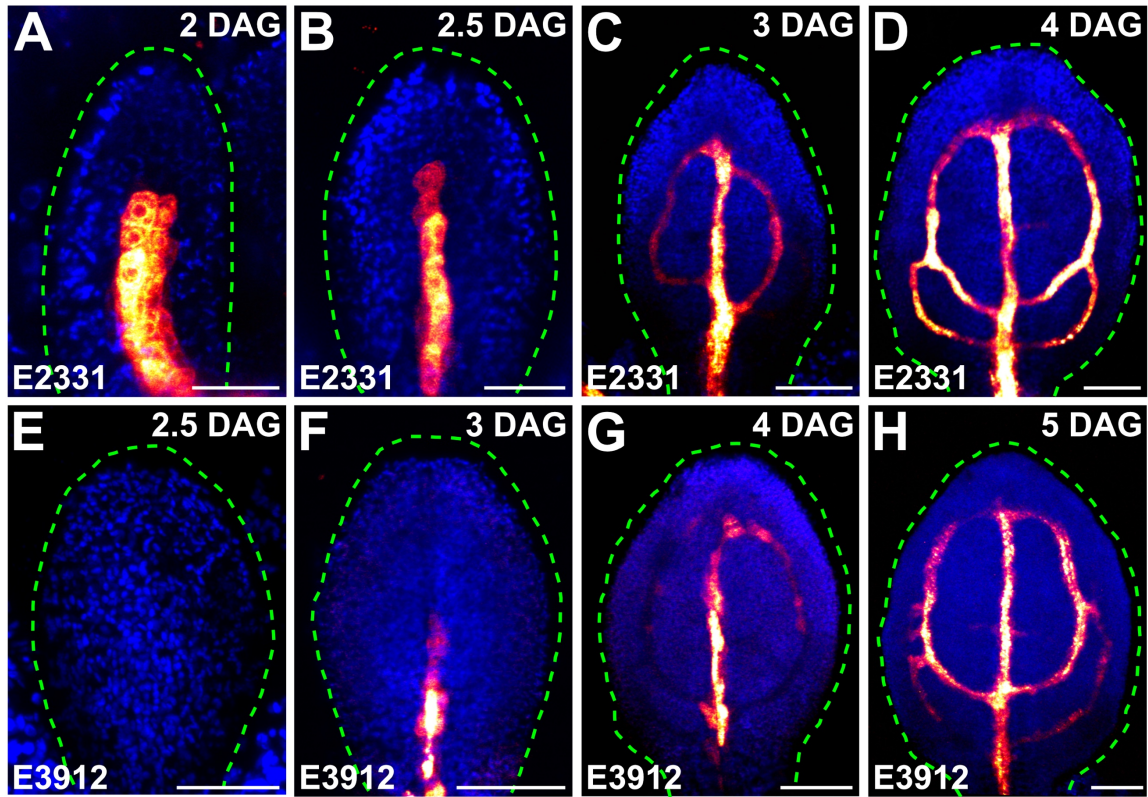


Figure 4.3. Expression of E2331>> and E3912>>erGFP in leaf development. (A–H) Confocal laser scanning microscopy. First leaves. Top right: leaf age in days after germination (DAG). Bottom left: genotype. Look-up table (ramp in Fig. 4.1J) visualizes erGFP expression levels. Blue: autofluorescence. Dashed green line delineates leaf outline. Median view (abaxial side to the left in A) . See Table 4.2 for reproducibility of expression features. Bars: (A,B,E) 30 μm ; (C,D,F–H) 60 μm .

To demonstrate the informative power of the lines reported here for plant developmental biology, we selected the E2331 line, which marks early stages of vein development (Fig. 4.3A–D).

In wild-type (WT) leaves, the elongated vascular cells are connected end-to-end to one another into continuous veins (Esau, 1965) (Fig. 4.4C). By contrast, in mature leaves of the *gnom* (*gn*) mutant, putative vascular cells fail to elongate and to connect end-to-end to one another into continuous veins; instead, they accumulate into shapeless clusters of seemingly disconnected and randomly oriented cells (Shevell et al., 2000) (Chapter 2) (Fig. 4.4D). Though the cells in these clusters have some features of vascular cells (e.g., distinctive patterns of secondary cell-wall thickenings), they lack others (e.g., elongated shape and end-to-end connection to form continuous veins); therefore, it is unclear whether these cells are abnormal vascular cells or nonvascular cells that have recruited a cellular differentiation pathway that is normally, but not always (e.g., (Solereder, 1908; Kubo et al., 2005; Yamaguchi et al., 2010)), associated with vascular development.

To address this question, we imaged E2331>>erGFP in developing leaves of WT and *gn*.

As shown above (Fig. 4.3D), E2331>>erGFP was expressed in midvein, first and second loops, and minor veins in WT (Fig. 4.4A). In *gn*, the pattern of E2331>>erGFP expression in developing leaves recapitulated that of vascular differentiation in mature leaves (Fig. 4.4B,D), suggesting that the putative vascular cells in the shapeless clusters are indeed vascular cells, albeit abnormal ones.

Auxin signaling is thought to be required for vein formation because mutations in genes involved in auxin signaling or treatment with inhibitors of auxin signaling leads to the formation of fewer, incompletely differentiated veins (Przemeck et al., 1996; Hardtke and Berleth, 1998; Mattsson et al., 2003) (Chapter 2). Furthermore, increasing auxin signaling by means of broadly expressed mutations or transgenes turns nearly every cell file in the developing leaf into a vein, suggesting that auxin signaling is also sufficient for vein formation (Garrett et al., 2012; Krogan et al., 2012). This interpretation is based on the assumption that it is the increased auxin signaling in the cell files that normally

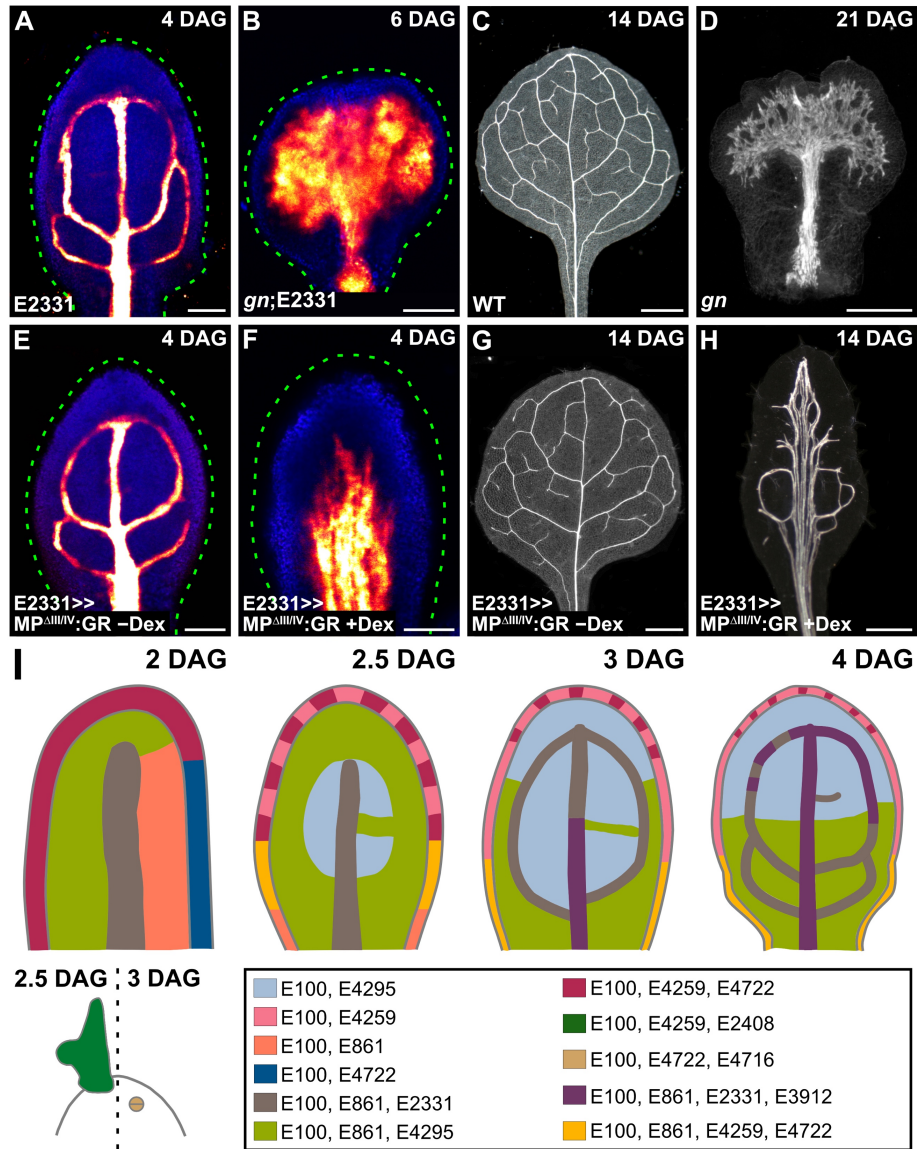


Figure 4.4. E2331-mediated visualization and manipulation of developing veins. (A–H) First leaves. Top right: leaf age in days after germination (DAG). Bottom left: genotype and treatment. (A,B,E,F) Confocal laser scanning microscopy. Look-up table (ramp in Figure 4.1 J) visualizes erGFP expression levels. Blue: autofluorescence. Dashed green line delineates leaf outline. Median view. (C,D,G,H) Dark-field microscopy of cleared leaves. See Table 4.2 for reproducibility of expression and pattern features. (I) Expression map of E100>>, E861>>, E4295>>, E4259>>, E4722>>, E2408>>, E4716>>, E2331>> and E3912>>erGFP in leaf development. See text for details. Bars: (A,B,E,F) 60 μ m; (C,D,G,H) 500 μ m.

would not differentiate into veins that leads those cell files to differentiate in fact into veins. However, it is also possible that, at least in part, it is the increased auxin signaling in the cell files that normally would differentiate into veins that leads the flanking cell files, which normally would not differentiate into veins, to do in fact so.

To discriminate between these possibilities, we increased auxin signaling in developing veins by expressing by the E2331 driver a dexamethasone (dex)-inducible MPΔIII/IV (Krogan et al., 2012; Ckurshumova et al., 2014; Smetana et al., 2019) (MPΔIII/IV:GR), and we imaged E2331>>erGFP in developing (4 DAG) leaves and vein patterns in mature (14 DAG) leaves of E2331>>MPΔIII/IV:GR grown in the presence or absence of dex.

Consistent with previous observations (Fig. 4.3D; Fig. 4.4A), in 4-DAG leaves of E2331>>MPΔIII/IV:GR grown in the absence of dex, E2331>>erGFP was expressed in narrow domains (Fig. 4.4E). By contrast, E2331>>erGFP was expressed in broad domains in 4-DAG leaves of dex-grown E2331>>MPΔIII/IV:GR (Fig. 4.4F). Whether in the presence or absence of dex, the patterns of E2331>>erGFP expression in 4-DAG leaves of E2331>>MPΔIII/IV:GR presaged those of mature veins in 14-DAG leaves: narrow zones of vein formation in the absence of dex; broad areas of vascular differentiation in the presence of dex, often with multiple veins running parallel next to one another (Fig. 4.4G,H).

Though the areas of vascular differentiation of dex-grown E2331>>MPΔIII/IV:GR are not as broad as those of leaves in which MPΔIII/IV is expressed in all the inner cells (Krogan et al., 2012), they are broader than those of E2331>>MPΔIII/IV:GR grown in the absence of dex. These observations suggest that, at least in part, it is the increased auxin signaling in the cell files that would normally differentiate into veins that leads the flanking cell files, which normally would not differentiate into veins, to do in fact so.

In conclusion, we provide a set of GAL4 enhancer-trap lines for the specific labeling of cells and tissues during leaf development (Fig. 4.4I), and we show that, just as in animal developmental biology, these lines can be used to address key questions in plant developmental biology.

4.3 Materials & Methods

4.3.1 Plants

Origin and nature of GAL4 enhancer-trap lines are in Table 4.1 *gn-13* (SALK_045424; ABRC) (Alonso et al., 2003)(Chapter 2) contains a T-DNA insertion after nucleotide +2835 of *GN* and was genotyped with the “SALK_045424 gn LP” (5'-TGATCCAAATCACTGGGTTTC-3') and “SALK_045424 gn RP” (5'-AGCTGAAGATAGGGAATTCGC-3') oligonucleotides (*GN*) and with the “SALK_045424 gn RP” and “LBb1.3” (5'-ATTTTGCCGATTCGGAAC-3') oligonucleotides (*gn*). To generate the UAS::MP Δ III/IV:GR construct, the UAS promoter was amplified with the “UAS Promoter Sali Forward” (5'-ATAGTCGACCCAAGCGCGCAATTAACCCTCAC-3) and the “UAS Promoter XhoI Reverse” (5'-AGCCTCGAGCCTCTCCAAATGAAATGAACTTCC-3); MP Δ III/IV was amplified with the “MP Delta XhoI Forward” (5'-AAACTCGAGATGATGGCTTCATTGTCTTGTGTT-3') and the “MP EcoRI Reverse” (5'-ATTGAATTCGGTTCGGACGCGGGGTGTCGCAATT-3') oligonucleotides; and a fragment of the rat glucocorticoid (GR) receptor gene was amplified with the “SpeI GR Forward” (5'-GGGACTAGTGGAGAAGCTCGAAAAACAAAG-3) and the “GR ApaI Reverse” (5'-GCGGGGCCCTCATTTTTGATGAAACAG-3'). Seeds were sterilized and sown as in (Sawchuk et al., 2008). Stratified seeds were germinated and seedlings were grown at 22°C under continuous fluorescent light ($\sim 80 \mu\text{mol m}^{-2} \text{s}^{-1}$). Plants were grown at 24°C under fluorescent light ($\sim 85 \mu\text{mol m}^{-2} \text{s}^{-1}$) in a 16-h-light/8-h-dark cycle. Plants were transformed and representative lines were selected as in (Sawchuk et al., 2008).

4.3.2 Chemicals

Dexamethasone (Sigma-Aldrich, catalogue no. D4902) was dissolved in dimethyl sulfoxide and was added to growth medium just before sowing.

4.3.3 Imaging

Developing leaves were mounted and imaged as in (Sawchuk et al., 2013), except that emission was collected from $\sim 1.5\text{--}5\text{-}\mu\text{m}$ -thick optical slices. Fluorophores were excited with the 488-nm line of a 30-mW Ar laser; GFP emission was collected with a BP 505–530 filter and autofluorescence was collected between 550 nm and 754 nm. Mature leaves were fixed in 3 : 1 or 6 : 1 ethanol : acetic acid, rehydrated in 70% ethanol and water, cleared briefly (few seconds to few minutes) — when necessary — in 0.4 M sodium hydroxide, washed in water, mounted in 80% glycerol or in 1 : 2 : 8 or 1 : 3 : 8 water : glycerol : chloral hydrate and imaged as in (Odat et al., 2014). In the Fiji distribution (Schindelin et al., 2012) of ImageJ (Schneider et al., 2012; Schindelin et al., 2015; Rueden et al., 2017), grayscale RGB color images were turned into 8-bit images; when necessary, 8-bit images were combined into stacks, and maximum-intensity projection was applied to stacks; look-up-tables were applied to images or stacks, and brightness and contrast were adjusted by linear stretching of the histogram.

Chapter 5: General discussion

5.1 Conclusion summary

The scope of my M.Sc. thesis was to understand the contribution of auxin transport and signaling to vein patterning in *Arabidopsis* (*Arabidopsis thaliana* (L.) Heynh) leaves.

For the past 20 years, the prevailing hypothesis of how auxin controls *PIN* function and derived polar formation of veins had been that the GNOM (GN) guanine-nucleotide exchange factor for ADP-rybosilation-factor GTPases, which regulates vesicle formation in membrane trafficking, coordinates the cellular localization of *PIN* proteins between cells (Steinmann et al., 1999); the resulting cell-to-cell, polar transport of auxin would coordinate *PIN* polarity between auxin-transporting cells and control polar developmental processes such as vein formation (reviewed in, e.g., (Berleth et al., 2000; Richter et al., 2010; Nakamura et al., 2012; Linh et al., 2018)). Contrary to predictions of the hypothesis, we found that auxin-induced polar vein-formation occurs in the absence of *PIN* proteins or any known intercellular auxin transporter, that the residual auxin-transport-independent vein-patterning activity relies on auxin signaling, and that GN controls both auxin transport and signaling to induce vein formation (Chapter 2).

Whereas mechanisms by which GN may control *PIN* polarity and derived polar auxin transport have been suggested (reviewed in (Richter et al., 2010; Luschnig and Vert, 2014); see also (Naramoto et al., 2014) and references therein), it is unclear how GN could control auxin signaling, which takes place in the nucleus and is inherently non-polar (reviewed in (Leyser, 2018)). The most parsimonious account is that auxin signaling leads to the production of proteins which control vein patterning and whose localization is controlled by GN; we identified four putative candidates for such proteins (Chapter 3).

The identification of such putative candidate proteins which are targets of auxin signaling, which control vein patterning and whose localization is controlled by GN required gene misexpression by different promoters. This imposed the burden of generating different constructs for different gene and promoter combinations. This approach could be simplified

if GAL4/GFP enhancer-trap lines existed in Columbia-0, the genotype of reference in Arabidopsis (Koornneef and Meinke, 2010), with which to drive expression of genes of interest in desired cells and tissues of developing leaves. Unfortunately, such lines had not been available. We addressed this limitation and provided GAL4/GFP enhancer-trap lines in the Col-0 background of Arabidopsis for the identification and manipulation of cells and tissues in developing leaves (Chapter 4).

In the Discussion section of the respective chapters, we provided an account of how we reached these conclusions from the experimental evidence, how these conclusions could be integrated with one another and with those of studies by others to advance our understanding of vein patterning, and what the implications of such conclusions are for aspects of plant development beyond the formation of veins. Here we instead wish to discuss whether accounts can be proposed to reconcile our findings in Chapter 2 with the canalization hypothesis, which was originally formulated to account for the formation of vascular strands in plant tissues that had been wounded and/or to which auxin had been applied (Sachs, 1968; Sachs, 1981), whose modern interpretations assume that PIN proteins are essential to auxin-induced vein formation (e.g., (Hartmann et al; Alim and Frey, 2010; Runions et al., 2014; Cieslak et al., 2015)), and which our findings therefore seem to challenge.

5.2 The Canalization hypothesis: challenges and alternatives

The “Canalization Hypothesis” was formulated 50 years ago — though not named as such until 1981 — by Tsvi Sachs to account for the formation of vascular strands in plant tissues that had been wounded and/or to which auxin had been applied (Sachs, 1968b; Sachs, 1981). In its simplest formulation, the hypothesis proposes that the movement of an auxin-dependent signal through a cell increases that cell’s ability to transport the signal. This positive feedback of the signal movement on itself would ultimately lead to the selection of cell files through which the signal would preferentially move — the “canals” the hypothesis refers to — and which would be induced by this preferential movement to differentiate into vascular strands.

The canalization hypothesis has provided an invaluable conceptual framework to understand the patterned formation of vascular strands, one which seems to have survived mathematical testing and to be supported by overwhelming experimental evidence. At the same time, however, evidence has been accumulating that seems to be incompatible with the hypothesis in its original formulation or current interpretation. Here we'll briefly discuss the most recent of this challenging evidence and whether accounts can be proposed to reconcile it with the canalization hypothesis. For comprehensive discussion of previous evidence, see instead, for example, (Sawchuk and Scarpella, 2013; Bennett et al., 2014; Runions et al., 2014).

5.2.1 The canalization hypothesis

In its most complete formulation, the canalization hypothesis proposes that when auxin is applied to a stem or root in which the vascular connection with the immature leaves above the auxin application site has been interrupted by wounding, an auxin-dependent signal, which includes auxin itself, diffuses from the auxin application site to the pre-existing vascular strands in the organ (Sachs, 1981; Sachs, 1991b; Sachs, 2000; Sachs, 2003) (Fig. 5.1A). By interrupting the connection between the pre-existing vascular strands in the organ and the immature leaves above the auxin application site, the pre-existing vascular strands basal to the auxin application site would be depleted of their supply of auxin and other signals that originate from the immature leaves and would thus become sinks toward which the applied auxin would diffuse. Though their supply of auxin-dependent signal would be low, the pre-existing vascular strands basal to the auxin application site would still be highly efficient and polarized signal transporters because the continuous flow of auxin-dependent signal that would be maintaining their transport polarity would only recently have been interrupted. As such, the pre-existing vascular strands basal to the auxin application site would polarize toward themselves signal movement in the neighboring, nonvascular cells.

The polarized signal movement in these neighboring, nonvascular cells would amplify itself because of the postulated positive feedback of signal movement on itself and drain signal from their lateral neighbors, thus preventing them from becoming better signal transporters. Instead, by becoming themselves better signal transporters, the nonvascular cells neighboring the pre-existing vascular strands basal to the auxin application site would become signal

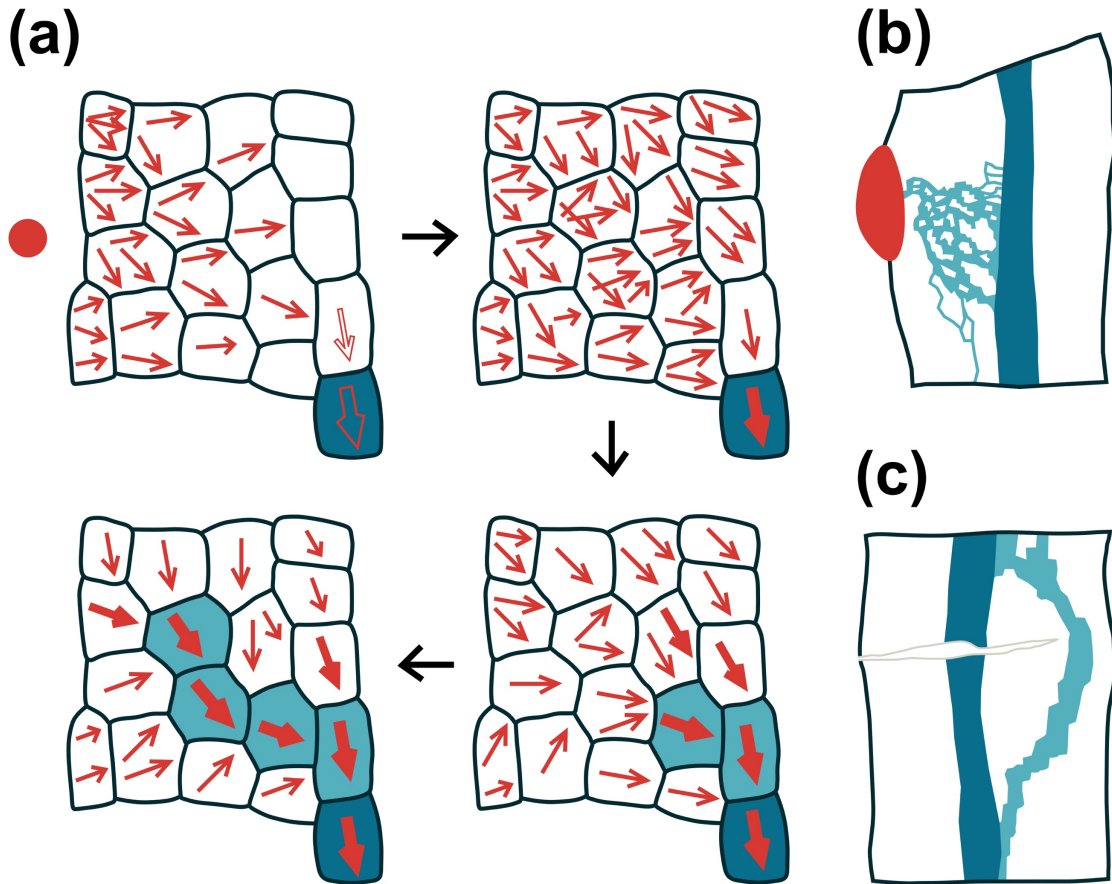


Figure 5.1. Induction of vascular strand formation by wounding and auxin application:

(a) Successive stages (connected by black arrows) of vascular strand formation in response to wounding and/or auxin application (red circle) according to the “Canalization Hypothesis”.

An auxin-dependent signal, which includes auxin itself, diffuses from the wounding or the auxin application site to the pre-existing vascular strands in the organ. The positive feedback of signal movement (red arrows) on itself gradually polarizes signal movement (increasingly thicker red-arrows). This occurs first in the cells in contact with the pre-existing vascular strands (dark blue fill), which are still polarized along the original, apical-basal polarity of the organ (empty red arrows) and thus orient signal movement toward themselves. Increased signal transport polarity, capacity and/or velocity in the selected cells leads to vascular differentiation (light blue fill) and drains signal away from neighboring cells, thus inhibiting their differentiation. The process continues until a vascular strand is formed that connects the applied auxin to the pre-existing vascular strands basal to the auxin application site. After

(Sachs, 1991a). (b) Application of auxin (red) to a mature stem or root in which the vascular connection with the immature leaves above the auxin application site has been interrupted by wounding induces the formation of vascular strands (light blue lines) that connect the applied auxin to the pre-existing vascular strands basal to the application site. After (Sachs, 1968a).

(c) Interruption of the supply of auxin and other signals that originate from the immature leaves by wounding a vascular strand in a mature stem or root induces the formation of vascular strands connecting the pre-existing vascular strand above and below the wound. After (Thompson and Jacobs, 1966; Benayoun et al., 1975).

sinks and polarize toward themselves signal movement in the cells above them. This process would repeat until cell files that transported the signal efficiently and polarly, and that would later differentiate into vascular strands, had been selected to connect the applied auxin with the pre-existing vascular strands basal to the auxin application site (Fig. 5.1B). These cell files would rarely be selected along the shortest path between the applied auxin and the pre-existing vascular strands because at every step of the process, multiple, nearly equivalent possibilities would exist and would be initiated, and the possibility that would eventually become stabilized would each time depend on choices made previously and, no less, on chance (Sachs, 1988).

Likewise, when the supply of auxin and other signals that originate from the immature leaves is interrupted by wounding a vascular strand, the auxin-dependent signal would accumulate above the wounding site (Sachs, 1991a) (Fig. 5.1A). Depleted of signal supply, the vascular strand below the wounding site would become a polarized sink for the signal, which would diffuse toward the vascular strand below the wounding site. This signal-depleted vascular strand would thus polarize signal movement toward itself and, through the same process described above, would lead to the formation of vascular strands connecting the pre-existing vascular strand above and below the wound (Fig. 5.1C). However, it seems that the wounded vascular strand is not repaired by the process; rather, new vascular strands form alongside it to re-establish the continuity of signal transport interrupted by the wounding (Benayoun et al., 1975); it's unclear whether this also applies to the vascular strands formed in response to auxin application.

5.2.2 Challenges to the canalization hypothesis

Even though the canalization hypothesis seems to be able to account for many of the available experimental observations, it makes assumptions that await experimental testing or that seem to be altogether unsupported: among them, that auxin can readily diffuse across tissues, that cells can measure auxin transport, and that cell files with high auxin transport have low auxin concentration. Many of such inconsistencies have been resolved by modifications of the original hypothesis that make assumptions that are based on known molecules and plausible parameters (e.g., (Hartmann et al; Kramer, 2004; Feugier et al.,

2005; Bayer et al., 2009; Alim and Frey, 2010; Cieslak et al., 2015)); however, these assumptions still await experimental support.

Moreover, nearly all the experiments that suggested the canalization hypothesis had been performed on mature axial organs — stems and roots — and only very few such experiments have been performed in immature axial organs or lateral organs like leaves (Sachs, 1989; Sachs, 1993; Aloni, 2001; Scarpella et al., 2006; Sawchuk et al., 2007). In those very few experiments, only a subset of the possible informative experiments have been performed, and often the response of the tissue to the interference seems to be inconsistent with predictions of the canalization hypothesis.

Predictions of the original formulation of the canalization hypothesis have especially been challenged in leaves: whereas the canalization hypothesis predicts the formation of networks in which veins connect to other veins on one side only, the leaves of many flowering plants have networks in which veins connect to other veins on both sides (Sachs, 1975) (Fig. 5.2A). However, it seems that the formation of such veins can be accounted for if the direction of signal transport is inverted regularly during early stages of vein formation (Sachs, 1975).

Though modern interpretations of the canalization hypothesis may differ in how they resolve its inconsistencies, they all rely on the presence of auxin efflux carriers that can be localized polarly at the plasma membrane (e.g., (Hartmann et al.; Alim and Frey, 2010; Runions et al., 2014; Cieslak et al., 2015)). Indole-3-acetic acid (IAA), the most abundant natural auxin, is in fact a weak acid that at the extracellular pH is undissociated and can therefore diffuse into the cell (Fig. 5.2B). At the higher pH of the cytoplasm, however, IAA is mostly dissociated and is thus unable to leave the cell, except through the action of auxin efflux carriers. Though the mechanism of action is still unclear (e.g., (Barbosa et al., 2018)), overwhelming evidence suggests that these efflux carriers are encoded by *PIN-FORMED* (*PIN*) genes (Paponov et al., 2005; Zazimalová et al., 2007; Krecek et al., 2009; Petrasek and Friml, 2009; Zazimalova et al., 2010; Balzan et al., 2014; Adamowski and Friml, 2015; Bennett, 2015); however, recent results seem to be confounding.

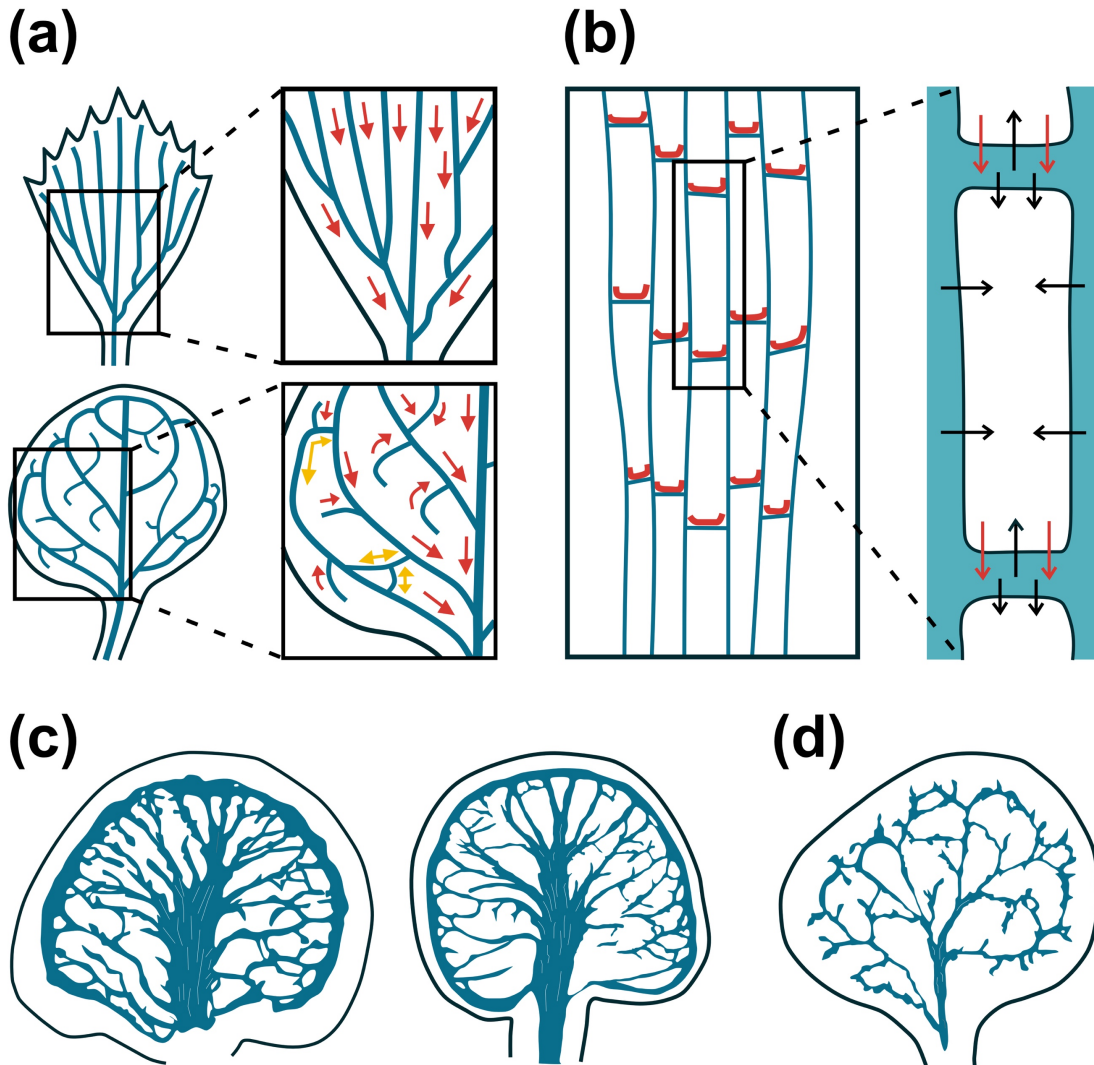


Figure 5.2. Leaf vein networks and carrier-mediated polar auxin transport: (a) Leaves have open (top) or closed (bottom) networks of veins. A unique shoot-to-root polarity (red arrow) can be assigned to each vein in open networks; attempts to assign shoot-to-root polarity to individual veins in closed networks lead to veins with ambiguous polarity (yellow double-headed arrows). (b) The shoot-to-root, apical-basal polarity of auxin transport derives from the polar localization of efflux carriers of the PIN-FORMED family (red) at the basal plasma-membrane of vascular cells. Specialized efflux carriers are required for auxin to leave the cell (red arrows) as auxin is mostly negatively charged at intracellular pH; by contrast, auxin is uncharged at extracellular pH and can thus diffuse into the cell (black arrows). (c) The vein networks of two *pin* sextuple mutants grown in the same conditions are

reproducible in their patterns but are variable in their details (drawn from (Chapter 2)); nevertheless, this variability is not associated with changes in leaf features. (d) The vein patterns of *pin* sextuple mutants can be modified by mutations in genes involved in auxin signaling without changing other leaf features.

Arabidopsis plants that lack function of six of the eight *PIN* genes (*pin* sextuple mutants hereafter) still form veins; moreover, these veins are oriented along the apical-basal axis of the leaf and are arranged in abnormal, yet reproducible, patterns (Chapter 2) (Fig. 5.2C). It's of course possible that in these plants the two remaining PIN proteins, PIN2 and PIN5, supply all the auxin transport activity required for the formation of those veins. However, mutation of *PIN2* fails to enhance the vein pattern defects of a mutant that lacks the function of four other *PIN* genes, and mutation of *PIN5* partially suppresses the vein pattern defects of a mutant that lacks function of three other *PIN* genes (Sawchuk et al., 2013; Verna et al., 2015) (Chapter 2). Furthermore, the auxin-transport and vein-patterning activity of PIN2 and PIN5 would have to be insensitive to all known auxin transport inhibitors because the vein pattern of *pin* sextuple mutants are phenocopied by treatment with at least three — but likely more — classes of chemically unrelated auxin transport inhibitors that are predicted to act through different mechanisms (Chapter 2) (Mattsson et al., 1999; Sieburth, 1999; Carland et al., 2016), and auxin transport inhibitors fail to induce additional defects in *pin* sextuple mutants (Chapter 2). Though it's possible that PIN2 and PIN5 are insensitive to all known auxin transport inhibitors, this is difficult to reconcile with the observation that such inhibitors completely inhibit auxin transport in plant tissue segments (e.g., (Okada et al., 1991; Kaneda et al., 2011)). And yet *pin* sextuple mutants can still respond to auxin application by forming veins that are oriented along the apical-basal axis of the leaf, which seems to suggest residual polar movement of auxin. But how would auxin move in those plants in the absence of the six PIN proteins with vein patterning function?

5.2.3 Alternatives to the canalization hypothesis

Available evidence suggests that auxin movement in *pin* sextuple mutants, if at all existing, does not depend on known intercellular transporters (Chapter 2). It's of course possible that it depends on known intracellular transporters — e.g., the PIN-LIKEs (Barbez et al., 2012) — or other unknown transporters. However, if so, such transporters would have to be insensitive to all known auxin transport inhibitors because treatment with these latter phenocopies the vein pattern of *pin* sextuple mutants (Chapter 2) (Mattsson et al., 1999; Sieburth, 1999; Carland et al., 2016); they would have to be specific to leaves or lateral organs, or transport

auxin inefficiently, because their activity is indistinguishable from diffusion in auxin transport measurements in stem and root segments (e.g., (Okada et al., 1991; Murphy et al., 2000; Kaneda et al., 2011)); and transport through them would have to be autocatalytic, to account for the formation of veins, as opposed to that of broad zones of vascular differentiation (Sachs, 1969). All these requirements make the existence of such transporters, though possible, less likely. But if not through auxin transporters, how would oriented veins be formed in *pin* sextuple mutants?

From a formal standpoint, we can think of two possibilities. The first one is that the vein patterns of *pin* sextuple mutants are the result of an auxin-dependent prepattern of chemical or physical nature. Veins would be rigidly specified together with all the other features of the leaf — for example, as overlaps between gene expression domains defining features in different areas of the leaf. If so, the vein patterns of *pin* sextuple mutants would be invariable, and the plasticity of such vein patterns, if at all existing, could not be uncoupled from that of other features of the leaf: any change in vein pattern could only occur as a consequence of changes in gene expression domains and would be associated with changes in other features in the corresponding leaf area, as it happens, for example, for the veins in insect wings (e.g., (De Celis, 1998)).

At least two pieces of evidence argue against such rigid specification of vein patterns in *pin* sextuple mutants. First, the vein networks of these mutants, just like those of WT, are reproducible in their patterns but are variable in their details; most important, this variability doesn't seem to be associated with changes in leaf features (Chapter 2) (Fig. 5.2C). Second, those vein patterns can be modified by mutations in genes involved in auxin signaling without changing other leaf features (Chapter 2) (Fig. 5.2D).

The second possibility is that the vein patterns of *pin* sextuple mutants are formed by a self-organizing mechanism that combines positive feedback with lateral inhibition. One such mechanism is the reaction-diffusion system developed by Alan Turing and applied to biological systems by Hans Meinhardt (Turing, 1952; Meinhardt, 1982); one other, conceptually similar to the canalization hypothesis, depends on the cell-to-cell flow of an inductive signal (e.g., (Berleth, 2000)). The main difference between a reaction-diffusion

system and the signal-flow hypothesis is that only the first one is compatible with discontinuous vein specification, i.e. the specification of isolated vein segments that successively merge into continuous veins; however, veins in auxin-transport-inhibited leaves seem to be specified as continuous veins from early on (Scarpella et al., 2006; Sawchuk et al., 2007; Wenzel et al., 2007) (Chapter 2); therefore, both mechanisms are compatible with available evidence.

Whichever the mechanism, available evidence suggests that the self-organizing specification of vein patterns in *pin* sextuple mutants depends on auxin signaling (Chapter 2). But how would auxin signaling control auxin movement, if at all existing, in those plants?

One possibility is that auxin moves by passive diffusion, whose direction is determined by gradients generated by localized auxin production and consumption. Passive diffusion of auxin depends on the proton gradient across the plasma membrane (Rubery and Shelldrake, 1974; Raven, 1975), which is regulated by proton transporters that are controlled by auxin signaling (Fendrych et al., 2016); therefore, it's possible to conceive how auxin movement could positively feedback on itself, but it's difficult to imagine how lateral inhibition would be brought about by this mechanism.

Alternatively, auxin could move by facilitated diffusion — for example, through the plasmodesmata intercellular channels — whose direction could still be determined by auxin gradients. Evidence of auxin movement through plasmodesmata had been hypothesized by Graeme Mitchison (Mitchison, 1980) and has recently received some experimental support (Han et al., 2014). There's also evidence that the size of plasmodesmata aperture is controlled by auxin signaling (Han et al., 2014), so also here it's possible to conceive how auxin movement could positively feedback on itself. Most important, however, here it's also possible to imagine how lateral inhibition could be brought about: for example, if auxin movement through the plasmodesmata in the transverse walls reduced movement through those in the lateral walls. However, there's currently no evidence of such mechanism or that plasmodesmata number or aperture controls vein patterning.

Finally, auxin may not be the mobile signal in *pin* sextuple mutants but it may be activating one, which could be of chemical nature, but also of physical one - for example, differences in cell wall composition between vascular and nonvascular cells (Couder et al., 2002; Laguna et al., 2008; Corson et al., 2009; Lee et al., 2014). However, whether signals of physical or unknown chemical nature control vein patterning remains at this stage speculative.

5.2.4 Conclusions

Current interpretations of the canalization hypothesis depend on PIN-mediated auxin transport for vein formation. The evidence discussed here suggests that this interpretation, even though intellectually pleasing, is at the very least incomplete, and that additional mechanisms, dependent on auxin but not on its carrier-mediated transport, are involved. These mechanisms may account for the inconsistencies between PIN-dependent interpretations of the canalization hypothesis and experimental observations. Surprisingly, however, the conceptual framework provided by the canalization hypothesis — the autocatalytic, cell-to-cell movement of an inductive signal that drains lateral neighbors from it — is still viable and compatible with the available evidence. The molecular details of such framework will have to be a priority for future research.

Literature cited

Adamowski, M. and Friml, J. (2015). PIN-dependent auxin transport: action, regulation, and evolution. *Plant Cell* **27**, 20-32.

Alim, K. and Frey, E. (2010). Quantitative predictions on auxin-induced polar distribution of PIN proteins during vein formation in leaves. *The European Physical Journal E* **33**, 165-173.

Aloni, R. (2001). Foliar and Axial Aspects of Vascular Differentiation: Hypotheses and Evidence. *Journal of Plant Growth Regulation* **20**, 22-34.

Aloni, R. (2010). The induction of vascular tissues by auxin. In *Plant hormones: biosynthesis, signal transduction, action* (ed. D. PJ), pp. 485-506. Dordrecht: Kluwer Academic Publishers.

Alonso-Peral, M. M., Candela, H., del Pozo, J. C., Martinez-Laborda, A., Ponce, M. R. and Micol, J. L. (2006). The HVE/CAND1 gene is required for the early patterning of leaf venation in Arabidopsis. *Development* **133**, 3755-3766.

Alonso, J. M., Stepanova, A. N., Leisse, T. J., Kim, C. J., Chen, H., Shinn, P., Stevenson, D. K., Zimmerman, J., Barajas, P., Cheuk, R. et al. (2003). Genome-wide insertional mutagenesis of Arabidopsis thaliana. *Science* **301**, 653-657.

Austin, R. S., Hiu, S., Waese, J., Ierullo, M., Pasha, A., Wang, T. T., Fan, J., Foong, C., Breit, R., Desveaux, D. et al. (2016). New BAR tools for mining expression data and exploring Cis-elements in Arabidopsis thaliana. *Plant J* **88**, 490-504.

Avery, G. S., Jr. (1935). Differential Distribution of a Phytohormone in the Developing Leaf of Nicotiana, and Its Relation to Polarized Growth. *Bulletin of the Torrey Botanical Club* **62**, 313-330.

Bailly, A., Sovero, V., Vincenzetti, V., Santelia, D., Bartnik, D., Koenig, B. W., Mancuso, S., Martinoia, E. and Geisler, M. (2008). Modulation of P-glycoproteins by

auxin transport inhibitors is mediated by interaction with immunophilins. *J. Biol. Chem.* **283**, 21817-21826.

Bainbridge, K., Guyomarc'h, S., Bayer, E., Swarup, R., Bennett, M., Mandel, T. and Kuhlemeier, C. (2008). Auxin influx carriers stabilize phyllotactic patterning. *Genes Dev.* **22**, 810-823.

Balzan, S., Johal, G. S. and Carraro, N. (2014). The role of auxin transporters in monocots development. *Front Plant Sci* **5**, 393.

Barbez, E., Kubes, M., Rolcik, J., Beziat, C., Pencik, A., Wang, B., Rosquete, M. R., Zhu, J., Dobrev, P. I., Lee, Y. et al. (2012). A novel putative auxin carrier family regulates intracellular auxin homeostasis in plants. *Nature* **485**, 119-122.

Barbosa, I. C. R., Hammes, U. Z. and Schwechheimer, C. (2018). Activation and Polarity Control of PIN-FORMED Auxin Transporters by Phosphorylation. *Trends Plant Sci* **23**, 523-538.

Bayer, E. M., Smith, R. S., Mandel, T., Nakayama, N., Sauer, M., Prusinkiewicz, P. and Kuhlemeier, C. (2009). Integration of transport-based models for phyllotaxis and midvein formation. *Genes Dev.* **23**, 373-384.

Beeckman, T., Przemeck, G. K., Stamatiou, G., Lau, R., Terry, N., De Rycke, R., Inze, D. and Berleth, T. (2002). Genetic complexity of cellulose synthase a gene function in Arabidopsis embryogenesis. *Plant Physiol* **130**, 1883-1893.

Belteton, S. A., Sawchuk, M. G., Donohoe, B. S., Scarpella, E. and Szymanski, D. B. (2018). Reassessing the Roles of PIN Proteins and Anticlinal Microtubules during Pavement Cell Morphogenesis. *Plant Physiol* **176**, 432-449.

Benayoun, J., Aloni, R. and Sachs, T. (1975). Regeneration around wounds and the control of vascular differentiation. *Annals of Botany* **39**, no. 161, 447-454.

- Benkova, E., Michniewicz, M., Sauer, M., Teichmann, T., Seifertova, D., Jurgens, G. and Friml, J.** (2003). Local, efflux-dependent auxin gradients as a common module for plant organ formation. *Cell* **115**, 591-602.
- Bennett, T.** (2015). PIN proteins and the evolution of plant development. *Trends Plant Sci* **20**, 498-507.
- Bennett, T., Hines, G. and Leyser, O.** (2014). Canalization: what the flux. *Trends Genet.* **30**, 41-48.
- Bennett, T., Hines, G., van Rongen, M., Waldie, T., Sawchuk, M. G., Scarpella, E., Ljung, K. and Leyser, O.** (2016). Connective Auxin Transport in the Shoot Facilitates Communication between Shoot Apices. *PLoS Biol.* **14**, e1002446.
- Berleth, T.** (2000). Plant development: Hidden networks. *Curr. Biol.* **10**, R658-R661.
- Berleth, T. and Jurgens, G.** (1993). The Role of the Monopteros Gene in Organizing the Basal Body Region of the Arabidopsis Embryo. *Development* **118**, 575-587.
- Berleth, T., Mattsson, J. and Hardtke, C. S.** (2000). Vascular continuity and auxin signals. *Trends Plant Sci* **5**, 387-393.
- Bilsborough, G. D., Runions, A., Barkoulas, M., Jenkins, H. W., Hasson, A., Galinha, C., Laufs, P., Hay, A., Prusinkiewicz, P. and Tsiantis, M.** (2011). Model for the regulation of Arabidopsis thaliana leaf margin development. *Proc. Natl. Acad. Sci. U S A* **108**, 3424-3429.
- Blakeslee, J. J., Bandyopadhyay, A., Lee, O. R., Mravec, J., Titapiwatanakun, B., Sauer, M., Makam, S. N., Cheng, Y., Bouchard, R., Adamec, J. et al.** (2007). Interactions among PIN-FORMED and P-glycoprotein auxin transporters in Arabidopsis. *Plant Cell* **19**, 131-147.
- Bosco, C. D., Dovzhenko, A., Liu, X., Woerner, N., Rensch, T., Eismann, M., Eimer, S., Hegermann, J., Paponov, I. A., Ruperti, B. et al.** (2012). The endoplasmic reticulum

localized PIN8 is a pollen specific auxin carrier involved in intracellular auxin homeostasis. *The Plant Journal*, **71**, 860-870.

Bouchard, R., Bailly, A., Blakeslee, J. J., Oehring, S. C., Vincenzetti, V., Lee, O. R., Paponov, I., Palme, K., Mancuso, S., Murphy, A. S. et al. (2006). Immunophilin-like TWISTED DWARF1 modulates auxin efflux activities of Arabidopsis P-glycoproteins. *J. Biol. Chem.* **281**, 30603-30612.

Boutte, Y., Ikeda, Y. and Grebe, M. (2007). Mechanisms of auxin-dependent cell and tissue polarity. *Curr Opin Plant Biol* **10**, 616-623.

Brand, A. H. and Perrimon, N. (1993). Targeted gene expression as a means of altering cell fates and generating dominant phenotypes. *Development* **118**, 401-415.

Braybrook, S. A. and Peaucelle, A. (2013). Mechano-chemical aspects of organ formation in Arabidopsis thaliana: the relationship between auxin and pectin. *PLoS One* **8**, e57813.

Calderon-Villalobos, L. I., Tan, X., Zheng, N. and Estelle, M. (2010). Auxin perception--structural insights. *Cold Spring Harb Perspect Biol* **2**, a005546.

Cande, W. Z. and Ray, P. I. M. (1976). Nature of cell-to-cell transfer of auxin in polar transport. *Planta* **129**, 43-52.

Candela, H., Alonso-Peral, M. M., Ponce, M. R. and Micol, J. L. (2007). Role of HEMIVENATA and the Ubiquitin Pathway in Venation Pattern Formation. *Plant Signal Behav* **2**, 258-259.

Candela, H., Martinez-Laborda, A. and Micol, J. L. (1999). Venation pattern formation in Arabidopsis thaliana vegetative leaves. *Dev. Biol.* **205**, 205-216.

Carland, F., Defries, A., Cutler, S. and Nelson, T. (2016). Novel Vein Patterns in Arabidopsis Induced by Small Molecules. *Plant Physiol* **170**, 338-353.

Chen, R., Hilson, P., Sedbrook, J., Rosen, E., Caspar, T. and Masson, P. H. (1998). The arabidopsis thaliana AGRAVITROPIC 1 gene encodes a component of the polar-auxin-transport efflux carrier. *Proc. Natl. Acad. Sci. U S A* **95**, 15112-15117.

- Chevalier, D., Batoux, M., Fulton, L., Pfister, K., Yadav, R. K., Schellenberg, M. and Schneitz, K.** (2005). STRUBBELIG defines a receptor kinase-mediated signaling pathway regulating organ development in Arabidopsis. *Proc. Natl. Acad. Sci. U S A* **102**, 9074-9079.
- Chomczynski, P. and Sacchi, N.** (1987). Single-step method of RNA isolation by acid guanidinium thiocyanate-phenol-chloroform extraction. *Anal. Biochem.* **162**, 156-159.
- Cieslak, M., Runions, A. and Prusinkiewicz, P.** (2015). Auxin-driven patterning with unidirectional fluxes. *J Exp Bot* **66**, 5083-5102.
- Ciruna, B., Jenny, A., Lee, D., Mlodzik, M. and Schier, A. F.** (2006). Planar cell polarity signalling couples cell division and morphogenesis during neurulation. *Nature* **439**, 220-224.
- Ckurshumova, W., Koizumi, K., Chatfield, S. P., Sanchez-Buelna, S. U., Gangaeva, A. E., McKenzie, R. and Berleth, T.** (2009). Tissue-specific GAL4 expression patterns as a resource enabling targeted gene expression, cell type-specific transcript profiling and gene function characterization in the Arabidopsis vascular system. *Plant Cell Physiol* **50**, 141-150.
- Ckurshumova, W., Smirnova, T., Marcos, D., Zayed, Y. and Berleth, T.** (2014). Irrepressible MONOPTEROS/ARF5 promotes de novo shoot formation. *New Phytol* **204**, 556-566.
- Corson, F., Adda-Bedia, M. and Boudaoud, A.** (2009). In silico leaf venation networks: growth and reorganization driven by mechanical forces. *J Theor Biol* **259**, 440-448.
- Couder, Y., Pauchard, L., Allain, C. and Adda-Bedia..., M.** (2002). The leaf venation as formed in a tensorial field. *The European Physical Journal B-Condensed Matter and Complex Systems*, **28**, 135-138.
- Crittenden, L. B. and Bitgood, J. J., Burt, D. W., de Leon, F., & Tixier-Boichard, M.** (1996). Nomenclature for naming loci, alleles, linkage groups and chromosomes to be used in poultry genome publications and databases. *Genetics, Selection, Evolution: GSE*, **28**, 289–297.

De Celis, J. F. (1998). Positioning and differentiation of veins in the *Drosophila* wing. *Int. J. Dev. Biol.* **42**, 335-343.

Dengler, N. G. (2006). The shoot apical meristem and development of vascular architecture. *Canadian Journal of Botany* **84**, 1660-1671.

Dharmasiri, N., Dharmasiri, S., Weijers, D., Lechner, E., Yamada, M., Hobbie, L., Ehrismann, J. S., Jurgens, G. and Estelle, M. (2005). Plant Development Is Regulated by a Family of Auxin Receptor F Box Proteins. *Dev. Cell* **9**, 109-119.

Dhonukshe, P., Grigoriev, I., Fischer, R., Tominaga, M., Robinson, D. G., Hasek, J., Paciorek, T., Petrasek, J., Seifertova, D., Tejos, R. et al. (2008). Auxin transport inhibitors impair vesicle motility and actin cytoskeleton dynamics in diverse eukaryotes. *Proc. Natl. Acad. Sci. U S A* **105**, 4489-4494.

Ding, Z., Wang, B., Moreno, I., Duplakova, N., Simon, S., Carraro, N., Reemmer, J., Pencik, A., Chen, X., Tejos, R. et al. (2012). ER-localized auxin transporter PIN8 regulates auxin homeostasis and male gametophyte development in *Arabidopsis*. *Nat Commun* **3**, 941.

Ditengou, F. A., Gomes, D., Nziengui, H., Kochersperger, P., Lasok, H., Medeiros, V., Paponov, I. A., Nagy, S. K., Náday, T. V., Mészáros, T. et al. (2018). Characterization of auxin transporter PIN6 plasma membrane targeting reveals a function for PIN6 in plant bolting. *New Phytol* **217**, 1610-1624.

Donnelly, P. M., Bonetta, D., Tsukaya, H., Dengler, R. E. and Dengler, N. G. (1999). Cell cycling and cell enlargement in developing leaves of *Arabidopsis*. *Dev. Biol.* **215**, 407-419.

Donner, T. J., Sherr, I. and Scarpella, E. (2009). Regulation of preprocambial cell state acquisition by auxin signaling in *Arabidopsis* leaves. *Development* **136**, 3235-3246.

Esau, K. (1942). Vascular Differentiation in the Vegetative Shoot of *Linum*. I. The Procambium. *American Journal of Botany* **29**, 738-747.

Esau, K. (1965). *Plant anatomy*. New York: John Wiley.

- Esteve-Bruna, D., Perez-Perez, J. M., Ponce, M. R. and Micol, J. L.** (2013). *incurvata13*, a novel allele of AUXIN RESISTANT6, reveals a specific role for auxin and the SCF complex in Arabidopsis embryogenesis, vascular specification, and leaf flatness. *Plant Physiol* **161**, 1303-1320.
- Etchells, J. P. and Turner, S. R.** (2010). The PXY-CLE41 receptor ligand pair defines a multifunctional pathway that controls the rate and orientation of vascular cell division. *Development* **137**, 767-774.
- Eyüboğlu, B., Pfister, K., Haberer, G., Chevalier, D., Fuchs, A., Mayer, K. F. and Schneitz, K.** (2007). Molecular characterisation of the STRUBBELIG-RECEPTOR FAMILY of genes encoding putative leucine-rich repeat receptor-like kinases in Arabidopsis thaliana. *BMC Plant Biol* **7**, 16.
- Fendrych, M., Leung, J. and Friml, J.** (2016). TIR1/AFB-Aux/IAA auxin perception mediates rapid cell wall acidification and growth of Arabidopsis hypocotyls. *Elife* **5**, e19048.
- Feugier, F. G., Mochizuki, A. and Iwasa, Y.** (2005). Self-organization of the vascular system in plant leaves: Inter-dependent dynamics of auxin flux and carrier proteins. *Journal of Theoretical Biology* **236**, 366-375.
- Fischer, U., Ikeda, Y., Ljung, K., Serralbo, O., Singh, M., Heidstra, R., Palme, K., Scheres, B. and Grebe, M.** (2006). Vectorial information for Arabidopsis planar polarity is mediated by combined AUX1, EIN2, and GNOM activity. *Curr. Biol.* **16**, 2143-2149.
- Fisher, K. and Turner, S.** (2007). PXY, a receptor-like kinase essential for maintaining polarity during plant vascular-tissue development. *Curr. Biol.* **17**, 1061-1066.
- Franzmann, L., Patton, D. A. and Meinke, D. W.** (1989). In vitro Morphogenesis of Arrested Embryos from Lethal Mutants of Arabidopsis-Thaliana. *Theoretical and Applied Genetics* **77**, 609-616.

- Friml, J., Benkova, E., Blilou, I., Wisniewska, J., Hamann, T., Ljung, K., Woody, S., Sandberg, G., Scheres, B., Jurgens, G. et al.** (2002a). AtPIN4 mediates sink-driven auxin gradients and root patterning in Arabidopsis. *Cell* **108**, 661-673.
- Friml, J., Vieten, A., Sauer, M., Weijers, D., Schwarz, H., Hamann, T., Offringa, R. and Jurgens, G.** (2003). Efflux-dependent auxin gradients establish the apical-basal axis of Arabidopsis. *Nature* **426**, 147-153.
- Friml, J., Wisniewska, J., Benkova, E., Mendgen, K. and Palme, K.** (2002b). Lateral relocation of auxin efflux regulator PIN3 mediates tropism in Arabidopsis. *Nature* **415**, 806-809.
- Galweiler, L., Guan, C., Muller, A., Wisman, E., Mendgen, K., Yephremov, A. and Palme, K.** (1998). Regulation of polar auxin transport by AtPIN1 in Arabidopsis vascular tissue. *Science* **282**, 2226-2230.
- Ganguly, A., Park, M., Kesawat, M. S. and Cho, H.-T.** (2014). Functional analysis of the hydrophilic loop in intracellular trafficking of Arabidopsis PIN-FORMED proteins. *The Plant Cell* **26**, 1570-1585.
- Gardiner, J., Donner, T. J. and Scarpella, E.** (2011). Simultaneous activation of SHR and ATHB8 expression defines switch to preprocambial cell state in Arabidopsis leaf development. *Dev Dyn* **240**, 261-270.
- Gardner, M. J., Baker, A. J., Assie, J. M., Poethig, R. S., Haseloff, J. P. and Webb, A. A.** (2009). GAL4 GFP enhancer trap lines for analysis of stomatal guard cell development and gene expression. *J Exp Bot* **60**, 213-226.
- Garrett, J. J., Meents, M. J., Blackshaw, M. T., Blackshaw, L. C., Hou, H., Styranko, D. M., Kohalmi, S. E. and Schultz, E. A.** (2012). A novel, semi-dominant allele of MONOPTEROS provides insight into leaf initiation and vein pattern formation. *Planta* **236**, 297-312.

Geisler, M. and Murphy, A. S. (2006). The ABC of auxin transport: the role of p-glycoproteins in plant development. *FEBS Lett.* **580**, 1094-1102.

Geisler, M., Blakeslee, J. J., Bouchard, R., Lee, O. R., Vincenzetti, V., Bandyopadhyay, A., Titapiwatanakun, B., Peer, W. A., Bailly, A., Richards, E. L. et al. (2005). Cellular efflux of auxin catalyzed by the Arabidopsis MDR/PGP transporter AtPGP1. *Plant J* **44**, 179-194.

Geisler, M., Kolukisaoglu, H. U., Bouchard, R., Billion, K., Berger, J., Saal, B., Frangne, N., Koncz-Kalman, Z., Koncz, C., Dudler, R. et al. (2003). TWISTED DWARF1, a unique plasma membrane-anchored immunophilin-like protein, interacts with Arabidopsis multidrug resistance-like transporters AtPGP1 and AtPGP19. *Mol. Biol. Cell* **14**, 4238-4249.

Geldner, N., Richter, S., Vieten, A., Marquardt, S., Torres-Ruiz, R. A., Mayer, U. and Jurgens, G. (2004). Partial loss-of-function alleles reveal a role for GNOM in auxin transport-related, post-embryonic development of Arabidopsis. *Development* **131**, 389-400.

Gillmor, C. S., Park, M. Y., Smith, M. R., Pepitone, R., Kerstetter, R. A. and Poethig, R. S. (2010). The MED12-MED13 module of Mediator regulates the timing of embryo patterning in Arabidopsis. *Development* **137**, 113-122.

Goodrich, L. V. and Strutt, D. (2011). Principles of planar polarity in animal development. *Development* **138**, 1877-1892.

Groszmann, M., Gonzalez-Bayon, R., Greaves, I. K., Wang, L., Huen, A. K., Peacock, W. J. and Dennis, E. S. (2014). Intraspecific Arabidopsis hybrids show different patterns of heterosis despite the close relatedness of the parental genomes. *Plant Physiol* **166**, 265-280.

Halder, G., Callaerts, P. and Gehring, W. J. (1995). Induction of ectopic eyes by targeted expression of the eyeless gene in Drosophila. *Science* **267**, 1788-1792.

- Hamant, O., Heisler, M. G., Jonsson, H., Krupinski, P., Uyttewaal, M., Bokov, P., Corson, F., Sahlin, P., Boudaoud, A., Meyerowitz, E. M. et al.** (2008). Developmental patterning by mechanical signals in Arabidopsis. *Science* **322**, 1650-1655.
- Han, X., Hyun, T. K., Zhang, M., Kumar, R., Koh, E. J., Kang, B. H., Lucas, W. J. and Kim, J. Y.** (2014). Auxin-callose-mediated plasmodesmal gating is essential for tropic auxin gradient formation and signaling. *Dev. Cell* **28**, 132-146.
- Hardtke, C. S. and Berleth, T.** (1998). The Arabidopsis gene MONOPTEROS encodes a transcription factor mediating embryo axis formation and vascular development. *EMBO J.* **17**, 1405-1411.
- Hardtke, C. S., Ckurshumova, W., Vidaurre, D. P., Singh, S. A., Stamatiou, G., Tiwari, S. B., Hagen, G., Guilfoyle, T. J. and Berleth, T.** (2004). Overlapping and non-redundant functions of the Arabidopsis auxin response factors MONOPTEROS and NONPHOTOTROPIC HYPOCOTYL 4. *Development* **131**, 1089-1100.
- Hartmann, F. P., Barbier de Reuille, P. and Kuhlemeier, C.** Toward a 3D model of phyllotaxis based on a biochemically plausible auxin-transport mechanism. *PloS Comp Biol* **15**, e1006896.
- Haseloff, J.** (1999). GFP variants for multispectral imaging of living cells. *Methods Cell Biol.* **58**, 139-151.
- Heisler, M. G., Hamant, O., Krupinski, P., Uyttewaal, M., Ohno, C., Jonsson, H., Traas, J. and Meyerowitz, E. M.** (2010). Alignment between PIN1 polarity and microtubule orientation in the shoot apical meristem reveals a tight coupling between morphogenesis and auxin transport. *PLoS Biol.* **8**, e1000516.
- Heisler, M. G., Ohno, C., Das, P., Sieber, P., Reddy, G. V., Long, J. A. and Meyerowitz, E. M.** (2005). Patterns of Auxin Transport and Gene Expression during Primordium Development Revealed by Live Imaging of the Arabidopsis Inflorescence Meristem. *Curr. Biol.* **15**, 1899-1911.

Hirakawa, Y., Shinohara, H., Kondo, Y., Inoue, A., Nakanomyo, I., Ogawa, M., Sawa, S., Ohashi-Ito, K., Matsubayashi, Y. and Fukuda, H. (2008). Non-cell-autonomous control of vascular stem cell fate by a CLE peptide/receptor system. *Proc. Natl. Acad. Sci. U S A* **105**, 15208-15213.

Hooper, C. M., Castleden, I. R., Tanz, S. K., Aryamanesh, N. and Millar, A. H. (2017). SUBA4: the interactive data analysis centre for Arabidopsis subcellular protein locations. *Nucleic Acids Res.* **45**, D1064-D1074.

Huang, T., Harrar, Y., Lin, C., Reinhart, B., Newell, N. R., Talavera-Rauh, F., Hokin, S. A., Barton, M. K. and Kerstetter, R. A. (2014). Arabidopsis KANAD11 acts as a transcriptional repressor by interacting with a specific cis-element and regulates auxin biosynthesis, transport, and signaling in opposition to HD-ZIPIII factors. *Plant Cell* **26**, 246-262.

Irani, N. G., Di Rubbo, S., Mylle, E., Van den Begin, J., Schneider-Pizoń, J., Hniliková, J., Šiša, M., Buyst, D., Vilarrasa-Blasi, J. and Szatmári, A.-M. (2012). Fluorescent castasterone reveals BRI1 signaling from the plasma membrane. *Nature chemical biology* **8**, 583.

Ito, K., Awano, W., Suzuki, K., Hiromi, Y. and Yamamoto, D. (1997). The Drosophila mushroom body is a quadruple structure of clonal units each of which contains a virtually identical set of neurones and glial cells. *Development* **124**, 761-771.

Ito, Y., Nakanomyo, I., Motose, H., Iwamoto, K., Sawa, S., Dohmae, N. and Fukuda, H. (2006). Dodeca-CLE peptides as suppressors of plant stem cell differentiation. *Science* **313**, 842-845.

Kamphausen, T., Fanghanel, J., Neumann, D., Schulz, B. and Rahfeld, J. U. (2002). Characterization of Arabidopsis thaliana AtFKBP42 that is membrane-bound and interacts with Hsp90. *Plant J* **32**, 263-276.

Kaneda, M., Schuetz, M., Lin, B. S., Chanis, C., Hamberger, B., Western, T. L., Ehltling, J. and Samuels, A. L. (2011). ABC transporters coordinately expressed during lignification

of Arabidopsis stems include a set of ABCBs associated with auxin transport. *J Exp Bot* **62**, 2063-2077.

Kang, J. and Dengler, N. (2002). Cell cycling frequency and expression of the homeobox gene ATHB-8 during leaf vein development in Arabidopsis. *Planta* **216**, 212-219.

Kang, J. and Dengler, N. (2004). Vein pattern development in adult leaves of Arabidopsis thaliana. *International Journal of Plant Sciences* **165**, 231-242.

Katekar, G. F. and Geissler, A. E. (1980). Auxin Transport Inhibitors: IV. EVIDENCE OF A COMMON MODE OF ACTION FOR A PROPOSED CLASS OF AUXIN TRANSPORT INHIBITORS: THE PHYTOTROPINS. *Plant Physiol* **66**, 1190-1195.

Kawanabe, T., Ishikura, S., Miyaji, N., Sasaki, T., Wu, L. M., Itabashi, E., Takada, S., Shimizu, M., Takasaki-Yasuda, T. and Osabe, K. (2016). Role of DNA methylation in hybrid vigor in Arabidopsis thaliana. *Proceedings of the National Academy of Sciences* **113**, E6704-E6711.

Kierzkowski, D., Lenhard, M., Smith, R. and Kuhlemeier, C. (2013). Interaction between meristem tissue layers controls phyllotaxis. *Dev. Cell* **26**, 616-628.

Kim, D., Langmead, B., & Salzberg, S. L. (2015). HISAT: a fast spliced aligner with low memory requirements. *Nature methods*, **12**, 357.

Kinsman, E. A. and Pyke, K. A. (1998). Bundle sheath cells and cell-specific plastid development in Arabidopsis leaves. *Development* **125**, 1815-1822.

Kleine-Vehn, J., Dhonukshe, P., Sauer, M., Brewer, P. B., Wisniewska, J., Paciorek, T., Benkova, E. and Friml, J. (2008). ARF GEF-dependent transcytosis and polar delivery of PIN auxin carriers in Arabidopsis. *Curr. Biol.* **18**, 526-531.

Koizumi, K., Sugiyama, M. and Fukuda, H. (2000). A series of novel mutants of Arabidopsis thaliana that are defective in the formation of continuous vascular network: calling the auxin signal flow canalization hypothesis into question. *Development* **127**, 3197-3204.

- Koornneef, M. and Meinke, D.** (2010). The development of Arabidopsis as a model plant. *The Plant Journal* **61**, 909-921.
- Kramer, E. M.** (2004). PIN and AUX/LAX proteins: their role in auxin accumulation. *Trends Plant Sci* **9**, 578-582.
- Krecek, P., Skupa, P., Libus, J., Naramoto, S., Tejos, R., Friml, J. and Zazimalova, E.** (2009). The PIN-FORMED (PIN) protein family of auxin transporters. *Genome Biol* **10**, 249.
- Krogan, N. T. and Berleth, T.** (2012). A dominant mutation reveals asymmetry in MP/ARF5 function along the adaxial-abaxial axis of shoot lateral organs. *Plant Signal Behav* **7**, 940-943.
- Krogan, N. T., Ckurshumova, W., Marcos, D., Caragea, A. E. and Berleth, T.** (2012). Deletion of MP/ARF5 domains III and IV reveals a requirement for Aux/IAA regulation in Arabidopsis leaf vascular patterning. *New Phytologist*, **194**, 391-401.
- Kubo, M., Udagawa, M., Nishikubo, N., Horiguchi, G., Yamaguchi, M., Ito, J., Mimura, T., Fukuda, H. and Demura, T.** (2005). Transcription switches for protoxylem and metaxylem vessel formation. *Genes Dev.* **19**, 1855-1860.
- Kwak, S. H. and Schiefelbein, J.** (2008). A feedback mechanism controlling SCRAMBLED receptor accumulation and cell-type pattern in Arabidopsis. *Curr. Biol.* **18**, 1949-1954.
- Kwak, S. H., Shen, R. and Schiefelbein, J.** (2005). Positional signaling mediated by a receptor-like kinase in Arabidopsis. *Science* **307**, 1111-1113.
- Kwak, S.-H. and Schiefelbein, J.** (2007). The role of the SCRAMBLED receptor-like kinase in patterning the Arabidopsis root epidermis. *Dev. Biol.* **302**, 118-131.
- Laguna, M. F., Bohn, S. and Jagla, E. A.** (2008). The role of elastic stresses on leaf venation morphogenesis. *PLoS computational biology*, **4**, e1000055.
- Lamesch P, Berardini TZ, Li D, Swarbreck D, Wilks C, Sasidharan R, Muller R, Dreher K, Alexander DL, Garcia-Hernandez M, Karthikeyan AS.** (2012) The

Arabidopsis Information Resource (TAIR): improved gene annotation and new tools. *Nucleic acids research*. D1202-10.

Laplaze, L., Parizot, B., Baker, A., Ricaud, L., Martinière, A., Auguy, F., Franche, C., Nussaume, L., Bogusz, D. and Haseloff, J. (2005). GAL4-GFP enhancer trap lines for genetic manipulation of lateral root development in *Arabidopsis thaliana*. *J Exp Bot* **56**, 2433-2442.

Larkin, J. C., Young, N., Prigge, M. and Marks, M. D. (1996). The control of trichome spacing and number in *Arabidopsis*. *Development* **122**, 997-1005.

Lee, S. W., Feugier, F. G. and Morishita, Y. (2014). Canalization-based vein formation in a growing leaf. *Journal of theoretical biology* , **353**, 104-120.

Leyser, O. (2018). Auxin Signaling. *Plant Physiol* **176**, 465-479.

Li, H., Handsaker, B., Wysoker, A., Fennell, T., Ruan, J., Homer, N., ... & Durbin, R. (2009). The sequence alignment/map format and SAMtools. *Bioinformatics*, **25**, 2078-2079.

Linh, N. M., Verna, C. and Scarpella, E. (2018). Coordination of cell polarity and the patterning of leaf vein networks. *Curr Opin Plant Biol* **41**, 116-124.

Lu, P., Porat, R., Nadeau, J. A. and O'Neill, S. D. (1996). Identification of a meristem L1 layer-specific gene in *Arabidopsis* that is expressed during embryonic pattern formation and defines a new class of homeobox genes. *The Plant Cell* **8**, 2155-2168.

Lukowitz, W., Gillmor, C. S. and Scheible, W. R. (2000). Positional cloning in *Arabidopsis*. Why it feels good to have a genome initiative working for you. *Plant Physiol* **123**, 795-805.

Luschnig, C. and Vert, G. (2014). The dynamics of plant plasma membrane proteins: PINs and beyond. *Development* **141**, 2924-2938.

Luschnig, C., Gaxiola, R. A., Grisafi, P. and Fink, G. R. (1998). EIR1, a root-specific protein involved in auxin transport, is required for gravitropism in *Arabidopsis thaliana*. *Genes & Development* **12**, 2175-2187.

- Marcos, D. and Berleth, T.** (2014). Dynamic auxin transport patterns preceding vein formation revealed by live-imaging of Arabidopsis leaf primordia. *Front Plant Sci* **5**, 235.
- Marhava, P., Bassukas, A. E. L., Zourelidou, M., Kolb, M., Moret, B., Fastner, A., Schulze, W. X., Cattaneo, P., Hammes, U. Z., Schwechheimer, C. et al.** (2018). A molecular rheostat adjusts auxin flux to promote root protophloem differentiation. *Nature* **558**, 297-300.
- Matthes, M. and Torres-Ruiz, R. A.** (2016). Boronic acids induce monopteros phenocopies by affecting PIN1 membrane stability and polar auxin transport in Arabidopsis thaliana embryos. *Development*, **143**, 4053-4062.
- Mattsson, J., Ckurshumova, W. and Berleth, T.** (2003). Auxin signaling in Arabidopsis leaf vascular development. *Plant Physiol* **131**, 1327-1339.
- Mattsson, J., Sung, Z. R. and Berleth, T.** (1999). Responses of plant vascular systems to auxin transport inhibition. *Development* **126**, 2979-2991.
- Mayer, U., Buttner, G. and Jurgens, G.** (1993). Apical-basal pattern formation in the Arabidopsis embryo: studies on the role of the gnom gene. *Development* **117**, 149-162.
- Meinhardt, H.** (1982). Models of biological pattern formation. London: Academic Press
- Mitchison, G. J.** (1980). Model for Vein Formation in Higher-Plants. *Proceedings of the Royal Society of London Series B-Biological Sciences* **207**, 79-109.
- Morgan, D. G. and Söding, H.** (1958). Über die Wirkungsweise von Phthalsäuremono- α -Naphthylamid (PNA) auf das Wachstum der Haferkoleoptile. *Planta* **52**, 235-249.
- Moriwaki, T., Miyazawa, Y., Fujii, N. and Takahashi, H.** (2014). GNOM regulates root hydrotropism and phototropism independently of PIN-mediated auxin transport. *Plant Sci* **215-216**, 141-149.
- Mravec, J., Kubes, M., Bielach, A., Gaykova, V., Petrasek, J., Skupa, P., Chand, S., Benkova, E., Zazimalova, E. and Friml, J.** (2008). Interaction of PIN and PGP transport mechanisms in auxin distribution-dependent development. *Development* **135**, 3345-3354.

- Mravec, J., Skupa, P., Bailly, A., Hoyerova, K., Krecek, P., Bielach, A., Petrasek, J., Zhang, J., Gaykova, V., Stierhof, Y. D. et al.** (2009). Subcellular homeostasis of phytohormone auxin is mediated by the ER-localized PIN5 transporter. *Nature* **459**, 1136-1140.
- Muller, A., Guan, C., Galweiler, L., Tanzler, P., Huijser, P., Marchant, A., Parry, G., Bennett, M., Wisman, E. and Palme, K.** (1998). AtPIN2 defines a locus of Arabidopsis for root gravitropism control. *EMBO J.* **17**, 6903-6911.
- Murphy, A., Peer, W. A. and Taiz, L.** (2000). Regulation of auxin transport by aminopeptidases and endogenous flavonoids. *Planta* **211**, 315-324.
- Nakamura, M., Kiefer, C. S. and Grebe, M.** (2012). Planar polarity, tissue polarity and planar morphogenesis in plants. *Curr Opin Plant Biol* **15**, 593-600.
- Nakano, R. T., Matsushima, R., Ueda, H., Tamura, K., Shimada, T., Li, L., Hayashi, Y., Kondo, M., Nishimura, M. and Hara-Nishimura, I.** (2009). GNOM-LIKE1/ERMO1 and SEC24a/ERMO2 are required for maintenance of endoplasmic reticulum morphology in Arabidopsis thaliana. *Plant Cell* **21**, 3672-3685.
- Nakayama, N., Smith, R. S., Mandel, T., Robinson, S., Kimura, S., Boudaoud, A. and Kuhlemeier, C.** (2012). Mechanical regulation of auxin-mediated growth. *Curr. Biol.* **22**, 1468-1476.
- Naramoto, S., Otegui, M. S., Kutsuna, N., de Rycke, R., Dainobu, T., Karampelias, M., Fujimoto, M., Feraru, E., Miki, D., Fukuda, H. et al.** (2014). Insights into the localization and function of the membrane trafficking regulator GNOM ARF-GEF at the Golgi apparatus in Arabidopsis. *Plant Cell* **26**, 3062-3076.
- Nelson, T. and Dengler, N.** (1997). Leaf Vascular Pattern Formation. *Plant Cell* **9**, 1121-1135.
- Nielsen, M. E., Feechan, A., Böhlenius, H., Ueda, T. and Thordal-Christensen, H.** (2012). Arabidopsis ARF-GTP exchange factor, GNOM, mediates transport required for

innate immunity and focal accumulation of syntaxin PEN1. *Proceedings of the National Academy of Sciences* **109**, 11443-11448.

Odat, O., Gardiner, J., Sawchuk, M. G., Verna, C., Donner, T. J. and Scarpella, E. (2014). Characterization of an allelic series in the MONOPTEROS gene of Arabidopsis. *Genesis* **52**, 127-133.

Okada, K., Ueda, J., Komaki, M. K., Bell, C. J. and Shimura, Y. (1991). Requirement of the Auxin Polar Transport System in Early Stages of Arabidopsis Floral Bud Formation. *Plant Cell* **3**, 677-684.

Okumura, K., Goh, T., Toyokura, K., Kasahara, H., Takebayashi, Y., Mimura, T., Kamiya, Y. and Fukaki, H. (2013). GNOM/FEWER ROOTS is required for the establishment of an auxin response maximum for arabidopsis lateral root initiation. *Plant Cell Physiol* **54**, 406-417.

Paponov, I. A., Teale, W. D., Trebar, M., Blilou, I. and Palme, K. (2005). The PIN auxin efflux facilitators: evolutionary and functional perspectives. *Trends Plant Sci* **10**, 170-177.

Parry, G., Marchant, A., May, S., Swarup, R., Swarup, K., James, N., Graham, N., Allen, T., Martucci, T., Yemm, A. et al. (2001). Quick on the uptake: Characterization of a family of plant auxin influx carriers. *Journal of Plant Growth Regulation* **20**, 217-225.

Peaucelle, A., Braybrook, S. A., Le Guillou, L., Bron, E., Kuhlemeier, C. and Höfte, H. (2011). Pectin-induced changes in cell wall mechanics underlie organ initiation in Arabidopsis. *Curr. Biol.* **21**, 1720-1726.

Peret, B., Swarup, K., Ferguson, A., Seth, M., Yang, Y. D., Dhondt, S., James, N., Casimiro, I., Perry, P., Syed, A. et al. (2012). AUX/LAX Genes Encode a Family of Auxin Influx Transporters That Perform Distinct Functions during Arabidopsis Development. *Plant Cell* **24**, 2874-2885.

Perez-Perez, J. M., Ponce, M. R. and Micol, J. L. (2004). The ULTRACURVATA2 gene of Arabidopsis encodes an FK506-binding protein involved in auxin and brassinosteroid signaling. *Plant Physiol* **134**, 101-117.

Pertea, M., Kim, D., Pertea, G. M., Leek, J. T., & Salzberg, S. L. (2016). Transcript-level expression analysis of RNA-seq experiments with HISAT, StringTie and Ballgown. *Nature protocols*, **11**, 1650.

Petrasek, J. and Friml, J. (2009). Auxin transport routes in plant development. *Development* **136**, 2675-2688.

Petrasek, J., Cerna, A., Schwarzerova, K., Elckner, M., Morris, D. A. and Zazimalova, E. (2003). Do phytohormones inhibit auxin efflux by impairing vesicle traffic? *Plant Physiol* **131**, 254-263.

Petrasek, J., Mravec, J., Bouchard, R., Blakeslee, J. J., Abas, M., Seifertova, D., Wisniewska, J., Tadele, Z., Kubes, M., Covanova, M. et al. (2006). PIN proteins perform a rate-limiting function in cellular auxin efflux. *Science* **312**, 914-918.

Przemeck, G. K., Mattsson, J., Hardtke, C. S., Sung, Z. R. and Berleth, T. (1996). Studies on the role of the Arabidopsis gene MONOPTEROS in vascular development and plant cell axialization. *Planta* **200**, 229-237.

Pyke, K. A., Marrison, J. L. and Leech, R. M. (1991). Temporal and Spatial Development of the Cells of the Expanding 1st Leaf of Arabidopsis-Thaliana (L) Heynh. *Journal of Experimental Botany* **42**, 1407-1416.

Raven, J. A. (1975). Transport of indole acetic acid in plant cells in relation to pH and electrical potential gradients, and its significance for polar IAA transport. *New Phytologist* **74**, 163-172.

Reinhardt, D., Pesce, E. R., Stieger, P., Mandel, T., Baltensperger, K., Bennett, M., Traas, J., Friml, J. and Kuhlemeier, C. (2003). Regulation of phyllotaxis by polar auxin transport. *Nature* **426**, 255-260.

- Richter, S., Anders, N., Wolters, H., Beckmann, H., Thomann, A., Heinrich, R., Schrader, J., Singh, M. K., Geldner, N., Mayer, U. et al.** (2010). Role of the GNOM gene in Arabidopsis apical-basal patterning--From mutant phenotype to cellular mechanism of protein action. *Eur. J. Cell Biol.* **89**, 138-144.
- Richter, S., Geldner, N., Schrader, J., Wolters, H., Stierhof, Y. D., Rios, G., Koncz, C., Robinson, D. G. and Jürgens, G.** (2007). Functional diversification of closely related ARF-GEFs in protein secretion and recycling. *Nature* **448**, 488-492.
- Rubery, P. H. and Shelldrake, A. R.** (1974). Carrier-Mediated Auxin Transport. *Planta* **118**, 101-121.
- Rueden, C. T., Schindelin, J., Hiner, M. C., DeZonia, B. E., Walter, A. E., Arena, E. T. and Eliceiri, K. W.** (2017). ImageJ2: ImageJ for the next generation of scientific image data. *BMC Bioinformatics* **18**, 529.
- Ruegger, M., Dewey, E., Hobbie, L., Brown, D., Bernasconi, P., Turner, J., Muday, G. and Estelle, M.** (1997). Reduced naphthylphthalamic acid binding in the tir3 mutant of Arabidopsis is associated with a reduction in polar auxin transport and diverse morphological defects. *Plant Cell* **9**, 745-757.
- Runions, A., Smith, R. S. and Prusinkiewicz, P.** (2014). Computational Models of Auxin-Driven Development. In *Auxin and Its Role in Plant Development* pp. 315-357. Vienna: Springer.
- Sabatini, S., Beis, D., Wolkenfelt, H., Murfett, J., Guilfoyle, T., Malamy, J., Benfey, P., Leyser, O., Bechtold, N., Weisbeek, P. et al.** (1999). An auxin-dependent distal organizer of pattern and polarity in the Arabidopsis root. *Cell* **99**, 463-472.
- Sachs, T.** (1968a). On determination of pattern of vascular tissues in peas. *Annals of Botany* **32**, 781-790.
- Sachs, T.** (1968b). The Role of the Root in the Induction of Xylem Differentiation in Peas. *Annals of Botany* **32**, 391-399.

- Sachs, T.** (1969). Polarity and the Induction of Organized Vascular Tissues. *Annals of Botany* **33**, 263-275.
- Sachs, T.** (1975). Control of Differentiation of Vascular Networks. *Annals of Botany* **39**, 197-204.
- Sachs, T.** (1981). The control of the patterned differentiation of vascular tissues. *Advances in Botanical Research* **9**, 151-262.
- Sachs, T.** (1988). Epigenetic selection: an alternative mechanism of pattern formation. *Journal of theoretical biology* **134**, 547-559.
- Sachs, T.** (1989). The development of vascular networks during leaf development. *Current Topics in Plant Biochemistry and Physiology* **8**, 168-183.
- Sachs, T.** (1991a). Cell Polarity and Tissue Patterning in Plants. *Development Suppl* **1**, 83-93.
- Sachs, T.** (1991b). Pattern Formation in Plant Tissues. *Development and cell biology series*. Cambridge: Cambridge University Press.
- Sachs, T.** (1991b). The canalization of vascular differentiation. In *Pattern Formation in Plant Tissues* pp. 70-87. Cambridge: Cambridge University Press.
- Sachs, T.** (1993). The role of auxin in the polar organisation of apical meristems. *Functional Plant Biology* **20**, 541-553.
- Sachs, T.** (2000). Integrating Cellular and Organismic Aspects of Vascular Differentiation. *Plant and Cell Physiology* **41**, 649-656.
- Sachs, T.** (2003). Collective specification of cellular development. *BioEssays* **25**, 897-903.
- Sawchuk, M. G. and Scarpella, E.** (2013). Polarity, continuity, and alignment in plant vascular strands. *J Integr Plant Biol* **55**, 824-834.

- Sawchuk, M. G., Donner, T. J., Head, P. and Scarpella, E.** (2008). Unique and overlapping expression patterns among members of photosynthesis-associated nuclear gene families in Arabidopsis. *Plant Physiol* **148**, 1908-1924.
- Sawchuk, M. G., Edgar, A. and Scarpella, E.** (2013). Patterning of leaf vein networks by convergent auxin transport pathways. *PLoS Genet.* **9**, e1003294.
- Sawchuk, M. G., Head, P., Donner, T. J. and Scarpella, E.** (2007). Time-lapse imaging of Arabidopsis leaf development shows dynamic patterns of procambium formation. *New Phytol* **176**, 560-571.
- Scacchi, E., Osmont, K. S., Beuchat, J., Salinas, P., Navarrete-Gómez, M., Trigueros, M., Ferrándiz, C. and Hardtke, C. S.** (2009). Dynamic, auxin-responsive plasma membrane-to-nucleus movement of Arabidopsis BRX. *Development* **136**, 2059-2067.
- Scacchi, E., Salinas, P., Gujas, B., Santuari, L., Krogan, N., Ragni, L., Berleth, T. and Hardtke, C. S.** (2010). Spatio-temporal sequence of cross-regulatory events in root meristem growth. *Proc. Natl. Acad. Sci. U S A* **107**, 22734-22739.
- Scarpella, E., Francis, P. and Berleth, T.** (2004). Stage-specific markers define early steps of procambium development in Arabidopsis leaves and correlate termination of vein formation with mesophyll differentiation. *Development* **131**, 3445-3455.
- Scarpella, E., Marcos, D., Friml, J. and Berleth, T.** (2006). Control of leaf vascular patterning by polar auxin transport. *Genes Dev.* **20**, 1015-1027.
- Schindelin, J., Arganda-Carreras, I., Frise, E., Kaynig, V., Longair, M., Pietzsch, T., Preibisch, S., Rueden, C., Saalfeld, S., Schmid, B. et al.** (2012). Fiji: an open-source platform for biological-image analysis. *Nat Methods* **9**, 676-682.
- Schindelin, J., Rueden, C. T., Hiner, M. C. and Eliceiri, K. W.** (2015). The ImageJ ecosystem: An open platform for biomedical image analysis. *Mol. Reprod. Dev.* **82**, 518-529.
- Schneider, C. A., Rasband, W. S. and Eliceiri, K. W.** (2012). NIH Image to ImageJ: 25 years of image analysis. *Nat Methods* **9**, 671-675.

- Schuetz, M., Berleth, T. and Mattsson, J.** (2008). Multiple MONOPTEROS-dependent pathways are involved in leaf initiation. *Plant Physiol* **148**, 870-880.
- Schwechheimer, C.** (2018). NEDD8-its role in the regulation of Cullin-RING ligases. *Curr Opin Plant Biol* **45**, 112-119.
- Sessions, A., Weigel, D. and Yanofsky, M. F.** (1999). The Arabidopsis thaliana MERISTEM LAYER 1 promoter specifies epidermal expression in meristems and young primordia. *Plant J* **20**, 259-263.
- Shevell, D. E., Kunkel, T. and Chua, N. H.** (2000). Cell wall alterations in the arabidopsis emb30 mutant. *Plant Cell* **12**, 2047-2060.
- Shevell, D. E., Leu, W. M., Gillmor, C. S., Xia, G., Feldmann, K. A. and Chua, N. H.** (1994). EMB30 is essential for normal cell division, cell expansion, and cell adhesion in Arabidopsis and encodes a protein that has similarity to Sec7. *Cell* **77**, 1051-1062.
- Shpak, E. D., Berthiaume, C. T., Hill, E. J. and Torii, K. U.** (2004). Synergistic interaction of three ERECTA-family receptor-like kinases controls Arabidopsis organ growth and flower development by promoting cell proliferation. *Development* **131**, 1491-1501.
- Sieburth, L. E.** (1999). Auxin is required for leaf vein pattern in Arabidopsis. *Plant Physiol* **121**, 1179-1190.
- Simon, S., Skůpa, P., Viaene, T., Zwiewka, M., Tejos, R., Klíma, P., Čarná, M., Rolčik, J., De Rycke, R. and Moreno, I.** (2016). PIN6 auxin transporter at endoplasmic reticulum and plasma membrane mediates auxin homeostasis and organogenesis in Arabidopsis. *New Phytologist* **211**, 65-74.
- Smetana, O., Mäkilä, R., Lyu, M., Amiryousefi, A., Sánchez Rodríguez, F., Wu, M. F., Solé-Gil, A., Leal Gavarrón, M., Siligato, R., Miyashima, S. et al.** (2019). High levels of auxin signalling define the stem-cell organizer of the vascular cambium. *Nature* **565**, 485-489.

Solereeder, H. (1908). *Systematic anatomy of the dicotyledons: a handbook for laboratories of pure and applied botany. II.* Oxford: Clarendon Press.

Steinmann, T., Geldner, N., Grebe, M., Mangold, S., Jackson, C. L., Paris, S., Galweiler, L., Palme, K. and Jurgens, G. (1999). Coordinated polar localization of auxin efflux carrier PIN1 by GNOM ARF GEF. *Science* **286**, 316-318.

Stewart, R. N. (1978). Ontogeny of the primary body in chimeral forms of higher plants. In *The Clonal Basis of Development* (ed. S. Subtelny and I. M. Sussex), 131-160. New York: Academic Press.

Steynen, Q. J. and Schultz, E. A. (2003). The FORKED genes are essential for distal vein meeting in Arabidopsis. *Development* **130**, 4695-4708.

Strabala, T. J., O'donnell, P. J., Smit, A. M., Ampomah-Dwamena, C., Martin, E. J., Netzler, N., Nieuwenhuizen, N. J., Quinn, B. D., Foote, H. C. and Hudson, K. R. (2006). Gain-of-function phenotypes of many CLAVATA3/ESR genes, including four new family members, correlate with tandem variations in the conserved CLAVATA3/ESR domain. *Plant Physiol* **140**, 1331-1344.

Suer, S., Agusti, J., Sanchez, P., Schwarz, M. and Greb, T. (2011). WOX4 imparts auxin responsiveness to cambium cells in Arabidopsis. *Plant Cell* **23**, 3247-3259.

Sussman, M. R. and Goldsmith, M. H. M. (1981). Auxin uptake and action of N-1-naphthylphthalamic acid in corn coleoptiles. *Planta* **151**, 15-25.

Swarup, K., Benkova, E., Swarup, R., Casimiro, I., Peret, B., Yang, Y., Parry, G., Nielsen, E., De Smet, I., Vanneste, S. et al. (2008). The auxin influx carrier LAX3 promotes lateral root emergence. *Nat. Cell Biol.* **10**, 946-954.

Takada, S. and Jürgens, G. (2007). Transcriptional regulation of epidermal cell fate in the Arabidopsis embryo. *Development* **134**, 1141-1150.

Teh, O.-k. and Moore, I. (2007). An ARF-GEF acting at the Golgi and in selective endocytosis in polarized plant cells. *Nature* **448**, 493.

- Telfer, A. and Poethig, R. S.** (1994). Leaf development in Arabidopsis. In *Arabidopsis* (ed. E. M. Meyerowitz and C. R. Somerville). **27**, New York: Cold Spring Harbor Press.
- Thimann, K. V. and Skoog, F.** (1934). On the Inhibition of Bud Development and other Functions of Growth Substance in *Vicia Faba*. *Proceedings of the Royal Society of London. Series B, Containing Papers of a Biological Character* **114**, 317-339.
- Thompson, N. P. and Jacobs, W. P.** (1966). Polarity of IAA effect on sieve-tube and xylem regeneration in *Coleus* and tomato stems. *Plant Physiology* , **41**, 673-682.
- Tilney-Bassett, R. A. E.** (1986). *Plant Chimeras*. London: Edward Arnold (Publishers) Ltd.
- Torii, K. U., Mitsukawa, N., Oosumi, T., Matsuura, Y., Yokoyama, R., Whittier, R. F. and Komeda, Y.** (1996). The Arabidopsis ERECTA gene encodes a putative receptor protein kinase with extracellular leucine-rich repeats. *Plant Cell* **8**, 735-746.
- Trapnell, C., Roberts, A., Goff, L., Pertea, G., Kim, D., Kelley, D. R., Pimentel, H., Salzberg, S.L., Rinn, J.L. & Pachter, L.** (2012). Differential gene and transcript expression analysis of RNA-seq experiments with TopHat and Cufflinks. *Nature protocols*, **7**, 562.
- Turing, A.** (1952). The Chemical Basis of Morphogenesis. *Philosophical Transactions of the Royal Society of London. Series B, Biological Sciences* **237**, 37-72.
- Verna, C., Sawchuk, M. G., Linh, N. M. and Scarpella, E.** (2015). Control of vein network topology by auxin transport. *BMC Biol* **13**, 94.
- Viaene, T., Delwiche, C. F., Rensing, S. A. and Friml, J.** (2012). Origin and evolution of PIN auxin transporters in the green lineage. *Trends in plant science*, **18**, 5-10.
- Wang, B., Bailly, A., Zwiewka, M., Henrichs, S., Azzarello, E., Mancuso, S., Maeshima, M., Friml, J., Schulz, A. and Geisler, M.** (2013). Arabidopsis TWISTED DWARF1 functionally interacts with auxin exporter ABCB1 on the root plasma membrane. *Plant Cell* **25**, 202-214.
- Wangermann, E.** (1974). The pathway of transport of applied indolyl-acetic acid through internode segments. *New Phytologist* **73**, 623-636.

- Weijers, D., Franke-van Dijk, M., Vencken, R. J., Quint, A., Hooykaas, P. and Offringa, R.** (2001). An Arabidopsis Minute-like phenotype caused by a semi-dominant mutation in a RIBOSOMAL PROTEIN S5 gene. *Development* **128**, 4289-4299.
- Weijers, D., Van Hamburg, J. P., Van Rijn, E., Hooykaas, P. J. and Offringa, R.** (2003). Diphtheria toxin-mediated cell ablation reveals interregional communication during Arabidopsis seed development. *Plant Physiol* **133**, 1882-1892.
- Went, F. W.** (1928). Wuchsstoff und Wachstum. *Recueil des travaux botaniques néerlandais* **25**, IV-116.
- Wenzel, C. L., Schuetz, M., Yu, Q. and Mattsson, J.** (2007). Dynamics of MONOPTEROS and PIN-FORMED1 expression during leaf vein pattern formation in Arabidopsis thaliana. *Plant J* **49**, 387-398.
- Whitford, R., Fernandez, A., De Groot, R., Ortega, E. and Hilson, P.** (2008). Plant CLE peptides from two distinct functional classes synergistically induce division of vascular cells. *Proc. Natl. Acad. Sci. U S A* **105**, 18625-18630.
- Wisniewska, J., Xu, J., Seifertova, D., Brewer, P. B., Ruzicka, K., Blilou, I., Rouquie, D., Benkova, E., Scheres, B. and Friml, J.** (2006). Polar PIN localization directs auxin flow in plants. *Science* **312**, 883.
- Wu, G., Otegui, M. S. and Spalding, E. P.** (2010). The ER-localized TWD1 immunophilin is necessary for localization of multidrug resistance-like proteins required for polar auxin transport in Arabidopsis roots. *Plant Cell* **22**, 3295-3304.
- Xu, J. and Scheres, B.** (2005). Dissection of Arabidopsis ADP-RIBOSYLATION FACTOR 1 function in epidermal cell polarity. *Plant Cell* **17**, 525-536.
- Yadav, R. K., Fulton, L., Batoux, M. and Schneitz, K.** (2008). The Arabidopsis receptor-like kinase STRUBBELIG mediates inter-cell-layer signaling during floral development. *Dev. Biol.* **323**, 261-270.

Yamaguchi, M., Goué, N., Igarashi, H., Ohtani, M., Nakano, Y., Mortimer, J. C., Nishikubo, N., Kubo, M., Katayama, Y., Kakegawa, K. et al. (2010). VASCULAR-RELATED NAC-DOMAIN6 and VASCULAR-RELATED NAC-DOMAIN7 effectively induce transdifferentiation into xylem vessel elements under control of an induction system. *Plant Physiol* **153**, 906-914.

Yang, H. and Murphy, A. S. (2009). Functional expression and characterization of Arabidopsis ABCB, AUX 1 and PIN auxin transporters in *Schizosaccharomyces pombe*. *Plant J* **59**, 179-191.

Yang, Y., Hammes, U. Z., Taylor, C. G., Schachtman, D. P. and Nielsen, E. (2006). High-affinity auxin transport by the AUX1 influx carrier protein. *Curr. Biol.* **16**, 1123-1127.

Yin, C., Kiskowski, M., Pouille, P. A., Farge, E. and Solnica-Krezel, L. (2008). Cooperation of polarized cell intercalations drives convergence and extension of presomitic mesoderm during zebrafish gastrulation. *J. Cell Biol.* **180**, 221-232.

Yoshida, S., van der Schuren, A., van Dop, M., van Galen, L., Saiga, S., Adibi, M., Möller, B., ten Hove, C. A., Marhavy, P., Smith, R. et al. (2019). A SOSEKI-based coordinate system interprets global polarity cues in Arabidopsis. *Nature Plants* **5**, 160-166.

Zadnikova, P., Petrasek, J., Marhavy, P., Raz, V., Vandenbussche, F., Ding, Z., Schwarzerova, K., Morita, M. T., Tasaka, M., Hejatko, J. et al. (2010). Role of PIN-mediated auxin efflux in apical hook development of Arabidopsis thaliana. *Development* **137**, 607-617.

Zazimalová, E., Krecek, P., Skůpa, P., Hoyerová, K. and Petrásek, J. (2007). Polar transport of the plant hormone auxin - the role of PIN-FORMED (PIN) proteins. *Cell Mol Life Sci* **64**, 1621-1637.

Zazimalova, E., Murphy, A. S., Yang, H., Hoyerova, K. and Hosek, P. (2010). Auxin transporters--why so many? *Cold Spring Harb Perspect Biol* **2**, a001552.

Zhang, Q., Wang, D., Lang, Z., He, L., Yang, L., Zeng, L., Li, Y., Zhao, C., Huang, H., Zhang, H. et al. (2016). Methylation interactions in Arabidopsis hybrids require RNA-directed DNA methylation and are influenced by genetic variation. *Proc. Natl. Acad. Sci. U S A* **113**, E4248-56.

Zourelidou, M., Absmanner, B., Weller, B., Barbosa, I. C., Willige, B. C., Fastner, A., Streit, V., Port, S. A., Colcombet, J., de la Fuente van Bentem, S. et al. (2014). Auxin efflux by PIN-FORMED proteins is activated by two different protein kinases, D6 PROTEIN KINASE and PINOID. *Elife* **3**, e02860.